

STOCHASTIC OPTIMIZATION OF COVERED CALL STRATEGIES

by

Mauricio Diaz

A thesis submitted in conformity with the requirements
for the degree of Doctor of Philosophy
Graduate Department of Mechanical and Industrial Engineering
University of Toronto

© Copyright 2019 by Mauricio Diaz

Abstract

Stochastic Optimization of Covered Call Strategies

Mauricio Diaz

Doctor of Philosophy

Graduate Department of Mechanical and Industrial Engineering

University of Toronto

2019

We present scenario-based stochastic optimization models to construct covered call strategies. Unlike existing studies which have tested heuristics for forming covered calls and have largely been descriptive in nature, our models prescribe the construction of optimal covered call strategies to produce either risk-return efficient or expected utility-maximized strategies. We present models where we define the sample expected return, sample risk, and sample expected utility based on the return of a covered call strategy in numerous simulated scenarios. All models we propose feature only linear constraints and either linear, quadratic, or convex objective functions. With some innovation all models we present are computationally tractable using over fifty assets and several hundred call options. In contrast to existing studies which typically focus on covered calls formed on a single asset by fully overwriting with an at-the-money or slightly out-of-the-money option, we explore covered call strategies of a more general form which include: multiple underlying assets, partial overwriting, and overwriting by simultaneously selling call options of different strike prices and maturity dates. We find that optimized covered call strategies exploit this generalized form. Popular heuristics in the literature and in practice which select strike prices based on a fixed level of moneyness or probability of exercise fail to consider the option market prices as part of the selection process. The call option market prices are critical inputs to our models. We show that expected return-maximized covered call strategies are directly linked to call risk premiums, one component of which are the option market prices. Covered calls are traditionally formed as an overlay on existing asset positions. Our analysis suggests that covered calls formed in two steps by first optimizing underlying

equity positions then selecting call overwriting weights are not risk-return optimal in general. We propose optimization frameworks which construct covered call portfolios by simultaneously selecting underlying asset positions and call options to sell. We detail the implementation and testing of various models, and draw insight into the structure of optimized covered call strategies.

Acknowledgements

Thank you to Professor Roy Kwon for his continued mentorship and guidance as my supervisor.

Thank you to Professor Daniel Frances for fatefully setting me on my academic journey.

Thank you to Professor Yuri Lawryshyn for his reviews and suggestions.

Thank you to my wife Ashley for her endless motivation and support.

Thank you to Oliver Gergelj for his words of wisdom.

Thank you to my friends and my family.

Thank you for reading my thesis.

Contents

Preface	1
1 Introduction	2
1.1 The Covered Call Strategy	2
1.2 Covered Call Literature	3
1.3 Covered Calls In Practice	5
1.4 Proposed Optimization of Covered Call Strategies	7
2 Optimizing a Single Asset Covered Call	11
2.1 Methodology	12
2.2 Policy Structure	15
2.3 Implementation	16
2.4 Results	18
2.5 Conclusion	21
3 Optimizing a Portfolio of Covered Calls	22
3.1 Methodology	23
3.2 Policy Analysis	28
3.3 Implementation	32
3.4 Results	34
3.5 Scaling	38
3.6 Performance	43
3.7 Conclusion	46

4 Two-stage Optimization of Covered Calls	48
4.1 Methodology	49
4.2 Implementation	57
4.3 Results	61
4.4 Implementing the Progressive Hedging Algorithm	68
4.5 Conclusion	74
5 Conclusion	76
Bibliography	80
A Monotonicity of a Single Asset Covered Call	85
B Linearity of Covered Call Constraints	87
C Convexity of Variance and Semivariance	90
D Description of Michaud Resampling	92
E Description of GARCH Volatility	94
F Two-Stage Covered Call Optimization Formulation	95
G Two-Stage Scenario Generation	99
H Option Market Price Estimation	103
I Utilities With Identical Arrow-Pratt Coefficients	105
J Progressive Hedging Penalties With Variable Rescaling	108

Preface

The bulk of chapters 2 and 3 has been published as Diaz and Kwon (2017) and Diaz and Kwon (2019). The bulk of chapter 4 is under review for publication with the title "Optimization of covered calls under uncertainty". This work was funded in part by Mitacs grant IT04115. This work was also funded by the Queen Elizabeth II Graduate Scholarship in Science and Technology Program and by the Ontario Graduate Scholarship Program.

Chapter 1

Introduction

1.1 The Covered Call Strategy

A covered call strategy, also called a buy-write strategy, involves selling European call options while holding units of the underlying asset. A naked short call position can potentially incur infinite losses, but a covered call is covered in the sense that the underlying asset is being held and is available for delivery at maturity if necessary. In down-side cases where the option expires out-of-the-money, the premium from selling the call provides a modest gain which offsets losses on the underlying equity. In up-side cases where the option expires in-the-money, the liability incurred caps the gains earned from the underlying equity. The short call position can thus be perceived as regulating the return of the long equity position. For this reason covered calls are often thought of as superior on a risk-adjusted basis versus the long position in the underlying asset.

Traditional covered calls are formed by selling one unit of a call option of a particular strike price and maturity date for each unit of underlying equity held. The maturity date is typically close to the present, e.g. one-month-to-maturity. The strike price is usually selected so that the option is at-the-money (ATM) or out-of-the-money (OTM). Options which are in-the-money (ITM) are rarely considered.

1.2 Covered Call Literature

Much of the existing covered call literature is descriptive in nature, typically using some heuristic to select strike prices and maturity dates of options to sell to form covered calls then analyzing the resulting performance. Existing studies have also focused on covered calls composed on a single asset, usually fully overwritten with one particular option. In contrast to the existing literature, in section 1.4 we propose models which: utilize optimization to create covered calls, consider portfolios of covered calls with multiple assets, provide a definitive solution for how to select strike prices, allow partial overwriting and overwriting with multiple options with different strike prices and maturity dates, and use the market prices of options as important inputs.

Authors consistently conclude that it is best to form covered call strategies using short-dated options, e.g. one month to maturity options (see Whaley 2002, Figelman 2008, and Maidel and Sahlin 2010). Figelman (2008) found that options with shorter terms usually had the highest volatility risk premiums and were most attractive when forming covered calls. Kapadia and Szado (2007) and Maidel and Sahlin (2010) reached similar conclusions. In contrast there is no consensus about how to best select strike prices.

In 2002, the Chicago Board Options Exchange (CBOE) introduced the CBOE S&P 500 BuyWrite Index. It was designed to track the performance of a covered call strategy where the underlying is the S&P 500 Index. When shorted, the calls have approximately a month until maturity and an at-the-money (ATM) strike price. Details about the index can be found in CBOE (2010). Robert Whaley, who was commissioned to design the index, showed in Whaley (2002) that from 1988–2001 the index provided nearly the same return as the S&P 500 while having a monthly standard deviation of returns one third lower than that of the S&P 500. Feldman and Roy (2005) and Callan Associates (2006) repeated Whaley’s analysis and drew similar conclusions. These studies were limited in only analyzing a covered call on the S&P 500 Index always fully overwritten using a one-month-to-maturity ATM option. Hill et al. (2006) explored covered calls using the S&P 500 Index and one-month call options of varying strike prices. They tested dynamic strategies where the strike price was set according to the volatility of the underlying asset. They concluded by recommending, based on historical performance,

options with less than a 30 percent probability of exercise or with a strike price at least 2 percent out-of-the-money. In contrast Maidel and Sahlin (2010) found that when forming a covered call on the S&P 500 Index ATM strikes provided the best Sharpe ratios. Che and Fung (2011) performed an analysis similar to Hill et al. (2006) using Hang Seng Index futures as the underlying. They concluded that the performance of the strategies depends greatly on market conditions, and that for the Hong Kong market the dynamic strategy may provide a benefit in bullish conditions. Though several strike prices were considered, combinations of options were not explored and positions were always fully overwritten.

McIntyre and Jackson (2007) showed that from a Black-Scholes perspective selling a call option simply ought to reduce exposure to the underlying equity, but also found that covered calls using equities in the Financial Times Stock Exchange (FTSE) 100 Index in many cases outperformed their underlying equity position. No conclusions or suggestions about optimal strike prices and maturity dates were drawn, and covered calls were formed by selecting one equity from the FTSE 100 at a time and fully overwriting it by selling call options of a fixed moneyness level and maturity date. Board et al. (2000) also investigated several covered call strategies formed using the FTSE 100 Index and found that according to a wide range of utility functions the covered calls were preferable to the underlying long position. Kapadia and Szado (2007) found that a covered call overlay improved the risk-return efficiency of the Russell 2000 Index. They tested covered calls formed on the Russell 2000 fully overwritten by selling calls of a fixed maturity and moneyness level on the index. They tested various moneyness levels, and one and two month maturities, but did not draw conclusions about which moneyness levels are best. He et al. (2015) tested covered call strategies using different maturity dates and strike prices with the S&P 500 as the underlying asset. The portfolio was always fully covered and shorting combinations of options was not explored. Yang (2011) proposed a dynamic strategy which alternates between selling at-the-money calls and at-the-money puts. As puts are sometimes sold, the Yang (2011) strategy is outside the scope of a covered call, however we note that when calls are sold it is at a fixed moneyness level, i.e. at-the-money.

Although selecting the moneyness level or strike price is important in determining the potential liability of a covered call at maturity, many studies failed to consider the effect of the option market prices. Figelman (2008) aimed to build a framework for evaluating a covered

call composed of a single asset with full overwriting. He highlighted the negative relationship between the covered call return and the call risk premium (CRP). He defines the CRP as the difference between the expected call liability less the call price, normalized by dividing by the underlying asset's spot price. Figelman's analysis demonstrates the importance of considering market prices when forming covered calls. Figelman also concluded that short-dated options have lower CRPs and are therefore preferable for covered call strategies. Figelman did not make conclusions about optimal strike prices and only considered a covered call with full overwriting on a single asset.

Despite the ubiquity of optimization in investing, there has been little research regarding optimization and options relevant to covered calls. Alexander et al. (2006) examined the well posedness of CVaR and VaR optimization for a portfolio of derivatives under broad conditions. They showed that the widely used formulation of Rockafellar and Uryasev (2000) is ill posed for a portfolio of options under some conditions. The optimization of covered calls introduces many constraints making the problem dissimilar to that studied in Alexander et al. Zymler et al. (2011) formulated a worst-case optimization for a portfolio including European options. Worst-case optimization is not suitable for covered call portfolios where managing up-side liability is as important as reducing down-side risk.

1.3 Covered Calls In Practice

Billions of US and Canadian dollars are currently being managed in a vast array of exchange-traded-funds (ETFs) and mutual funds which utilize covered call strategies. Thus there is immense practical value in trying to improve the construction and performance of covered call strategies. Covered call literature has typically focused on holding a single asset with full overwriting. In contrast covered call funds are often portfolios of covered calls on multiple assets without full overwriting. Thus there is practical value in broadening the scope of covered call literature to include such cases.

Many popular covered call ETFs can effectively be thought of as covered calls on a single asset, e.g. an index or commodity. According to Global X (2019) their NASDAQ 100 Covered Call ETF aims to replicate the return of holding the NASDAQ 100 and selling a one-month-to-

maturity ATM call option each month. Similarly, according to Invesco (2019) their S&P 500 BuyWrite ETF aims to replicate the return of the CBOE S&P 500 BuyWrite Index, i.e. long S&P 500 fully overwritten by selling a one-month-to-maturity ATM call option. According to Credit Suisse (2019) the X-Links Gold Shares Covered Call ETN fully overwrites a long position in gold bullion by selling roughly 3% out-of-the-money (OTM) one-month-to-maturity call options each month. Countless additional examples can easily be found.

There are also many covered call funds which hold positions in a large number of individual securities. Some Canadian examples include series of covered call ETFs offered by Horizons, CI Financial, and Bank of Montreal. Some of their ETFs are covered call portfolios on: Canadian financial equities, Canadian materials equities, Canadian energy companies, Canadian large cap equities, US large cap equities, international large cap equities, US health care companies, US technology companies, and US financial equities. Horizons covered call ETFs currently hold up to 40 equities, occasionally rebalanced to be equally weighted, and according to Horizons (2019) fully overwritten by selling roughly 5% OTM call options with one to two months to expiry. CI Financial First Asset covered call ETFs currently hold up to 50 equities, also equally weighted, and according to CI Financial (2019) have overwriting on roughly one quarter of the underlying investments. Bank of Montreal covered call ETFs currently hold up to 90 assets, and according to Bank of Montreal (2019) have overwriting on one quarter of underlying holdings by selling one to two month to maturity options. They short options with lower strikes when volatility is low, and options further out-of-the-money when volatilities are high; this is roughly equivalent to targeting a certain probability of execution. An abundance of other funds of covered call portfolios exists.

Covered call funds are consistent with the literature in selling options with near expiry dates, e.g. less than two months to maturity. However, funds also vary wildly in their overwriting amounts and strike selection methods. Many funds also include a large number of assets, in contrast to the single asset case that has typically been studied in existing literature. In section 1.4 we will propose models which are useful for constructing covered call portfolios as they are used in practice.

1.4 Proposed Optimization of Covered Call Strategies

The main objective of this dissertation is to apply stochastic optimization to improve the construction of covered call strategies. This can be subdivided into two main goals. The first is to broaden the scope of covered call strategies by analyzing portfolios of covered calls on multiple assets, with full or partial overwriting, and with overwriting with call options of different strike prices and maturity dates. The second is to leverage operations research to improve the construction and performance of such portfolios of covered calls.

Existing studies have largely focused on covered calls on a single asset fully overwritten by selling an ATM or slightly OTM call option with a nearby maturity date. The effects of simultaneously holding covered calls on different assets, with different strike prices and maturity dates, have been unexplored. The majority of the published evidence suggests that it is preferable to sell short-dated call options (e.g. with one month to maturity), though there is no consensus regarding the strike price. Given that there is no consensus on how to best form a covered call with full overwriting on a single asset, how can we hope to provide meaningful guidance on constructing covered call portfolios of the much more general form which we propose? Despite its prevalence in investing in the last half-century, financial optimization has not yet been applied to covered call strategies. We propose several optimization models which prescribe the optimal construction of covered call strategies of a very general form to best satisfy one of two common objectives: risk-return efficiency, and expected utility maximization. By varying the return target when performing risk-return optimization, or the utility curvature when performing expected utility maximization, the proposed models can provide optimal portfolios for varying risk appetites.

Optimization may also reveal that covered calls can be beneficial from a pure return perspective, contrary to popular belief. A call option should have an arbitrage-free price computed under a risk-neutral probability measure. However, Figelman (2008) showed that the expected return of a covered call strategy is related to the expected option payoff computed under the real-world probability measure. A short call position has a positive expected return if its price exceeds its discounted expected payoff. The price is dictated by the market, but estimating the expected payoff under the real world measure is highly subjective and ultimately depends

upon an investor's world view. Consider also the existence of the volatility risk premium: the Black-Scholes implied volatility of an option's market price is typically higher than the realized volatility of the underlying asset during the option's lifetime. Kapadia and Szado (2007), Figelman (2008), Maidel and Sahlin (2010), and Che and Fung (2011) all noted the contribution of the volatility risk premium to the empirical performance of covered calls. From a Black-Scholes perspective, option market prices are generally high. The combination of high implied volatilities (market prices) and potentially low expected payoffs (under the investor's view) may suggest that some short call position has a positive expected return. If the investor's view is correct then this short position forms a covered call with an expected return larger than the underlying equity position alone. Optimization may aid in identifying and selecting such options to sell as part of a covered call strategy. In general, an important part of our models is the use of observed option market prices as an input.

We begin in chapter 2 by applying risk-return optimization to a covered call on a single asset. Since its introduction by Markowitz (1952) risk-return efficiency has formed the backbone of modern portfolio theory. We note that the current literature has analyzed the effect of various call maturity dates and strike prices. Varying the proportion of calls being sold and the possibility of shorting a combination of different calls have not been considered. We develop an optimization framework that selects quantities of calls with different strikes and common maturity dates to sell to form a covered call strategy on a given asset position. This framework is tested by forming covered calls using the S&P 500 Index to explore the risk-return profile and structure of the resulting portfolios. Return variance, semivariance, Value-at-Risk (VaR), and Conditional Value-at-Risk (CVaR) are used as risk measures. This framework is new in that it considers selling less options than units of the underlying held, it considers selling combinations of different strike prices, and it selects strike prices and quantities of options to sell based on risk-return optimality.

The work of chapter 2 is limited in considering a covered call on a single asset position. In practice there are many institutional funds which hold portfolios of covered calls using dozens of underlying assets. In chapter 3 we extend the framework of chapter 2 to optimize a portfolio of covered calls. The optimization model provides a prescriptive method of constructing covered call portfolios based on risk-return optimality using variance, semivariance, and CVaR as risk

measures. As in chapter 2 the market prices of the options are critical in modeling the expected return. Unlike the single asset model which only optimizes option positions the extended model optimizes the overwritten call options and simultaneously selects the underlying asset positions. One question we seek to answer is whether knowledge of the available call options affects the optimal equity positions. The model explores covered calls of a general form which includes the possibility of holding multiple assets, selling multiple call options of different strike prices on each asset, and having all or part of the underlying asset weights without overwriting. The model is tested by solving for portfolios with 92 US large-cap equities and several hundred options, as might be used in a practical setting.

The model of chapter 3 is limited in requiring that all options under consideration have the same maturity date. From a practical perspective an investor may want to form a covered call portfolio using the shortest dated options available, and the nearest maturities may differ across assets. For example the CBOE offers two-week-to-maturity options for the S&P 500 Index, while the shortest dated options offered for the EAFE and EM indices are one-month-to-maturity. From another perspective an investor may have conviction on the long-term behaviour of some assets but not others, and may wish to sell longer dated options where they have conviction and shorter dated options where they do not. In chapter 4 we extend the framework of chapter 3 in two ways: we augment the model with a second stage which allows the sale of call options with different maturity dates, and we generalize the objective by optimizing an expected utility. Risk-return optimization problems are not easily extensible to additional risk measures, but many popular risk measures have equivalent expected utility maximization models. Mean-variance optimization is equivalent to maximizing a quadratic utility for wealth, Estrada (2004) presents a utility model equivalent to mean-semivariance optimization, and Bassett et al. (2004) presents a utility optimization equivalent to mean-CVaR optimization. Conventional risk measures must be computed with knowledge of an entire return distribution and are not amenable to decomposition techniques. An expected utility can be modeled as the average of the utility achieved in a number of scenarios, this allows us to apply decomposition techniques to improve solution times.

Paralleling the shift from the mean-variance optimization of Markowitz (1952) to the expected utility maximization of Hanoch and Levy (1970) and finally to modern financial multi-

stage stochastic problems (an array of which can be found in Mulvey and Ziemba 1998, Zenios and Ziemba 2007, and Bertocchi et al. 2011), in chapter 4 we propose a two-stage stochastic program with recourse to maximize the expected utility of a portfolio of covered calls with mixed maturity dates. Chapter 4 emphasizes the problem of computational tractability. In contrast with the models from chapters 2 and 3, the model in chapter 4: is more general in considering covered call portfolios on multiple equities which possibly involve selling multiple options with different strike prices and maturity dates per asset, is more general in optimizing under an arbitrary payoff preference captured in the utility function, and incorporates an additional stage and rebalancing point to make better use of available market information. The model selects underlying asset weights, and quantities, strikes, and maturities of calls to sell to form optimal expected utility covered call portfolios, and allows rebalancing between stages. For testing we use 67 US large cap equities, and three utility functions popular in portfolio construction: the quadratic, negative exponential, and power utilities, but any concave (i.e. risk-averse) utility function can readily be substituted. To improve solution times we implement a progressive hedging decomposition.

Each of the models in chapters 2, 3, and 4 is presented in detail and accompanied by implementation notes, results, and analysis. In chapter 5 we provide concluding remarks and possible directions for future study.

Chapter 2

Optimizing a Single Asset Covered Call

In this chapter we propose an optimization model to construct risk-return efficient covered call strategies on a given asset position. To our knowledge this is the first application of optimization to covered call strategies in the literature. The model also solves for strategies of a more general form than has typically been studied in the literature. The model permits partial overwriting, including no overwriting (i.e. pure long equity) and full overwriting at the extremes, and permits overwriting with different strike prices. In theory, this could allow for pure long equity positions for an investor who is seeking to maximize return or in a bull market where an investor expects the asset price to rise considerably, while also allowing overwriting for risk-averse investors or in sideways or bear markets where an investor does not expect the asset price to rise.

We present the framework and test it using the S&P 500 Index as the underlying asset. A critical part of the model is the use of scenarios which we generate by assuming that the S&P 500 Index price follows the stochastic volatility with correlated jumps model of Eraker et al. (2003). We display sample results from performing risk-return optimization with variance of the return, semivariance of the return, VaR, and CVaR as risk measures.

2.1 Methodology

Suppose an investor wishes to create a covered call overlay on an existing asset position. The investor is long n units of an asset with current price S_0 . The investor can form a covered call strategy using this asset by shorting any of N_c European call options with maturity date T days away and varying strike prices. Up to n call options in total can be shorted beyond which some calls are not covered. The decision variable p is a vector of overwriting ratios where we short $p_j n$ units of call option j which has strike price k_j and best current market bid C_j . We consider only options which are not in-the-money, i.e. options whose strike prices are above the current asset price S_0 . We assume n is large enough that we can ignore the option contract size and treat p as continuous. We assume that proceeds gained from shorting the call option are invested into the risk-free asset with a constant interest rate. An alternative is to put this money against the cost of the underlying asset, but as in Figelman (2008) we find that the difference is negligible. We obtain p by solving the following optimization problem:

$$\begin{aligned} & \underset{p}{\text{minimize}} && \lambda(risk) - (1 - \lambda)\mathbb{E}(r) \\ & \text{subject to} && \sum_{j=1}^{N_c} p_j \leq 1 \\ & && 0 \leq p_j \leq 1, \quad j = 1, \dots, N_c \end{aligned}$$

Where:

- $\lambda \in [0, 1]$ represents risk aversion.
- r is the return of the covered call strategy.
- $risk$ is one of: variance of the return, semivariance of the return, Value-at-Risk (VaR), or Conditional Value-at-Risk (CVaR).

For maturity price S_T the return of the covered call is given by:

$$\begin{aligned} r &= \frac{nS_T + \eta D - nS_0 + \sum_{j=1}^{N_c} p_j n(C_j e^{r_f T} - \max(S_T - k_j, 0))}{nS_0} \\ &= \frac{S_T + \frac{\eta}{n} D - S_0 + \sum_{j=1}^{N_c} p_j (C_j e^{r_f T} - \max(S_T - k_j, 0))}{S_0} \end{aligned}$$

Where r_f is the continuously compounded risk-free rate, D is the value of the dividend paid out grown at the risk-free rate, and η is the number of units of the asset held on the dividend record date. Even if they are tractable for some price models, analytical expressions for the expected return and risk of a covered call strategy are highly non-linear and undesirable from an optimization perspective. For examples see Figelman (2008) for analytical expressions assuming geometric Brownian motion. We instead simulate the underlying asset price at maturity in scenario i , S_T^i , then formulate the sample returns r_i . The sample returns and expected return can be defined according to the following linear equality constraints, for N simulations:

$$r_i = \frac{S_T^i + \frac{\eta}{n}D - S_0 + \sum_{j=1}^{N_c} p_j(C_j e^{r_f T} - \max(S_T^i - k_j, 0))}{S_0}, \quad i = 1, \dots, N$$

$$\mathbb{E}(r) = \frac{1}{N} \sum_{i=1}^N r_i$$

We address each of the risk measures separately. The sample variance of the simulated values is given by:

$$\sigma_r^2 = \frac{1}{N-1} \sum_{i=1}^N (r_i - \mathbb{E}(r))^2$$

This formulation has a quadratic objective, which with our linear constraints can be solved rapidly even for a large number of simulations.

The sample semivariance below the risk-free rate is given by:

$$\text{semivariance} = \frac{1}{N} \sum_{i=1}^N z_i^2$$

$$-z_i \leq r_i - e^{r_f T}, \quad i = 1, \dots, N$$

$$z_i \geq 0, \quad i = 1, \dots, N$$

The latter sets of constraints ensure that $z_i = \min(r_i - e^{r_f T}, 0)$, i.e. that positive deviations are set to zero. An investor can easily replace the risk-free rate with their own specified level. As for variance, this leads to a quadratic optimization problem.

Suppose we are interested in optimizing VaR_α . In general this poses a significant challenge

as it may lead to a non-convex problem. In our case, since there is only one source of uncertainty which is the maturity price of the underlying asset, the problem is greatly simplified. Suppose we rearrange the index i of the simulated values S_T^i so that the simulated prices at maturity $S_T^1 \dots S_T^N$ are sorted from smallest to largest. In appendix A we show that the return is a monotonically increasing function of the asset price at maturity S_T . Thus, if the simulated asset values are sorted, i.e. $S_T^1 \leq S_T^2 \leq \dots \leq S_T^N$, then the sample return values must also be sorted, i.e. $r_1 \leq r_2 \leq \dots \leq r_N$. Suppose that the number of simulations, N , is chosen such that $(1 - \alpha)N$ is an integer. Then we can directly obtain the $(1 - \alpha)$ quantile of returns by looking at r_i where the index $i = (1 - \alpha)N$. Since the sample VaR_α is the α quantile of sample losses, we must multiply the $(1 - \alpha)$ quantile of sample returns by negative one to convert to a loss:

$$\text{VaR}_\alpha = -r_{(1-\alpha)N}$$

Similarly, if we know the sample returns are sorted, $r_1 \leq r_2 \leq \dots \leq r_N$, then the sample CVaR_α is given by averaging the $(1 - \alpha)N$ lowest returns and multiplying by negative one to convert to a loss:

$$\text{CVaR}_\alpha = \frac{-1}{(1 - \alpha)N} \sum_{i=1}^{(1-\alpha)N} r_i$$

Numerical examples of the implementation of VaR and CVaR are given in section 2.3.

In appendix B we show that all constraints for all risk measures are linear, that sample VaR and CVaR have linear objective functions, and that sample variance and semivariance have quadratic objective functions. Additionally, in appendix C we show that the quadratic objectives are convex, so that minimizing them is tractable. All formulations are thus of the simplest classes of optimization problems, namely quadratic and linear programs. These formulations are rapidly solvable even for large numbers of available call options and large numbers of simulations.

2.2 Policy Structure

To understand the structure of the optimal policy we consider the case of minimal risk aversion, $\lambda = 0$. The objective is then to maximize the expected return.

Theorem 1. *Maximizing the expected return of a covered call strategy on a given asset position is equivalent to minimizing the call risk premium of options sold.*

Proof. By substituting the simulated return values into the expected return the problem becomes:

$$\underset{\sum p_j \leq 1, p \geq 0}{\text{maximize}} \quad \frac{1}{N} \sum_{i=1}^N \frac{S_T^i + \frac{\eta}{n} D - S_0 + \sum_{j=1}^{N_c} p_j (C_j e^{r_f T} - \max(S_T^i - k_j, 0))}{S_0}$$

Ignoring constants gives:

$$\begin{aligned} & \underset{\sum p_j \leq 1, p \geq 0}{\text{maximize}} \quad \frac{1}{N} \sum_{i=1}^N \frac{\sum_{j=1}^{N_c} p_j (C_j e^{r_f T} - \max(S_T^i - k_j, 0))}{S_0} \\ & \underset{\sum p_j \leq 1, p \geq 0}{\text{maximize}} \quad \frac{\sum_{j=1}^{N_c} p_j (C_j e^{r_f T} - \frac{1}{N} \sum_{i=1}^N \max(S_T^i - k_j, 0))}{S_0} \end{aligned}$$

For large N the simulated mean call payoff is approximately equal to the expectation:

$$\begin{aligned} & \underset{\sum p_j \leq 1, p \geq 0}{\text{maximize}} \quad \frac{\sum_{j=1}^{N_c} p_j (C_j e^{r_f T} - \mathbb{E}(\max(S_T^i - k_j, 0)))}{S_0} \\ & \underset{\sum p_j \leq 1, p \geq 0}{\text{maximize}} \quad \sum_{j=1}^{N_c} -p_j \text{CRP}_j \end{aligned}$$

□

The coefficient of p_j , the future value of the call price minus the expected call payoff as a fraction of the asset price, is the negative of the call risk premium (CRP) defined in Figelman (2008) for option j . Maximizing the expected return is equivalent to minimizing the CRP of options sold. If according to our simulations the risk premia of all available calls are positive then $p = 0$, selling no options, maximizes the expected return. If there is a call with a negative

risk premium then $p_j = 1$ maximizes the expected return where option j has the lowest CRP. In theory, the CRP should always be positive since investors expect to be compensated for risk. However, as noted in Figelman (2008), implied volatility has often been higher than realized volatility. This implies that some options had negative risk premiums and were effectively overpriced.

Selling calls produces a liability which reduces up-side returns and provides a premium that increases down-side returns. Call options with high premiums and low strike prices provide the largest down-side benefit and largest up-side liability making them most effective in minimizing risk. Therefore, to minimize variance, semivariance, VaR, or CVaR, it is optimal to set $p_j=1$ where option j has the lowest strike price of the options available. Thus, if we are not considering options which are in-the-money, a sufficiently risk averse investor always ought to sell the maximum amount of ATM options.

All risk measures lead to the same optimal solution in the case of either minimal or maximal risk aversion. From an analytical perspective it is not clear what the optimal mix should be for intermediate risk aversion settings. However, it is clear that the balance between risk and return is equivalent to the balance between minimizing risk and minimizing the CRP of options sold. Intermediate risk aversion cases are explored experimentally for all four risk measures under consideration.

2.3 Implementation

We use the S&P 500 index as the underlying asset of our covered call for the period from 1996 to 2014.

To utilize our formulation we must produce simulations of the S&P 500, this requires a model for the price path. Eraker et al. (2003) argue that, versus a number of alternatives, their stochastic volatility with correlated jumps (SVCJ) model best explains the price path of the S&P 500 index in their examined time period of 1980 to 1999. The SVCJ model is similar to vanilla geometric Brownian motion for prices but with a few additional features. Volatility is modelled as a mean reverting stochastic process which has noise which is negatively correlated to noise in the return. There are positive jumps in volatility which are negatively correlated

with jumps in returns. This is consistent with market dynamics; in times of stress there are sharp increases in volatility and large drops in price.

Figelman (2009) shows that compared to geometric Brownian motion the SVCJ model produces similar expected call payoffs for ATM and near the money options, but may produce significantly different expected call payoffs (and thus CRPs) for further out-of-the-money options. Following Figelman (2009) we employ the SVCJ model using the parameter estimates provided for the S&P 500 in Eraker et al. (2003). We adjust the parameter estimate of μ from the SVCJ model so that the expected annual return matches the long run historical average return of the S&P 500 of about 6.5% annually. We do not adjust the volatility parameters as the expected volatility of 16% annually is close to the long run historical volatility.

While the SVCJ model holds strong explanatory power, it may not hold strong predictive power beyond the time period for which the parameters were calibrated. We employ the model and parameter estimates from Eraker et al. (2003) for the purposes of examining the structure of optimal covered calls. In practice an investor seeking performance should employ a predictive model and should continually update their estimates using newly available information. An investor can readily substitute maturity prices simulated according to their preferred price model into our formulations.

We adjust some parts of our optimization formulation to account for the effectively continuous dividends of the S&P 500. The return of the S&P 500 gross of dividends, S_T^G , was modelled as the return of the S&P 500 index plus a logarithmic return of $7E-5$ per day. This is consistent with the approximately 2% annual return provided by dividends. Where S_T appears outside of the call settlement formula, it is replaced with S_T^G and the dividend D is set to zero. The constraint for return r_i becomes:

$$r_i = \frac{S_T^{Gi} - S_0 + p(Ce^{r_f T} - \max(S_T^i - k, 0))}{S_0}, \quad i = 1, \dots, N$$

All other constraints and objectives were unchanged and implemented as presented in section 2.1.

We closely follow the methodology used to construct the CBOE BuyWrite Index with a few noted differences. Call option data was obtained from OptionMetrics which only provides

closing prices. Thus, the call premium was taken to be the best closing bid. Lastly, we consider only out-of-the-money options, thus the option with the lowest strike price above the current asset price was taken as the at-the-money option. Each month on the dates where the BuyWrite Index shorts the at-the-money call (the date on which the previous call expires) we instead perform our optimization over all available out-of-the-money (OTM) options to solve for optimal overwriting ratios. Since we are only considering one month maturity dates, the 30 day US treasury rate is used as the risk-free rate.

Each formulation used $N = 10,000$ simulations of the asset price at maturity. For all risk measures this creates 10,000 variables and equality constraints to model r_i . For semivariance this produces an additional 10,000 variables and inequality constraints to model z_i . Additional variables are required for the overwriting ratios of the available options, usually less than fifty. One additional constraint is required to ensure that the sum of overwriting ratios does not exceed one. Lastly one constraint is required to define the expected return variable. Since the scenario return variables r_i and the expected return variable $\mathbb{E}(r)$ are defined by linear equality constraints, it is possible to eliminate them from the formulation by substituting them with their defining expressions. In practice there is no motivation for doing so since such variables introduce very little overhead from an efficiency perspective. All formulations were implemented and solved using CPLEX.

When optimizing VaR and CVaR we select $\alpha = 95\%$. Before optimizing, we rearrange the arbitrary index i of the simulated asset prices at maturity S_T^i so that the prices are arranged in ascending order as described in section 2.1. Since $N = 10,000$, $\text{VaR}_{95\%}$ is given by $-r_{500}$. Similarly, $\text{CVaR}_{95\%}$ is given by multiplying the average of the 500 worst cases by negative one, i.e. $\frac{-1}{500} \sum_{i=1}^{500} r_i$.

2.4 Results

In all tested cases the solution time using CPLEX did not exceed one second. The production of efficient frontiers of 20 to 30 points usually required less than 10 seconds.

For minimal and maximal risk aversion the optimal solution follows the predicted policy structure. We find that for intermediate risk aversion there is a non-trivial optimal mix involving

several options in most months. Example efficient frontiers and optimal mixes for all risk measures can be seen in figure 2.1. The left endpoints of the frontiers correspond to high risk aversion. On the left sides of the mix charts we see that for high risk aversion it is optimal to sell the maximum number of ATM calls. The right endpoints of the frontiers correspond to maximizing the expected return. We see in the mix charts that for low risk aversion or risk-neutrality it was optimal in this example to sell the maximum amount of the 9.4% OTM option, i.e. the option whose strike price was 9.4% higher than the asset's price at the time it was sold. This is because the 9.4% OTM option had a negative simulated CRP value which was lowest among all options examined in this particular month. The existence of this slightly negative CRP allows us to achieve a slightly greater expected return than the long position, as seen in the frontiers. When using vanilla geometric Brownian motion to simulate the underlying instead of the SVCJ model, we found portfolio structures similar to figure 2.1.

In the literature there is no consensus on how to best select strike prices of options to sell. Our methodology selects strike prices of options to sell based on risk-return optimality. Intermediate risk aversion values lead us to sell a blend of the ATM, 1.5% OTM, 2.4% OTM, 8.1% OTM, and 9.4% OTM options. Although there were many other options which could have been sold in this month the optimal mixes contain only these five. In this particular month these options were more efficient from a risk-return perspective than others due to their low CRP values.

Although the current literature has only examined covered calls where a single call option is sold in a one to one ratio to the underlying asset, our results suggest that from a risk-return perspective it is often optimal to sell combinations of call options with different strike prices for intermediate risk aversion. This result is relevant since in practice investors tend to have intermediate risk aversion since maximum return portfolios might have excessively high risk while minimum risk portfolios might provide very poor returns.

We observe that the sample mixes resulting from optimizing semivariance, VaR, and CVaR are all similar, but differ substantially versus variance. This is likely since the first three are all down-side risk measures, while the latter penalizes up-side deviations. The differences in mix observed in figure 2.1 highlight the importance of deciding between variance and a down-side risk measure given that covered call returns are highly asymmetrical.

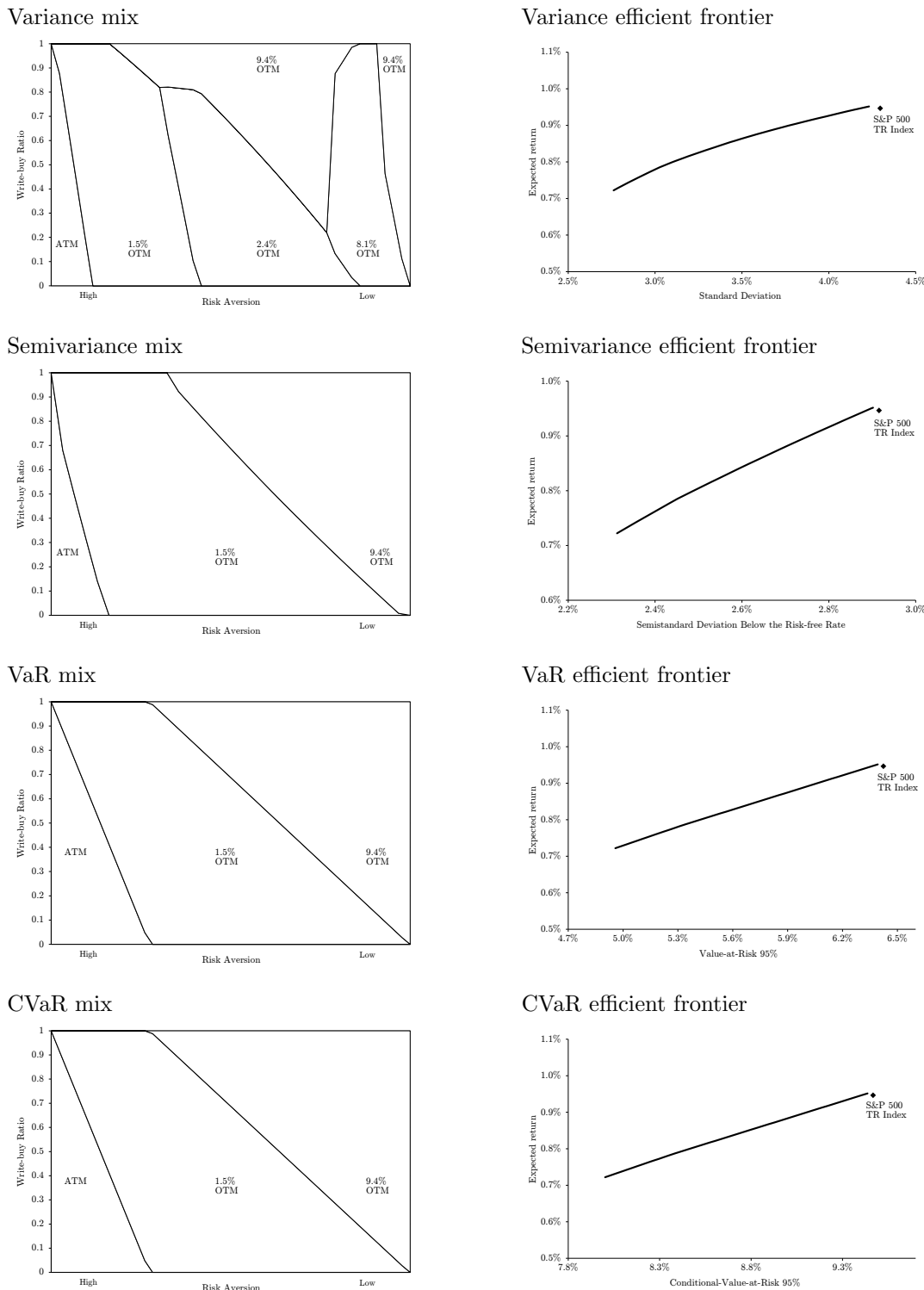


Figure 2.1: Sample optimal mixes and frontiers for different risk measures on a given single asset position.

The optimal mixes for VaR and CVaR in figure 2.1 are identical. This is a general phenomena which stems from our choice of $\alpha = 95\%$ and our choice not to consider selling in-the-money options. In the 95th percentile of losses and beyond none of the options under consideration were in the money. Thus, any improvement to the VaR gained by selling an option and not incurring a liability was also an improvement to the CVaR. Conversely, any improvement to the CVaR also caused an improvement to the VaR. Thus, the problems of optimizing VaR and CVaR for $\alpha = 95\%$ were identical and led to identical mixes. This would not hold if there were any options that were in-the-money at the α percentile of losses but still out-of-the-money in worse scenarios which are included in the calculation for CVaR. This could occur if a lower value of α were selected, if in-the-money options were considered for sale, or if the price model simply produced scenarios such that the α percentile of losses contained in-the-money options.

2.5 Conclusion

For all tested risk measures we find that from a risk-return perspective it is often optimal to sell a mix of options with different strike prices. This stands in contrast to previous literature which had only examined covered calls with one option shorted with an overwriting ratio of one. While the literature has not reached a consensus on how to select the strike prices of the options to be sold, our methodology selects strike prices and quantities on the basis of risk-return optimality. We have shown that a sufficiently risk averse investor ought to sell the full amount of ATM calls as in the BuyWrite index in order to minimize the risk measures under consideration, while a risk-neutral investor need only concern themselves with assessing the CRP of available options in order to maximize expected return. The methodology can be used to obtain optimal risk-return covered calls in the nontrivial case of intermediate risk aversion. The optimization formulations have few constraints and are thus easy to implement. Since all constraints are linear and the objectives are linear or quadratic they are rapidly solvable for all risk measures considered. In this chapter we have considered optimizing covered calls as an overlay to an existing position in a single asset. In the next chapter we build upon this framework by simultaneously optimizing covered calls for multiple assets as well as their underlying positions.

Chapter 3

Optimizing a Portfolio of Covered Calls

In chapter 2 we developed an optimization framework to select calls (i.e. strike prices, since the maturity date was fixed at one month) to sell to form a covered call strategy on a single long asset position. The framework of chapter 2 is limited to optimizing a covered call overlay on an existing equity position, and almost all studies reviewed in chapter 1 only examined covered calls using a single equity position. Although there are a number of single position (e.g. an index or commodity) covered call funds in practice, there are also many covered call funds which hold positions in a large number of individual securities. These include the Bank of Montreal US High Dividend Covered Call Fund (see Bank of Montreal 2018), the BlackRock Enhanced Capital and Income Fund (see BlackRock 2018), and the Manulife Covered Call US Equity Fund (see Manulife 2018). For these types of funds we propose an integrated approach where underlying asset positions and overwritten call options are simultaneously optimized.

In this chapter we extend the framework of chapter 2 to optimize a portfolio of covered calls. The extended optimization model produces risk-return efficient covered call portfolios using variance, semivariance, and CVaR as risk measures. As in chapter 2 the market prices of the options form a critical part of the model. The extended framework simultaneously optimizes long asset positions and short call positions. One question we seek to answer is whether knowledge of the available call options affects the optimal equity positions. The extended model

permits covered calls of a very general form which includes the possibility of holding multiple assets, selling multiple call options of different strike prices on each asset, and having all or part of the underlying asset weights without overwriting. Previous studies examined covered calls using a single asset typically fully overwritten with a single call option. Another question we seek to answer is whether risk-return efficient covered call portfolios exploit the general form we propose, i.e. with partial overwriting and overwriting using different strike prices on a single asset, as they did in chapter 2.

The remainder of the chapter is laid out as follows: in section 3.1 the general framework is developed and presented, section 3.2 examines the optimal call overwriting policy from an analytical perspective, section 3.3 details implementation of the model, section 3.4 analyzes sample results when using three indices as the underlying, section 3.5 analyzes how the model scales to solving portfolios with 92 US large-cap equities and several hundred options as it might be used in a practical setting, and section 3.6 analyzes possible improvements to performance versus conventional covered call strategies.

3.1 Methodology

Suppose an investor wishes to create a covered call portfolio using up to n available assets. The investor has W total wealth and spends w_j wealth on each asset j . If the current price of asset j is S_{0j} then the investor purchases $x_j = w_j/S_{0j}$ units of asset j . We assume no shortselling of the underlying assets. To form a covered call the investor can sell up to x_j total units of n_j available one-month European call options for asset j . We assume all options under consideration have the same maturity date. Letting p_{jl} denote the number of units of call option l sold for asset j , the relationships are summarized below.

$$\begin{aligned} W &= \sum_{j=1}^n w_j \\ x_j &= \frac{w_j}{S_{0j}} \quad \text{for } j = 1, \dots, n \\ \sum_{l=1}^{n_j} p_{jl} &\leq x_j \quad \text{for } j = 1, \dots, n \end{aligned}$$

These constraints are linear since the market price of the assets is known. Assuming the premiums from shorted calls are invested in the risk-free rate, at the maturity date in T days the investor's wealth is given by:

$$W_T = \sum_{j=1}^n x_j (S_{Tj} + D_j) + \sum_{j=1}^n \sum_{l=1}^{n_j} p_{jl} (C_{jl} e^{r_f T} - \max(S_{Tj} - k_{jl}, 0))$$

Where D_j is the value of any dividend paid out by asset j grown at the risk-free rate, C_{jl} and k_{jl} are the current market price and strike price of call option l for asset j respectively, r_f is the risk-free rate, and S_{Tj} is the price of asset j at the maturity date. Without loss of generality we can set the total wealth W to 1. We then interpret w_j as the proportion of each dollar of wealth invested into asset j , x_j as the number of units of asset j purchased for each dollar of wealth, and p_{jl} as the number of units of call option l for asset j sold for each dollar of wealth. We assume that the total wealth is large enough such that w_j , x_j , and p_{jl} are effectively continuous. The return of the portfolio at the maturity date is given by:

$$r = \frac{W_T}{W} - 1 = \sum_{j=1}^n x_j (S_{Tj} + D_j) + \sum_{j=1}^n \sum_{l=1}^{n_j} p_{jl} (C_{jl} e^{r_f T} - \max(S_{Tj} - k_{jl}, 0)) - 1$$

Risk-return optimization finds the optimal tradeoff between the expected value of r and some risk measure of the distribution of r . Deriving analytical expressions for these quantities would require multiple integrals over the joint distribution of the underlying assets. Whether such integrals would be tractable depends on the assumed underlying joint distribution and the chosen risk measure. Even if solutions were obtainable the resulting expressions would likely be impractical from an optimization perspective. For example, Figelman (2008) derived analytical expressions for the expected return, variance of the return, and semivariance of the

return for a covered call on a single asset by assuming a log-normal distribution for returns. The resulting expressions are highly nonlinear and convoluted, and they are only relevant if a log-normal distribution is assumed. Instead of seeking analytical expressions we propose using the sample expected return and sample risk based on a number of simulated scenarios. From an optimization perspective the simulated scenarios are constants, thus we can readily input values produced using any distribution or method which we like.

If we simulate values of S_{Tj} for all assets j then the return is linear in the decision variables x and p . Thus, for each simulation i we can capture the return in this scenario, r_i , using linear constraints:

$$r_i = \sum_{j=1}^n x_j (S_{Tj}^i + D_j) + \sum_{j=1}^n \sum_{l=1}^{n_j} p_{jl} (C_{jl} e^{r_f T} - \max(S_{Tj}^i - k_{jl}, 0)) - 1 \quad \text{for } i = 1, \dots, N$$

The sample expected return is given by a linear constraint, where N is the total number of simulations:

$$\mathbb{E}(r) = \frac{1}{N} \sum_{i=1}^N r_i$$

The sample variance is given by:

$$risk = \sigma_r^2 = \frac{1}{N-1} \sum_{i=1}^N (r_i - \mathbb{E}(r))^2$$

This formulation has a quadratic objective, which with our linear constraints can be solved rapidly even for a large number of simulations.

The sample semivariance below the risk-free rate is given by:

$$risk = semivariance = \frac{1}{N} \sum_{i=1}^N z_i^2$$

$$z_i \leq r_i - (e^{r_f T} - 1) \quad \text{for } i = 1, \dots, N$$

$$z_i \leq 0 \quad \text{for } i = 1, \dots, N$$

The latter sets of constraints ensure that $z_i = \min(r_i - (e^{r_f T} - 1), 0)$, i.e. that positive deviations are set to zero. As for variance, this leads to a quadratic optimization problem. Though

we choose the risk-free rate as the target, a different reference point can readily be substituted, e.g. $\mathbb{E}(r)$ to optimize the sample semivariance below the expected return.

The sample CVaR $_{\alpha}$ of the simulated returns can be optimized using the following formulation from Rockafellar and Uryasev (2000):

$$\begin{aligned} \min \quad & q + \frac{1}{N(1-\alpha)} \sum_{i=1}^N z_i \\ z_i \geq -r_i - q, \quad & \text{for } i = 1, \dots, N \\ z_i \geq 0, \quad & \text{for } i = 1, \dots, N \end{aligned}$$

The objective function provides the sample CVaR $_{\alpha}$. Alexander et al. (2006) show that the Rockafellar and Uryasev (2000) formulation may be ill posed for portfolios of options. In particular, there may be multiple optimal or near optimal solutions when the feasible set is defined only by the budget constraint and an expected return constraint. Our own formulation has a vastly different feasible set and produces stable results.

Using the expressions presented thus far, we have formulations of risk-return covered call optimization for variance, semivariance, and CVaR. Risk is minimized while the expected return is constrained to exceed a target:

Variance optimization:

$$\underset{w,x,p,\mathbb{E}(r),r}{\text{minimize}} \quad \frac{1}{N-1} \sum_{i=1}^N (r_i - \mathbb{E}(r))^2$$

Semivariance optimization:

$$\underset{w,x,p,\mathbb{E}(r),r,z}{\text{minimize}} \quad \frac{1}{N} \sum_{i=1}^N z_i^2$$

CVaR optimization:

$$\underset{w,x,p,\mathbb{E}(r),r,z,q}{\text{minimize}} \quad q + \frac{1}{N(1-\alpha)} \sum_{i=1}^N z_i$$

Common constraints:

$$\begin{aligned} w_j &\geq 0 \quad \text{for } j = 1, \dots, n \\ p_{jl} &\geq 0 \quad \forall j, l \\ \sum_{j=1}^n w_j &= 1 \\ \frac{w_j}{S_{0j}} - x_j &= 0 \quad \text{for } j = 1, \dots, n \\ -x_j + \sum_{l=1}^{n_j} p_{jl} &\leq 0 \quad \text{for } j = 1, \dots, n \\ \sum_{j=1}^n \sum_{l=1}^{n_j} p_{jl} (C_{jl} e^{r_f T} - \max(S_{Tj}^i - k_{jl}, 0)) \\ + \sum_{j=1}^n x_j (S_{Tj}^i + D_j) - r_i &= 1 \quad \text{for } i = 1, \dots, N \\ \mathbb{E}(r) - \frac{1}{N} \sum_{i=1}^N r_i &= 0 \\ -\mathbb{E}(r) &\leq -r_{target} \end{aligned}$$

Additional constraints for semivariance optimization:

$$\begin{aligned} z_i - r_i &\leq -(e^{r_f T} - 1) \quad \text{for } i = 1, \dots, N \\ z_i &\leq 0 \quad \text{for } i = 1, \dots, N \end{aligned}$$

Additional constraints for CVaR optimization:

$$\begin{aligned} -r_i - z_i - q &\leq 0 \quad \text{for } i = 1, \dots, N \\ z_i &\geq 0 \quad \text{for } i = 1, \dots, N \end{aligned}$$

All constraints are linear. Additionally, the CVaR objective function is linear. The variance and semivariance objectives are convex, quadratic functions.

It must now be noted that the chosen risk measures are not without limitations. Generally, since the sale of call options limits return on the up-side, the return distribution of a covered call strategy has a significant negative skew. Therefore variance of the return is not an appropriate risk measure for a covered call investor who has a preference towards skewness. Nonetheless we have included variance due to its ubiquity in asset management. Figelman (2008) suggested using semivariance to focus on down-side cases and address the problem of skewness. One problem with semivariance is that it is defined relative to an arbitrary point, e.g. semivariance below the risk-free rate. A better choice still may be CVaR which is widely used in asset management and simply averages returns in the worst scenarios. It is intuitive to understand and also addresses the problem of skewness.

Even semivariance and CVaR are limited risk measures in that they only capture preferences of the lower tail end of the return distribution. Since we are considering a portfolio composed of covered calls on numerous assets with varied correlations, it isn't clear what distribution the resulting portfolio's return will have. A covered call portfolio's return distribution is likely highly irregular with high order moments involved. An investor could very well have preferences regarding higher moments beyond just the left tail portion of the return distribution. In this case CVaR and semivariance would not suffice. One possible solution may be to use a utility function and maximize the expected utility of the return rather than optimize the risk-return tradeoff, a topic which we leave for future work. Later we discuss a structured solution policy which results from all risk measures under consideration. Though exact solutions may differ, we expect that the structured policy also exists when using other risk measures or maximizing an expected utility.

3.2 Policy Analysis

When performing risk-return optimization it is common practice to solve for portfolios along the entire risk spectrum. At one extreme this involves finding the largest expected return target,

r_{target} , for which the problem remains feasible. This is done by maximizing the expected return and ignoring the portfolio's risk level.

Under the constraints listed in section 3.1, it is possible to analytically derive the optimal policy to maximize the expected return. Consider the expected return:

$$\begin{aligned}\mathbb{E}(r) &= \sum_{i=1}^N \frac{1}{N} r_i \\ \mathbb{E}(r) &= \sum_{i=1}^N \frac{1}{N} \left(\sum_{j=1}^n \sum_{l=1}^{n_j} p_{jl} (C_{jl} e^{r_f T} - \max(S_{Tj}^i - k_{jl}, 0)) + \sum_{j=1}^n x_j (S_{Tj}^i + D_j) - 1 \right)\end{aligned}$$

Substituting x_j with its defining expression:

$$\mathbb{E}(r) = \sum_{i=1}^N \frac{1}{N} \left(\sum_{j=1}^n \sum_{l=1}^{n_j} p_{jl} (C_{jl} e^{r_f T} - \max(S_{Tj}^i - k_{jl}, 0)) + \sum_{j=1}^n w_j \frac{(S_{Tj}^i + D_j)}{S_{0j}} - 1 \right)$$

Rearranging the summation order and simplifying:

$$\mathbb{E}(r) = \sum_{j=1}^n \sum_{l=1}^{n_j} p_{jl} \left(C_{jl} e^{r_f T} - \sum_{i=1}^N \frac{1}{N} (\max(S_{Tj}^i - k_{jl}, 0)) \right) + \sum_{j=1}^n w_j \frac{(\sum_{i=1}^N \frac{1}{N} (S_{Tj}^i) + D_j)}{S_{0j}} - 1$$

For a sufficiently large number of simulations N the sample averages are approximately equal to expectations:

$$\mathbb{E}(r) = \sum_{j=1}^n \sum_{l=1}^{n_j} p_{jl} (C_{jl} e^{r_f T} - \mathbb{E}(\max(S_{Tj} - k_{jl}, 0))) + \sum_{j=1}^n w_j \frac{(\mathbb{E}(S_{Tj}) + D_j)}{S_{0j}} - 1$$

The difference between the expected call payout at the maturity date and the call price grown at the risk-free rate is the call risk premium (CRP) as defined in Figelman (2008):

$$\begin{aligned}\text{CRP}_{jl} &= \mathbb{E}(\max(S_{Tj} - k_{jl}, 0)) - C_{jl} e^{r_f T} \\ \text{CRP}_{jl} &= \sum_{i=1}^N \frac{1}{N} \max(S_{Tj}^i - k_{jl}, 0) - C_{jl} e^{r_f T} \\ \mathbb{E}(r) &= \sum_{j=1}^n \sum_{l=1}^{n_j} p_{jl} (-\text{CRP}_{jl}) + \sum_{j=1}^n w_j \frac{(\mathbb{E}(S_{Tj}) + D_j)}{S_{0j}} - 1\end{aligned}\tag{3.1}$$

Now consider the problem of maximizing the expected return; we may ignore variables and constraints related to modeling risk:

$$\begin{aligned}
 & \underset{w,p}{\text{maximize}} \quad \mathbb{E}(r) = \sum_{j=1}^n \sum_{l=1}^{n_j} p_{jl}(-\text{CRP}_{jl}) + \sum_{j=1}^n w_j \frac{(\mathbb{E}(S_{Tj}) + D_j)}{S_{0j}} - 1 \quad (3.2) \\
 & \text{subject to} \quad \sum_{j=1}^n w_j = 1 \\
 & \quad w_j \geq 0 \quad \text{for } j = 1, \dots, n \\
 & \quad p_{jl} \geq 0 \quad \forall j, l \\
 & \quad \sum_{l=1}^{n_j} p_{jl} \leq \frac{w_j}{S_{0j}} \quad \text{for } j = 1, \dots, n
 \end{aligned}$$

Since we are only interested in maximizing the expected return, the problem above is applicable to all risk measures. Consider the problem of selecting p for fixed asset weights w . The expression involving w in the objective function is then constant and can be ignored:

$$\begin{aligned}
 & \underset{p}{\text{maximize}} \quad \sum_{j=1}^n \sum_{l=1}^{n_j} p_{jl}(-\text{CRP}_{jl}) \\
 & \text{subject to} \quad p_{jl} \geq 0 \quad \forall j, l \\
 & \quad \sum_{l=1}^{n_j} p_{jl} \leq \frac{w_j}{S_{0j}} \quad \text{for } j = 1, \dots, n
 \end{aligned}$$

Since for $j \neq k$ the variables p_{jl} and p_{kl} do not share any constraints and do not interact in the objective function, the problem above can be decomposed into n subproblems. We can examine the subproblem of finding p_{jl} for each asset j individually:

$$\begin{aligned}
 & \underset{p}{\text{maximize}} \quad \sum_{l=1}^{n_j} p_{jl}(-\text{CRP}_{jl}) \\
 & \text{subject to} \quad p_{jl} \geq 0 \quad \text{for } l = 1, \dots, n_j \\
 & \quad \sum_{l=1}^{n_j} p_{jl} \leq \frac{w_j}{S_{0j}}
 \end{aligned}$$

The solution to the subproblem is evident. We find option l which has the lowest CRP amongst the available options for asset j . If the CRP of this option is negative, the solution is to set p_{jl}

to its maximum value of w_j/S_{0j} and all other variables to 0. If all options have a positive CRP then the solution is to set all variables to zero, i.e. no call overwriting on asset j . The value of the objective function at optimality is therefore:

$$\left(\underset{p}{\text{maximize}} \quad \sum_{l=1}^{n_j} p_{jl}(-\text{CRP}_{jl}) \right) = \frac{w_j}{S_{0j}} (-\min(\text{CRP}_{j1}, \dots, \text{CRP}_{jn_j}, 0))$$

For convenience, we use V_j to denote the minimum of the CRP of all available options for asset j and 0:

$$\begin{aligned} \min(\text{CRP}_{j1}, \dots, \text{CRP}_{jn_j}, 0) &= V_j \\ \left(\underset{p}{\text{maximize}} \quad \sum_{l=1}^{n_j} p_{jl}(-\text{CRP}_{jl}) \right) &= \frac{w_j}{S_{0j}} (-V_j) \end{aligned} \tag{3.3}$$

We know that for any given value of w_j we should follow the optimal policy for p_{jl} derived above and obtain the return benefit shown in (3.3). Therefore, the objective of problem (3.2) becomes:

$$\begin{aligned} \underset{w}{\text{maximize}} \quad \mathbb{E}(r) &= \sum_{j=1}^n \sum_{l=1}^{n_j} p_{jl}(-\text{CRP}_{jl}) + \sum_{j=1}^n w_j \frac{(\mathbb{E}(S_{Tj}) + D_j)}{S_{0j}} - 1 \\ &= \sum_{j=1}^n \frac{w_j}{S_{0j}} (-V_j) + \sum_{j=1}^n w_j \frac{(\mathbb{E}(S_{Tj}) + D_j)}{S_{0j}} - 1 \\ &= \sum_{j=1}^n w_j \frac{(\mathbb{E}(S_{Tj}) + D_j - V_j)}{S_{0j}} - 1 \end{aligned} \tag{3.4}$$

If w is only constrained by the budget constraint $\sum w_j = 1$, upper bound constraints $w_j \leq U_j$, and no shortselling, then to maximize expected return we place as much weight as possible into w_j which has the largest coefficient in (3.4) until it reaches its upper bound, then place as much weight as possible into w_j which has the second largest coefficient in (3.4), and so on until the budget constraint is binding. The coefficient of w_j in (3.4) assumes that after w has been decided the optimal policy for p_{jl} will be followed, i.e. for each asset j we look for the option with the lowest CRP as defined in (3.1); if the lowest CRP is negative then the option is sold in the maximum amount (w_j/S_{0j}), if the lowest CRP is positive we do not overwrite calls

on asset j .

Many arguments can be made that CRP values ought to be positive. Figelman (2008) assumed that CRP values should be positive if the underlying equity has a positive equity risk premium. McIntyre and Jackson (2007) show that from a Black-Scholes perspective holding a call is equivalent to holding some portion of the underlying equity, which presumably ought to have a positive risk premium. A long call option position is risky, so a purchaser may expect to be compensated for accepting that risk. However, a short call position is also extremely risky for the seller who may incur potentially unlimited losses. It isn't clear why a seller would be willing to accept this risk without expecting a risk premium themselves. Market prices contain some evidence that option prices may favour sellers. It has been empirically observed that the implied volatility by assuming that option prices follow the Black-Scholes model is frequently higher than the realized volatility of the underlying asset. This suggests that from a Black-Scholes perspective, i.e. if assets have log-normally distributed returns, options may be overpriced. Figelman (2009) argued that the volatility premium still existed in the presence of non-normality. If an option is overpriced its CRP would be negative and there would be an expected return benefit for a seller and an expected loss for a buyer. It is important to note that the call risk premiums as computed in this methodology in (3.1) are dependent on the inputted scenarios. As such, the particular method used to produce the scenarios could also lead to erratic CRP estimates.

Though we have derived the optimal policy for the risk-neutral goal of maximizing the expected return, it is not clear what the optimal policy is for a risk-averse investor. Regardless of the asset positions, we expect the optimal minimum risk portfolios to involve selling at-the-money (ATM) options, or selling in-the-money (ITM) options if they are under consideration. Further in-the-money options reduce variance and down-side risk by providing larger premiums, and also reduce variance by more severely restricting up-side gain.

3.3 Implementation

We test the methodology by using the S&P 500 Index, the Morgan Stanley Capital International (MSCI) Europe, Australasia and Far East (EAFE) Index, and the MSCI Emerging Markets

(EM) Index as underlying assets. We form covered call portfolios by selling call options on these assets. Following the findings of other authors, we consider only options with a one month maturity date which tend to have the highest implied volatility. We consider only options which are ATM or out-of-the-money (OTM) at the time the optimization is performed. In practice an investor may wish to include ITM options as they may be appropriate to sell given a bearish outlook. Historical data is limited since exchange-traded European call options for the EAFE and EM indices were only introduced by the Chicago Board Options Exchange (CBOE) in April 2015. Call option data for May 2015 to August 2015 was obtained from OptionMetrics. Data for September 2015 to May 2016 was obtained via Bloomberg. As bid-ask spreads were often large, we used the average of the best bid and best ask prices as the market price of an option; in practice an investor should be careful to use values which they believe best predict the execution price. The optimization is conducted once a month on the day which the previous month's options expired. The 30 day US Treasury Bill rate is used as the risk-free rate.

In order to use the methodology we must simulate asset prices at maturity. According to Figelman (2009), the expected return of far out-of-the-money options may be poorly estimated by using standard geometric Brownian motion versus a more realistic process. In chapter 2 we utilized a stochastic volatility with correlated jumps (SVCJ) model for stock returns and found that optimal covered call positions were similar when using the SVCJ model and classic geometric Brownian motion. We again use geometric Brownian motion for the purposes of examining the structure of covered call portfolios.

We simulate asset values at maturity by simulating multivariate standard normal variables, $Z^i = (Z_1^i, Z_2^i, Z_3^i)$, with correlation equal to that of the log returns of the three underlying assets. These values are then used to simulate asset prices at maturity via geometric Brownian motion, for asset j and scenario i :

$$S_{Tj}^i = S_{0j} e^{(\mu_j - 0.5\sigma_j^2)T + \sigma_j \sqrt{T} Z_j^i}$$

Values of μ and σ used reflect the long term return and volatility of the three assets, summarized in table 3.1. While we have used these simulations for illustrative purposes, in practice an investor should simulate asset prices which they believe best predict the behaviour of the

Asset	Annualized Return	Annualized Volatility	Annual Dividend Rate
S&P 500	6.5%	16%	2.2%
EAFE	6.1%	15.5%	3.4%
EM	7.3%	18%	2.7%

Table 3.1: Drift and volatility rates used for simulation. Dividend rates used in optimization.

underlying assets; a wealth of literature already exists in this topic.

We optimize using $N = 15,000$ simulations which we find is sufficiently large to produce consistent results. All problems were solved using CPLEX. Optimization of CVaR is a linear program and utilized the CPLEX simplex method. Optimization of semivariance and variance are quadratic programs and utilized the CPLEX quadratic simplex method.

3.4 Results

Sample results are shown in figure 3.1 for the month of August 2015; optimal solutions showed complex structures as in figure 3.1 for most months tested. We find that production of efficient frontiers of 50 points generally takes 2 to 3 minutes for variance and CVaR optimization, and 5 to 6 minutes for semivariance optimization.

As expected, the maximum return portfolio is the same across all risk measures for any given month. The result in figure 3.1 for the maximum return portfolio matches our prediction from section 3.2. All options for the S&P 500 and EAFE have positive CRP estimates, thus from an expected return perspective it is optimal not to overwrite either of these assets. The 13% OTM option has the lowest estimated CRP amongst all EM options, and this estimate is negative. The greatest expected return for an EM position therefore occurs when the position is fully overwritten using this call option. Since a long EM position overwritten with the 13% OTM call has the greatest expected return, the optimal solution from an expected return perspective is to put as much weight as possible into this combination. This matches the empirical result seen in figure 3.1.

The optimal mixes for all three risk measures prominently feature EM. It has often been noted that risk-return optimization using point estimates for the risk and expected return produces concentrated portfolios which are sensitive to the input values. Because EM has

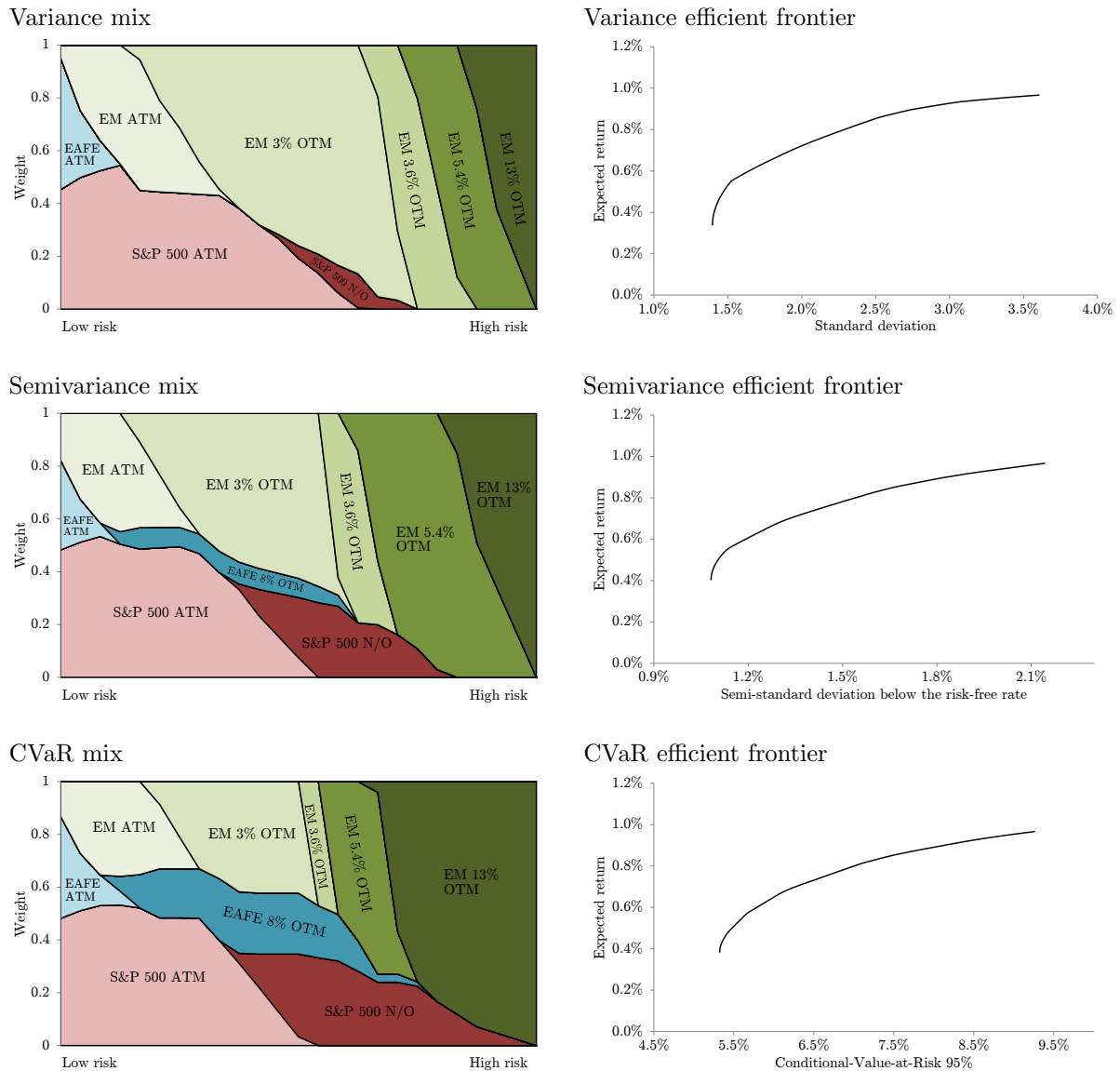


Figure 3.1: Sample optimal mixes and frontiers for different risk measures. Areas simultaneously indicate asset weights and call overwriting weights. "N/O" indicates that an asset was held but some of its units were not overwritten. All values are monthly.

a slightly higher expected total return in table 3.1, it has a very large portfolio weight at higher expected return targets. One way to combat this sensitivity is to perform resampled optimization, for example as in the Resampled Efficient Frontier in Chapter 6 of Michaud and Michaud (2008). In short, we produce multiple optimal mixes using resampled estimates of the data in table 3.1 and blend the resulting mixes. The resampling and blending procedures are described in detail in appendix D.

An alternative to Michaud resampling is distributionally robust stochastic optimization (DSRO, see Gao and Kleywegt 2016 for details). In standard stochastic optimization a quantity (e.g. risk) is optimized over a distribution of random variables (e.g. asset returns). In DSRO a quantity is optimized over the worst case distribution from a set of distributions. Michaud resampling blends the solutions from optimizing over a set of distributions one distribution at a time. Compared to Michaud resampling DSRO is conceptually more complex and difficult to implement, this may preclude its usefulness in a practical asset management setting. Furthermore there is an existing precedent for the use of Michaud resampling; it is widely used and well known in portfolio management. Because Michaud resampling optimizes using a range of distributions it can provide insight into optimal solutions across a wide range of input parameters.

The resulting mix from Michaud resampling for August 2015 is shown in figure 3.2. We observe in figure 3.2 that all minimum risk portfolios continue to overwrite exclusively with ATM options. This is intuitive since ATM options provide the largest premiums to counter down-side losses and the largest liabilities against up-side gain (given that ITM options are not under consideration). These facts do not change when resampling since the premiums and strike prices are fixed. However, the blended maximum return portfolio differs substantially from the concentrated portfolio in figure 3.1. Whereas previously EM had the highest total expected return leading to a concentrated position, there are resampling cases where the S&P 500 or EAFE offer the highest expected total return. This leads to some resampling cases where the maximum return portfolio has a concentrated position in S&P 500 or EAFE. When blended these lead to the maximum return weights seen in the resampled optimal mix; approximately 0.46 in EM, 0.28 in S&P 500, and 0.26 in EAFE. These weights can be interpreted as the probability that each asset (and its corresponding optimal call overwrite) has the highest expected

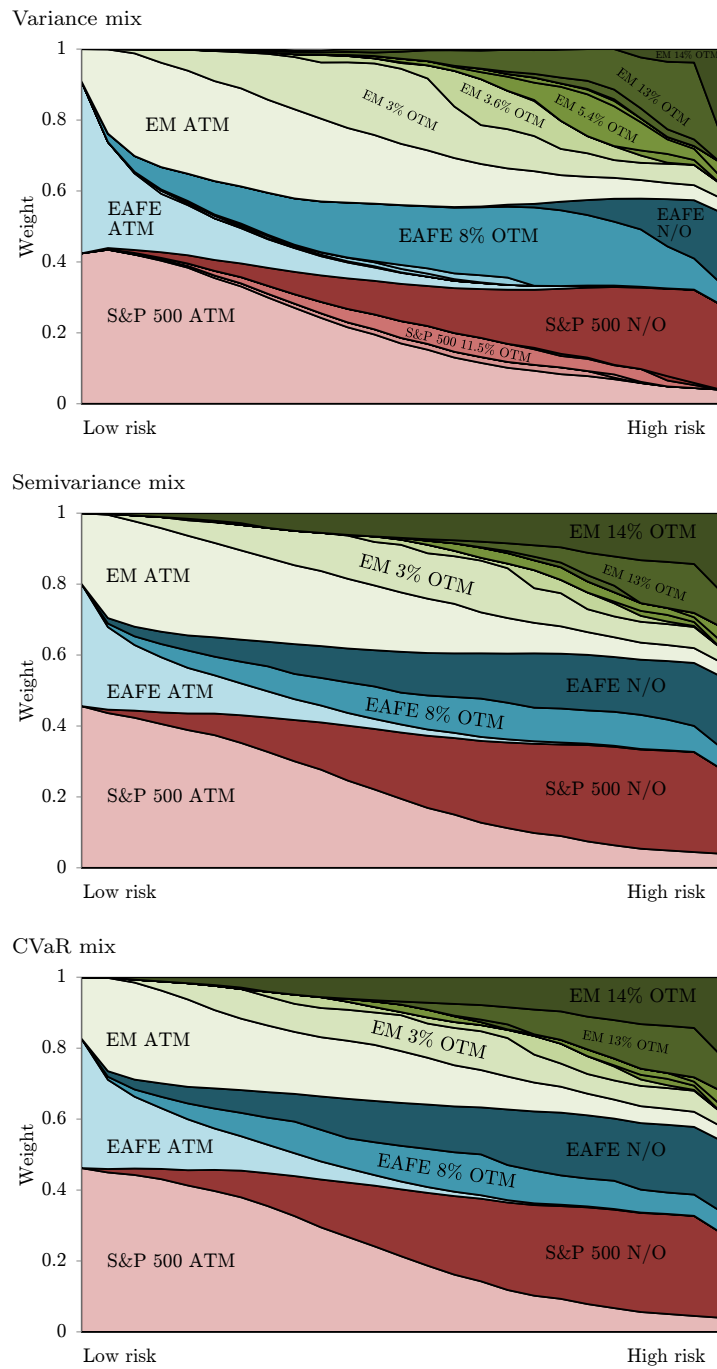


Figure 3.2: Sample optimal mixes for different risk measures using Michaud resampling. Areas simultaneously indicate asset weights and call overwriting weights. "N/O" indicates that an asset was held but some of its units were not overwritten.

total return according to the view reflected in our estimates in table 3.1 and our degree of confidence implicit in the resampling scheme.

Aside from the underlying asset weights, the resampling of the expected return and risk also creates diversity in the optimal call overwriting positions. The resampled parameters cause changes to the expected call payoffs at maturity, these in turn effect changes to the CRP estimates. Thus optimal call positions differ between resampling iterations. We still observe that some call options are never sold. This is likely because other options consistently offered more attractive risk-return tradeoffs.

The results of Michaud resampling demonstrate that optimal covered call portfolios are sensitive to assumptions about the expected return and volatility of the underlying assets. Another assumption we have made is that the underlying asset prices follow geometric Brownian motion. We test the sensitivity of the results to the shape of the underlying distributions by rerunning the results from figure 3.2 assuming a GARCH(1,1) model for the assets' volatilities (see appendix E for details). When using geometric Brownian motion with constant volatilities the resulting distribution of log-returns is of course normal with no skewness and kurtosis of 3. When using the GARCH driven volatilities skewness remains negligible but substantial kurtosis is produced; the kurtosis of the resulting distributions of log-returns of the S&P 500, EAFE, and EM indices are 3.8, 3.3, and 4.1 respectively. The resulting optimal mixes shown in figure 3.3 differ moderately from those in figure 3.2. It appears that the results are less sensitive to changes in kurtosis than to changes in the first or second moments. Another possibility is that geometric Brownian motion with GARCH volatility is not sufficiently irregular to accurately model the higher moments of the underlying asset returns.

3.5 Scaling

A commercial covered call fund may have many more than three assets. To examine how the formulation scales we test it on individual equities. For the test we select the largest 5, 10, 20, 40, 60, and 92 equities in the S&P 500 Index by market capitalization. Since exchange traded options on these assets are only offered with American exercise style, data for European options on these assets is unavailable. As a proxy we use American option prices for these assets; the

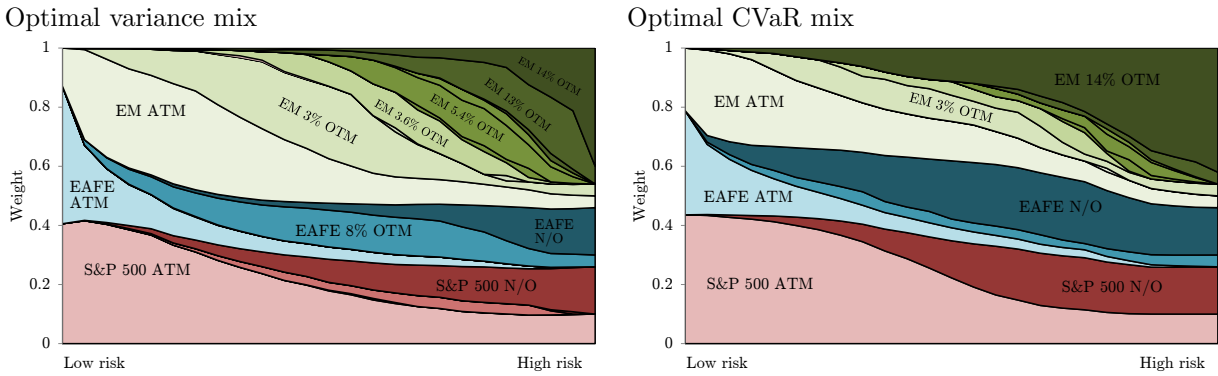


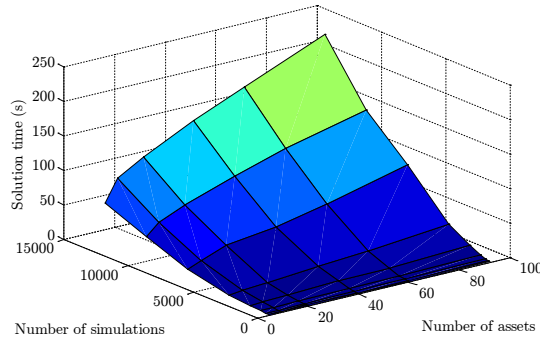
Figure 3.3: Sample optimal mixes for different risk measures using Michaud resampling and GARCH volatility. Areas simultaneously indicate asset weights and call overwriting weights. "N/O" indicates that an asset was held but some of its units were not overwritten. Results for semivariance are omitted as they closely resemble those of CVaR.

call price is taken as the highest closing bid. To avoid arbitrage the price of an American style option must always be higher than any immediate payout from exercising it. Thus American options are rarely executed before their maturity date and can readily be used as a substitute to European options in a covered call strategy.

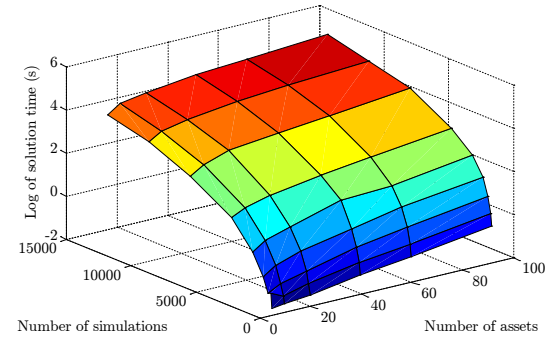
The expected returns and volatilities of the equities were estimated using one year of historical data leading up to the beginning of the sample period. We use these estimates only to analyze the structure of optimal covered calls. In practice a manager should carefully estimate the distributions which they believe best reflect the behaviour of assets for the time period under consideration; an abundance of literature exists on this subject. Simulations are produced as in section 3.3. We vary the number of simulations from 100 to 12800. As the number of assets and simulations increases, the times to produce efficient frontiers grow as shown in figure 3.4. Although semivariance solution times become extremely large, variance and CVaR solution times remain viable.

Sample solution results for the month of August 2015 are shown in figure 3.5. The 92 assets had a total of 702 call options available to sell, for comparison the S&P 500, EM, and EAFE indices had a total of 72 call options available to sell in the same month. Using point estimates without further constraints again leads to concentrated positions, and we again use Michaud resampling to optimize portfolios of the 92 assets. As in section 3.4 this leads to an enormous variety of assets and call options in the optimal portfolios, but this time the number of positions

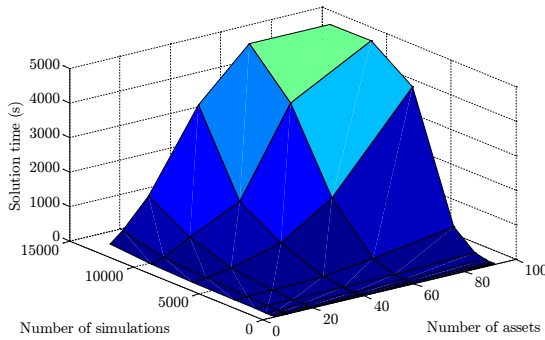
Variance solution times



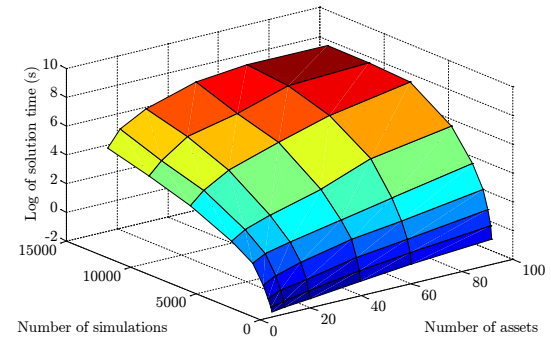
Log of variance solution times



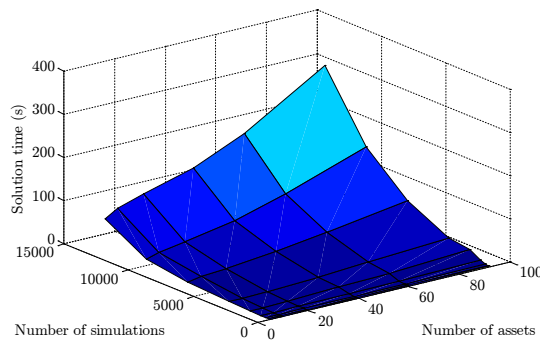
Semivariance solution times



Log of semivariance solution times



CVaR solution times



Log of CVaR solution times

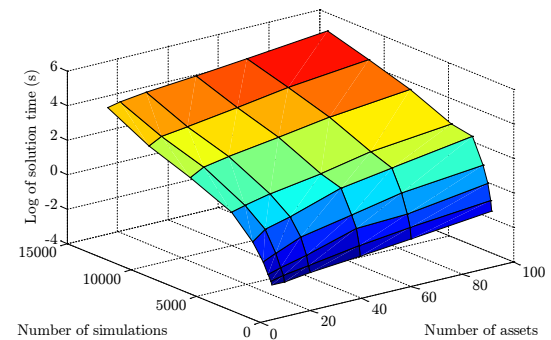


Figure 3.4: Solution times for different risk measures varying the number of assets and simulations. Data points represent the mean time to produce an efficient frontier of 50 points for 9 trial months. Solution times were capped at 5,000 seconds.

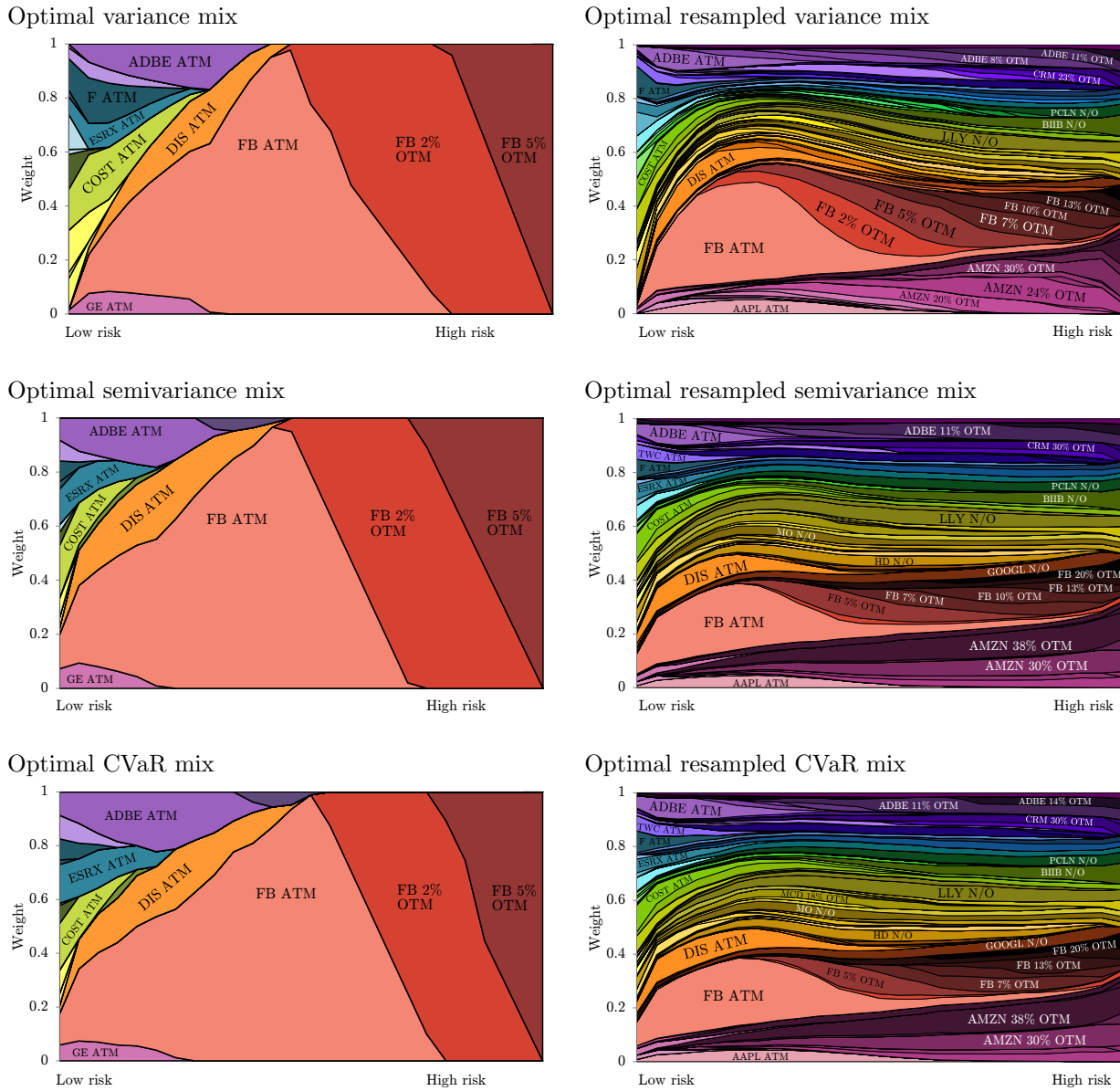


Figure 3.5: Optimal portfolios mixes using 92 large-cap US equities in August 2015. Major positions are labelled. Left without resampling, right with Michaud resampling. Areas simultaneously indicate asset weights and call overwriting weights. "N/O" indicates that an asset was held but some of its units were not overwritten.

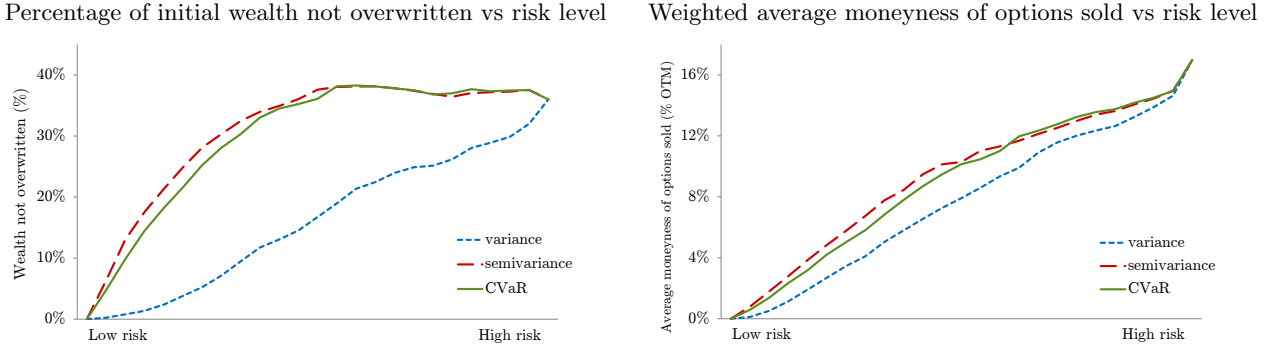


Figure 3.6: Both charts display information relating to the resampled portfolios in figure 3.5. The left chart displays the percentage of wealth without call option overwriting as a function of portfolio risk. The right chart displays the average moneyness of options sold as a function of portfolio risk. The average moneyness is weighted by the amount of wealth overwritten by each option.

may be problematic. In the worst case one of the variance optimized portfolios holds 52 equities and sells 230 different call options, far too many option positions for practical use. However, many positions are very small; over 95% of the wealth is overwritten with just 65 options. Thus some rounding may be all that is needed to produce a portfolio with a practical number of positions while still being nearly optimal.

In figures 3.5 and 3.6 we observe a structured policy where to minimize risk all assets are fully overwritten with ATM options. At this end of the risk spectrum we ought to simply seek the options with the lowest strike prices and thus the highest market prices, the other portion of the CRP estimate (the expected call payoff) is irrelevant. As risk-averseness decreases the amount of wealth overwritten drops, and the options sold have higher strike prices, lower expected payoffs, and likely lower CRP estimates. Finally, a risk-neutral investor should seek to sell only the options with the lowest estimated CRP values (those thought to be the most overpriced). The maximum return portfolio still features 64% of all wealth overwritten. This indicates that CRP estimates were negative across a wide range of expected return and volatility inputs. We also note that the optimal portfolios frequently hold equity weight without overwriting, and sell multiple options with different strike prices on a single asset. Previous studies had typically assumed that the equity position is fully overwritten using a single call option.

In all cases tested we found that semivariance and CVaR optimized portfolios were nearly identical, unsurprising since they are both down-side risk measures. We recommend using CVaR

instead since using semivariance requires longer solution times and offers no clear advantage. When using a point estimate for the expected return and volatility, we find that over 10,000 simulations are needed to produce consistent results. However, when using resampling we find 2,000 simulations per each of the 50 resampling iterations is sufficiently large to produce consistent results. Since the solution time scales rapidly as a function of the number of simulations this means that solving for stable resampled frontiers is faster than solving for stable results using point estimates. I.e., for a given risk measure, solving for one frontier using 15,000 simulations is far slower than solving for 50 frontiers using 2,000 simulations each, even when these frontiers are not optimized in parallel.

3.6 Performance

In practice covered calls are sometimes formed as an overlay on an existing equity portfolio. However, a covered call portfolio constructed by optimizing the underlying asset positions then applying a short call overlay is not risk-return optimal in general. The sample results in figure 3.7 suggest that to form a risk-return optimal covered call portfolio it is necessary to simultaneously optimize the call overwriting weights and the underlying asset positions. The top row of figure 3.7 displays optimal equity mixes when call options are not under consideration. A covered call overlay could then be applied to these fixed portfolios. The resulting covered call strategies from this two-step process differ substantially from the optimal mixes shown in the middle and bottom rows of figure 3.7 where equity and option positions were optimized simultaneously. When call options are not included, the optimal portfolio weights are well diversified over the available assets. However, using data from December 2014 when calls are included in the optimization much of the equity weight shifts to a handful of assets. In this particular month these assets had ATM call options trading at relatively high market prices, thus, selling these calls and holding the assets created a very attractive covered call position. In order to form risk-return optimal covered call portfolios, asset positions must sometimes be selected to exploit the market prices of available call options. This is only possible when call positions and underlying asset positions are optimized simultaneously. It isn't necessarily the case that the presence of call options dramatically alters the optimal equity positions. The

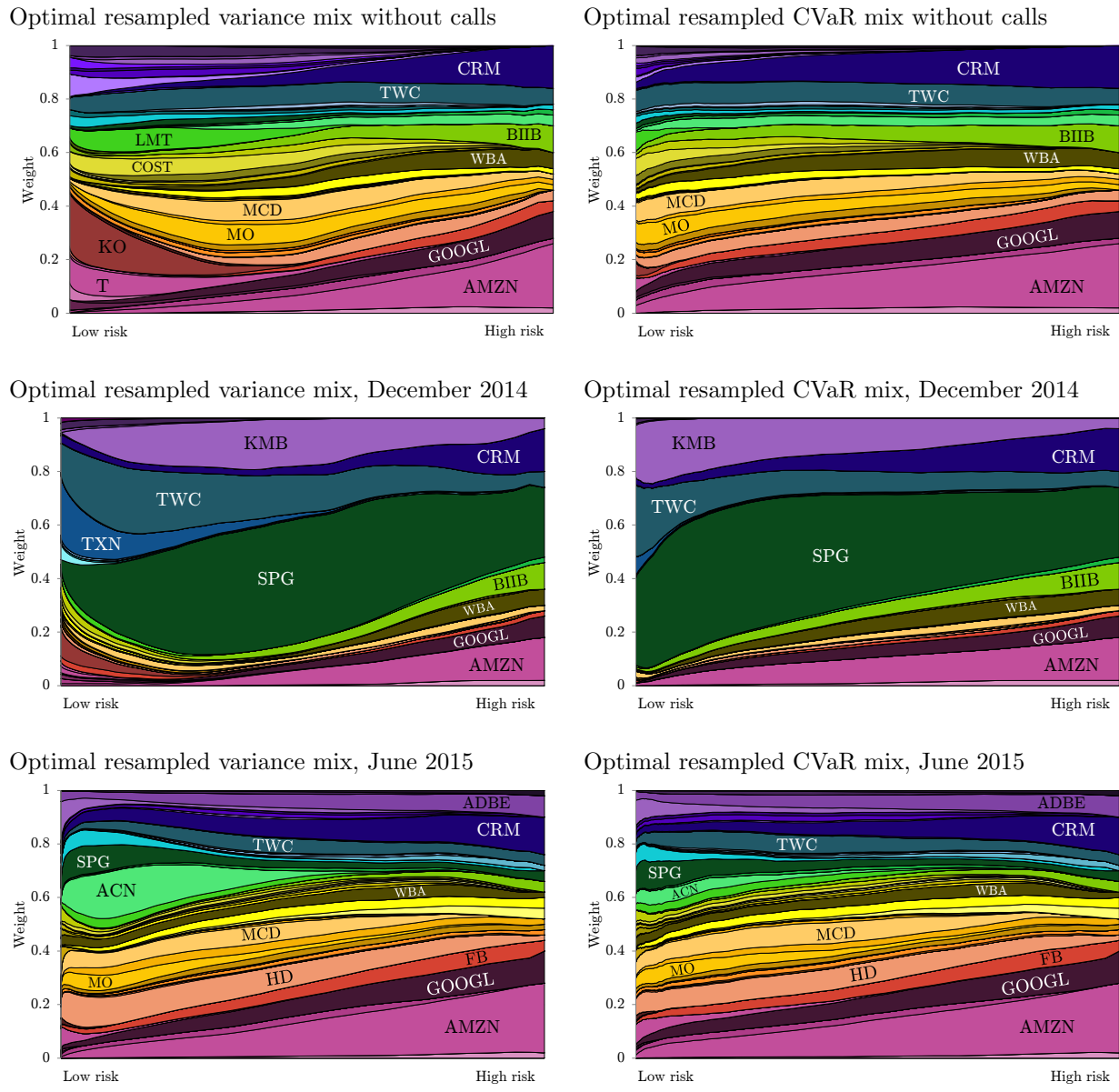


Figure 3.7: Optimal equity mixes using 92 large-cap US equities. Major positions are labelled. Top row optimized without options available, middle and bottom rows optimized using the options available in December 2014 and June 2015 respectively. Note that for clarity call overwriting weights are not shown, only the underlying equity weights are displayed. Results for semivariance are omitted as they closely resemble those of CVaR.

Strategy:	Optimized covered call	Optimized covered call, equity only	ATM Overlaid	5% Overlaid	OTM Overlaid	10% Overlaid	OTM Overlaid	Optimized equity, no overlay
Total return:	28.8%	28.0%	9.9%	15.9%	18.5%	18.5%	24.1%	

Table 3.2: Realized returns of sample portfolios. Overlay portfolios are short call positions overlaid on the optimized equity portfolio. Total return is the sum of realized monthly returns over the nine month sample period.

equity positions of the optimal covered call portfolios in June 2015 resemble the positions when equities were optimized alone.

We can also compare the performance of the optimized covered call portfolios versus the optimal equity only portfolios with call overlays applied. We form three conventional call strategies by taking the optimal equity portfolios and fully overwriting it with ATM calls, 5% OTM calls, and 10% OTM calls in each month. The actual moneyness of options sold varies around these targets since the offered strike prices have discrete increments. In each of the nine sample months we select the optimized covered call and conventional covered call portfolios which provide the maximum in-sample expected return and evaluate their out-of-sample realized return at maturity one month later. The total returns over the nine month sample period are displayed in table 3.2. For reference, we have also included the total return of the equity positions of the optimized covered call portfolios and the total return of the optimized equity portfolio without a covered call overlay. About 4% of the difference in total return between the optimized and conventional covered calls is accounted for by the difference in equity positions, the remainder of the differences are due to the option positions. The conventional overlays which targeted a level of moneyness all produced significant liabilities. Covered calls are not usually thought to improve returns except perhaps on a risk adjusted basis. However, as Figelman (2008) notes and as we demonstrated in section 3.2, a short call option's contribution to the expected return is given by the negative of its CRP. The CRP is defined as the expected liability at maturity less the price of the option grown at the risk free rate until maturity. Forming a covered call overlay based on a fixed moneyness level ignores the information provided by the options' market prices. This could lead to selling options which generally have unfavourable prices and could reduce the expected and realized returns as in

table 3.2. In contrast, our optimization model uses the option market prices as an input, and to maximize returns sells options that are suspected to have a negative CRP based on the views implicit in the simulation scheme. We see in table 3.2 that the option positions in the optimal covered call strategy added about 80 basis points of total return versus the underlying equity position over the nine month sample period. This provides evidence that calls with negative call risk premiums exist, and that selling call options can provide an increase to expected return if selected carefully. Over the nine month period, the optimal covered call portfolios sell options over a wide range of moneyness. This suggests that negative CRP estimates do not occur at a specific moneyness level. Though we have only tested the maximum expected return portfolios, the optimization model ought to significantly improve out-of-sample risk-return efficiency by identifying options which offer a disproportionately large reduction to risk via their selling premium (the market price) versus their potential liability. Additional data and more extensive testing is required to understand the out-of-sample risk and return characteristics of optimized covered call portfolios versus conventional covered calls.

3.7 Conclusion

Covered call portfolios formed by overlaying short option positions on an existing portfolio are not optimal in general, and conventional strategies which sell options at a fixed level of moneyness fail to consider the impact of the options' market prices. Our risk-return optimization framework is able to simultaneously select underlying asset positions and call option overwriting weights to produce optimal covered call portfolios. An essential part of the model is the use of the options' market prices in order to assess risk and return, as in chapter 2. When optimizing variance and semivariance the model is quadratic, while when optimizing CVaR the model is linear. Thus the models are easy to implement and can be solved by a wide range of commercial solvers. We find that the model scales without major difficulty to portfolios using 92 assets and over 500 call options. In all cases we find that solutions from optimizing semivariance closely resemble solutions from optimizing CVaR. Optimal portfolio mixes generally exhibit a structured policy where a sufficiently risk averse investor should only overwrite using ATM options and as they become less risk averse should sell further OTM options and gradually decrease

the amount of wealth being overwritten. We find that optimal portfolios often involve holding equity positions without call overwriting and overwriting an equity position with more than one call option. This contrasts previous studies which typically considered covered calls composed of a single asset fully overwritten with a single call option and agrees with findings from the single asset model of the previous chapter. In many cases we find that the solution of resampled frontiers involves a significant amount of overwriting even when attempting to maximize the expected return. This suggests that there are some call options which have prices higher than their expected liabilities according to a wide range of views. In the next chapter we extend the model yet again to permit the sale of options with different maturity dates and under an arbitrary payoff preference.

Chapter 4

Two-stage Optimization of Covered Calls

In chapters 2 and 3 we used optimization models to produce risk-return efficient covered call portfolios. The model of chapter 3 simultaneously selects asset positions and overwritten call positions of varying strikes and quantities, however it requires that all options under consideration have the same expiry date. From a practical perspective an investor may want a covered call portfolio with short calls of different maturity dates simply because options on the underlying assets have different maturity dates. From another perspective an investor may have conviction on the behaviour of some asset on a longer or shorter term than another asset, and may only wish to sell options expiring over the period where they have conviction. We extend the model of chapter 3 in two ways: we augment the model with a second stage which allows the sale of call options with different maturity dates, and we generalize the objective by optimizing an expected utility. The risk-return frameworks of the last two chapters are not easily extensible to additional risk measures. In contrast it is straightforward to model the sample expected utility of wealth in a number of scenarios for an arbitrary utility function. This allows us to optimize any arbitrary payoff preference and allows us to apply decomposition techniques to improve solution times.

We propose a two-stage stochastic program to maximize the expected utility of a portfolio of covered calls with mixed maturity dates. At the beginning of the first stage a combination of

options maturing at the end of the first stage and second stage may be sold. At the end of the first stage asset positions can be rebalanced and additional short call positions can be selected. The objective is to maximize the expected utility of wealth at the end of the two stage time horizon. We test using three functions popular in portfolio construction; the quadratic utility, the negative exponential utility, and the power utility, but any concave utility function can readily be substituted. The model is tested using 67 large cap US equities, which we assume follow geometric Brownian motion with GARCH volatilities. The optimization is scenario based as in the previous chapters, and when producing scenarios we employ moment matching so that sample returns match nominal first and second order moments. This moment matching aids in reducing the number of scenarios required to obtain stable results. In order to improve solution times we use the progressive hedging decomposition of Rockafellar and Wets (1991).

The main goals of this chapter are: to investigate the computational tractability of a two-stage covered call model, to observe the structure of covered call portfolios when optimizing an expected utility, and to investigate the use of mixed maturity dates in covered call strategies. In section 4.1 we present the two-stage covered call utility optimization model, in section 4.2 we discuss the model's implementation, in section 4.3 we present and analyze sample results, and in section 4.4 we apply a progressive hedging decomposition.

4.1 Methodology

We pose a two-stage formulation to maximize the expected utility of a portfolio of covered calls with mixed maturity dates. The full formulation and list of symbols is available in appendix F. The formulation here has explanations interspersed.

Suppose an investor would like to form a portfolio of covered calls using up to n available assets by selling a mix of call options which mature in either T_1 days or $T_1 + T_2$ days. We assume that short option positions are held until maturity. This covered call portfolio can be formed by optimizing the expected utility of wealth after $T_1 + T_2$ days. To do this we propose a two-stage scenario based stochastic program, the form of which is shown graphically in figure 4.1. The model has constraints, variables, and constants associated with three distinct dates. At time zero there are decision variables which define the initial portfolio, constants which define

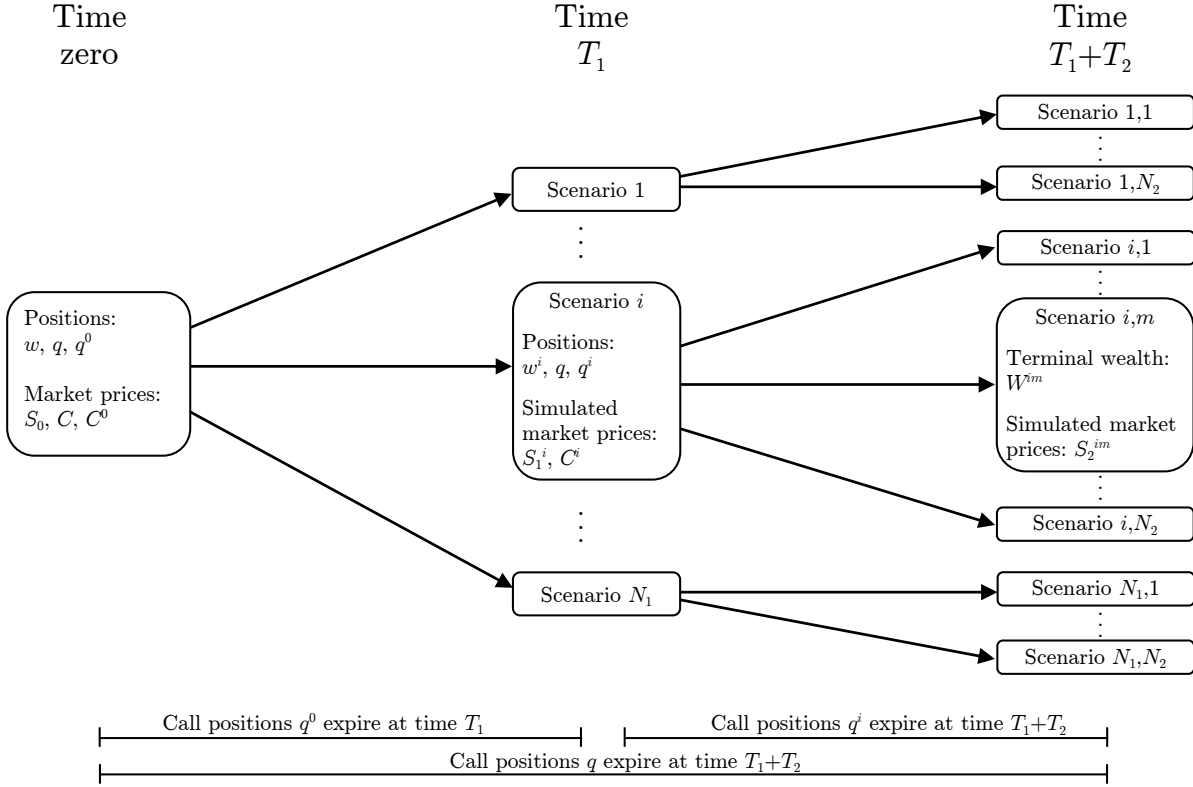


Figure 4.1: A tree representation of the problem's structure. Prominent decision variables and constants are labeled.

the observed market state, constraints which define the portfolio budget, and constraints which prohibit the sale of naked call options. From time zero to T_1 there are N_1 branches which define the possible scenarios at time T_1 , at this time the shorter-dated call options expire. For each scenario i at time T_1 there are decision variables which define a rebalanced portfolio, constants which define the state of the market, constraints which define the budget based on the market state, and constraints which prohibit the sale of naked call options. For each scenario i at time T_1 there are N_2 branches which define the possible scenarios at time $T_1 + T_2$. At this time all remaining call options expire. The terminal wealth in each scenario im at time $T_1 + T_2$ is modelled through a constraint based on the scenario's market state. The problem objective is taken to be the sample expectation of the utility of the terminal wealth across all scenarios at time $T_1 + T_2$.

We now present the model in detail. Let w_j denote the proportion of initial wealth invested in asset j at time zero. Only long equity positions are permitted, and all wealth must be

invested:

$$w_j \geq 0 \quad \text{for } j = 1, \dots, n \quad (4.1)$$

$$\sum_{j=1}^n w_j = 1 \quad (4.2)$$

Covered calls are formed by taking short call option positions. Suppose that at time zero there are n_j^0 available call options on asset j of varying moneyness but with a common maturity date at the end of the first stage in T_1 days. Suppose that at time zero there are also n_j available call options on asset j with a common maturity date at the end of the second stage in $T_1 + T_2$ days. We let q_{jl}^0 denote the proportion of initial wealth overwritten by selling option l on asset j with maturity date T_1 at time zero, similarly we let q_{jl} denote the proportion of initial wealth overwritten by selling option l on asset j with maturity date $T_1 + T_2$ at time zero. Only short call positions are permitted:

$$q_{jl} \geq 0 \quad \forall j, l \quad (4.3)$$

$$q_{jl}^0 \geq 0 \quad \forall j, l \quad (4.4)$$

The number of units of call options sold on asset j cannot exceed the number of units of asset j held, i.e. the sale of naked call options is not permitted:

$$\sum_{l=1}^{n_j} \frac{q_{jl}}{S_{0j}} + \sum_{l=1}^{n_j^0} \frac{q_{jl}^0}{S_{0j}} \leq \frac{w_j}{S_{0j}} \quad \text{for } j = 1, \dots, n$$

The use of the inequality sign permits a long equity position with partial overwriting or without a call overlay at all. On the right-hand side dividing w_j by the price of asset j at time zero, S_{0j} , provides the number of units of asset j purchased per unit of initial wealth. Similarly, dividing q_{jl} by S_{0j} produces the number of units of option l on asset j sold per unit of initial wealth. The constraint can of course be simplified by removing the common denominator:

$$\sum_{l=1}^{n_j} q_{jl} + \sum_{l=1}^{n_j^0} q_{jl}^0 \leq w_j \quad \text{for } j = 1, \dots, n \quad (4.5)$$

The above constraint can be interpreted as constraining the proportion of initial wealth overwritten by selling options on asset j not to exceed the proportion of initial wealth invested in asset j .

Obtaining an analytical expression for the expected utility of a portfolio of covered calls is likely impossible, regardless of the chosen utility function or the multivariate distribution assumed to produce the asset returns. Instead we may approximate the expected utility by the sample average of the portfolio's realized utility in a number of scenarios. This method is widely known as sample average approximation (SAA). Shapiro et al. (2009) proves in section 5.8.1 that the sample average converges with probability one to the true objective function as the number of scenarios goes to infinity.

Suppose that there are N_1 simulations of the asset prices at the end of the first stage, T_1 days after time zero. Shorted option positions denoted by q_{jl}^0 mature at this time. We define the wealth in each scenario i and set it equal to the budget for the second stage:

$$\begin{aligned} \sum_{j=1}^n \sum_{l=1}^{n_j^0} \frac{q_{jl}^0}{S_{0j}} (C_{jl}^0 e^{r_f T_1} - \max(S_{1j}^i - k_{jl}^0, 0)) \\ + \sum_{j=1}^n \frac{w_j}{S_{0j}} (S_{1j}^i + D_{1j}) = \sum_{j=1}^n w_j^i \quad \text{for } i = 1, \dots, N_1 \end{aligned} \quad (4.6)$$

On the left-hand side is the value of the covered call portfolio in scenario i at the end of the first stage per unit of initial wealth. The wealth gained from selling one unit of option l on asset j is given by the call's market price at time zero, C_{jl}^0 , grown at the risk free rate r_f for T_1 days, less the call liability. The liability is given by the maximum of the price of asset j at the end of the first stage in scenario i , S_{1j}^i , less the call's strike price k_{jl} and zero. Since presumably the scenario's asset prices are known, the maximum function may be replaced by its output, i.e. a constant, when the formulation is implemented. The constraint is thus linear in terms of q_{jl}^0 . The value of one unit of asset j at the end of the first stage in scenario i is given by S_{1j}^i plus any dividends paid since time zero grown at the risk-free rate until the end of the first stage, D_{1j} .

Constraint set (4.6) assumes that proceeds from selling call options and dividends are held in cash until the next rebalancing period (the end of the stage). Alternatively, the proceeds

from selling call options could be used to increase the initial budget, and dividend payments could be reinvested in the covered call portfolio. It isn't clear if or how these alternatives could be formulated. In any case, the difference in return caused by these assumptions is negligible.

The value of the covered call portfolio at the end of the first stage in scenario i is set to be equal to the budget of the equity positions for the second stage in constraint set (4.6). It is assumed that the start of the second stage coincides with the end of the first stage, i.e. once the short positions denoted by q_{jl}^0 mature the equity positions and call overlays are immediately rebalanced. At the beginning of the second stage there is a new set of decision variables in each scenario i . The covered call portfolio held during the second stage after scenario i occurs is given by the equity positions w_j^i and the short call positions q_{jl}^i . Only long equity positions and short call positions are permitted:

$$w_j^i \geq 0 \quad \text{for } i = 1, \dots, N_1 \text{ and } j = 1, \dots, n \quad (4.7)$$

$$q_{jl}^i \geq 0 \quad \text{for } i = 1, \dots, N_1 \text{ and } \forall j, l \quad (4.8)$$

At the start of the second stage in scenario i , there are n_j^i call options on asset j available to sell; call option l on asset j has market price C_{jl}^i and strike price k_{jl}^i . Short call positions denoted by q_{jl}^i are assumed to mature T_2 days from the end of the first stage, i.e. $T_1 + T_2$ days from time zero. Thus, these are the very same options that may have been shorted at the beginning of the first stage, those with positions denoted by q_{jl} . The variables q_{jl}^i can be thought of as rebalancing the initial positions in the longer-dated options. This rebalancing is one-directional in the sense that we may only increase the short position since we have assumed that short option positions must be held until maturity. Noting that the positions q_{jl} are still active, the number of units of call options sold on asset j in scenario i must not exceed the number of units of asset j held in scenario i :

$$\sum_{l=1}^{n_j} \frac{q_{jl}}{S_{0j}} + \sum_{l=1}^{n_j^i} \frac{q_{jl}^i}{S_{1j}^i} \leq \frac{w_j^i}{S_{1j}^i} \quad \text{for } i = 1, \dots, N_1 \text{ and } j = 1, \dots, n$$

We can multiply this constraint by the simulated asset price S_{1j}^i to obtain a constraint which can again be interpreted as constraining the proportion of wealth overwritten with call options

on each asset not to exceed the proportion of wealth invested in the corresponding asset:

$$\sum_{l=1}^{n_j} q_{jl} \frac{S_{1j}^i}{S_{0j}} + \sum_{l=1}^{n_j} q_{jl}^i \leq w_j^i \quad \text{for } i = 1, \dots, N_1 \text{ and } j = 1, \dots, n \quad (4.9)$$

In this form the constraint also has better scaling.

Suppose that for each first stage scenario i there are N_2 simulations of the asset prices at the end of the second stage. The price of asset j at the end of the second stage in scenario im is given by S_{2j}^{im} , and the value of any dividends paid for asset j grown at the risk free rate until the end of the second stage is given by D_{2j} . The wealth at the end of the second stage can be formulated:

$$\begin{aligned} & \sum_{j=1}^n \sum_{l=1}^{n_j} \frac{q_{jl}}{S_{0j}} (C_{jl} e^{r_f(T_1+T_2)} - \max(S_{2j}^{im} - k_{jl}, 0)) \\ & + \sum_{j=1}^n \sum_{l=1}^{n_j} \frac{q_{jl}^i}{S_{1j}^i} (C_{jl}^i e^{r_f T_2} - \max(S_{2j}^{im} - k_{jl}^i, 0)) \\ & + \sum_{j=1}^n \frac{w_j^i}{S_{1j}^i} (S_{2j}^{im} + D_{2j}) - \sum_{j=1}^n c_z z_j^i = W^{im} \end{aligned} \quad (4.10)$$

for $i = 1, \dots, N_1$ and $m = 1, \dots, N_2$

Constraint set (4.10) is the second stage equivalent of constraint set (4.6) with two differences. First, since this is the end of the investment horizon the right-hand side contains the terminal wealth in scenario im per unit of initial wealth, W^{im} . Second, a transaction cost is included to reflect the equity rebalancing at the beginning of the second stage.

The cost to buy or sell equity per unit of wealth is given by c_z . The turnover in asset j between the first and second stages in scenario i per unit of initial wealth is given by z_j^i which is defined using a pair of constraints:

$$z_j^i \geq w_j^i - w_j \frac{S_{1j}^i}{S_0} \quad \text{for } i = 1, \dots, N_1 \text{ and } j = 1, \dots, n \quad (4.11)$$

$$z_j^i \geq w_j \frac{S_{1j}^i}{S_0} - w_j^i \quad \text{for } i = 1, \dots, N_1 \text{ and } j = 1, \dots, n \quad (4.12)$$

This pair of constraints ensures that the value of z_j^i is equal to the absolute value of the difference

between the equity position in asset j at the end of the first stage and at the beginning of the second stage. Turnover has a cost $c_z > 0$ associated with it and thus decreases the utility, since the expected utility is being maximized the value of z_j^i will be pushed down until one of the two constraints is binding.

The transaction costs as formulated make a few implicit assumptions. The first is that the transaction cost is proportional to the amount of wealth being transferred. The second is that any options which expire in the money are settled in cash rather than delivery of the underlying asset. A transaction cost may then be incurred when some assets must be liquidated in order to meet the cash settlement liabilities unless sufficient cash was generated from dividends and premia of calls sold. The last implicit assumption is that the transaction costs do not affect the budget at the time they are incurred. Rather, the transaction cost is deducted from the total return at the end of the stage. If desired a cost of borrowing can be embedded into the transaction cost parameter c_z . In addition to imposing the transaction cost, we can also explicitly constrain the total turnover incurred at the beginning of the second stage in each scenario i :

$$\sum_{j=1}^n z_j^i \leq 2z_{max} \quad \text{for } i = 1, \dots, N_1 \quad (4.13)$$

The parameter z_{max} is equal to the maximum proportion of initial wealth which can be reinvested into a different asset between the first and second stages.

Using W^{im} which was defined in constraint set (4.10) we can maximize the expected utility of terminal wealth:

$$\underset{w,p,z,W}{\text{maximize}} \quad \frac{1}{N_1 N_2} \sum_{i=1}^{N_1} \sum_{m=1}^{N_2} U(W_0 W^{im}) \quad (4.14)$$

The terminal wealth in scenario im is given by multiplying W^{im} by the initial wealth W_0 . This can conveniently be used as the input to the utility function. Without loss of generality we can assume that $W_0 = 1$ and that any desired scaling is embedded in the utility function. The optimization problem is defined by the objective (4.14) and the constraints (4.1) through (4.13). Note that all constraints are linear, the chosen utility function U dictates the complexity

of the optimization model. In general investors are risk averse, thus appropriate utility functions are concave functions. Multiplying the objective by negative one thus produces a convex optimization problem. Convex optimization problems are highly tractable in general.

Three utility functions for wealth prevalent in risk modelling are the quadratic utility, the negative exponential utility, and the power utility (also called the isoelastic utility).

$$\text{The quadratic utility:} \quad U_Q(W) = W - \frac{W^2}{2s}, \quad W < s$$

$$\text{The negative exponential utility function:} \quad U_E(W) = \frac{1}{a}(1 - e^{-aW}), \quad a > 0$$

$$\text{The power utility function:} \quad U_P(W) = \frac{W^{1-c} - 1}{1 - c}, \quad c \geq 0, c \neq 1$$

$$\text{The limiting case of the power utility:} \quad U_L(W) = \ln W, \quad c = 1$$

These utility functions are concave functions of wealth and thus assume that the investor is risk averse. Detailed information on these utility functions can be found in Gerber and Pafumi (1998). When $c = 0$ the power utility becomes a linear utility function, and as $a \rightarrow 0$ and $s \rightarrow \infty$ the negative exponential and quadratic utilities converge to linear utilities. Maximizing a linear utility is equivalent to maximizing expected return. As risk aversion decreases the solutions from maximizing the expectation of all three utilities will converge to the same solution, the maximum expected return portfolio. However these utility functions have differing Arrow-Pratt absolute risk aversion (ARA) coefficients (see Pratt 1964) and reflect different risk attitudes. The quadratic utility has an increasing risk aversion coefficient, the negative exponential utility has a constant risk aversion coefficient, and the power utility has a decreasing risk aversion coefficient. Thus, as risk aversion increases the optimal portfolios for each utility may differ substantially.

It is straightforward to generalize the formulation to accommodate any number of option exercise dates by increasing the number of stages. However, the amount of computational effort required to produce near-optimal solutions rapidly becomes prohibitive as stages are added (see 5.8.2 of Shapiro et al. 2009 for a discussion on the convergence of sample average approximation problems).

4.2 Implementation

We implement the formulation of section 4.1 to optimize a portfolio using 67 large cap US equities from the S&P 500 Index. Since options with short maturity dates typically form the most attractive covered call strategies, we implement the model by setting each stage to two weeks. Covered calls are formed by selling a mix of two-week-to-maturity and one-month-to-maturity options. Option data on these assets from November 2016 to November 2017 was retrieved from OptionMetrics. Although options on these assets are of American exercise style, special considerations are not required since they are seldom exercised early. Only options which are at-the-money (ATM) or out-of-the-money (OTM) are included in the model. Since the asset's spot price most often does not exactly match the strike price of any of the options, the least in-the-money option is treated as the ATM option and is included in the model. The optimization is performed on the day that the previous month's one-month-to-maturity options expire, generally the third Friday of each month. For a particular month, we require data for options with one month to maturity and two weeks to maturity. We obtained sufficient data to perform the optimization in nine sample months.

Bid-ask spreads in the option prices are often sizeable. We assume that for ATM options the seller can sell at the asking price, and as options become further out-of-the-money the seller must sell closer to the best bid. The underlying logic is that liquidity is typically high for ATM options but becomes lower as the strike price increases. We use these assumptions to obtain the premiums C_{jl} and C_{jl}^0 from the bid-ask spreads. Options with a best bid of zero are discarded regardless of their asking price.

We treat dividends as if they are paid on the ex-dividend date since the payment date may be beyond the end of the second stage. The 30 day US treasury yield was used as the risk-free rate. The transaction cost parameter c_z was set to 0.00015; this is equivalent to a transaction cost of three basis points of wealth traded. The maximum turnover parameter z_{max} was set to 0.125; this corresponds to a maximum annual turnover of 300%.

Scenario simulations were produced by assuming that the price paths of the assets follow geometric Brownian motion (GBM). According to Figelman (2009) the liability of out-of-the-money options may be significantly underestimated if high moment market dynamics are not

accounted for. To accommodate such dynamics we model the variance of each asset's daily return as a GARCH process (see Bollerslev 1986 for details). This introduces significant skewness and kurtosis in the return distribution of most assets. Each asset's drift and correlations were estimated using the historical returns gross of dividends during the ten year period up to November 2016. The estimated drifts and GARCH processes are used to simulate daily asset returns via GBM. Although GARCH volatilities are useful in capturing high moment effects, it is prudent to use a forward-looking measure of volatility. We linearly rescale the simulated returns so that the sample variance of each asset's return at time T_1 matches the implied variance of the two-week-to-maturity ATM option at time zero, and the variance of each asset's return at time $T_1 + T_2$ matches the implied variance of the four-week-to-maturity ATM option at time zero. To improve convergence we also rescale the simulated returns so that the sample expected simple returns match those which are implied by the historical drifts. The rescaling transformation we employ preserves sample moments of the third order and above, and also preserves sample correlations of log-returns. Essentially then, for each asset's return distribution the first moment is driven by a historical estimate, the second moment is driven by observed implied volatilities of ATM options at time zero, and higher moments are driven by a fitted GARCH process. Scenario production is described in greater detail in appendix G. In practice it is an investor's prerogative to produce scenarios which reflect their beliefs of the behaviour of the assets for the time period in consideration.

The number of simulations, N_1 and N_2 , must be sufficiently large to produce optimal results. In order to accurately model the distribution of possible payoffs of two-week-to-maturity options sold at time zero, we require N_1 to be large. In order to do the same for options sold at time T_1 we require N_2 to be large. To accurately capture possible payoffs of the four-week-to-maturity options we need the total number of scenarios, $N_1 N_2$, to be large. From a convergence standpoint it is sensible to use $N_1 = N_2$ so that the first and second stage option payoffs are approximated at a similar level of accuracy. We use up to $N_1 = 110$ and $N_2 = 110$; at this upper limit a total of 12,100 simulations are used. For a given number of simulations, we rerun test cases several times using different random number seeds; Shapiro (2009) refers to this as different 'replications'. As a measure of stability we examine the optimal first-stage solutions as the random number seed is varied while all other parameters are fixed, i.e. across

the replications. It has long been noted, for example in Saliby (1990), that simple random sampling is problematic in that sample characteristics do not perfectly match those of the assumed sampling distribution. This is particularly damaging in our case where decisions on the two-week-to-maturity-options are being made based on a very small sample, $N_1 = N_2$. Moment matching (see Høyland et al. 2003) is a widely used scenario generation technique which ensures that multidimensional scenarios have sample moments which match nominal values. We apply moment matching on the first two sample moments: per appendix G we adjust the randomly generated scenarios so that the sample expected simple returns match the historical simple returns, and so that the sample volatilities match the implied volatilities of the ATM options. We find that this adjustment greatly improves stability and convergence with respect to the number of samples, N_1 and N_2 . A wide variety of other scenario generation techniques exists; a good overview is provided by Römisch (2010).

The quantity C_{jl}^i in constraint set (4.10) is the market price of option l on asset j in the beginning of the second stage in scenario i , and must be estimated. We employ a simple model where we assume that the implied volatility of an option as a function of moneyness is fixed over time for a fixed maturity date; this is known as the 'sticky delta' rule. Details are discussed in appendix H.

When using the quadratic utility, the resulting quadratic problems were solved using the quadratic simplex method in CPLEX. When using the power utility and the negative exponential utility, the resulting convex problems were solved using the interior point solvers of MOSEK. Without loss of generality, we assume that the initial wealth $W_0 = 1$. Any desired scaling could be embedded into the relevant utility function. In each of the sample months, we solve the optimization problem using each of the three utility functions. In order to explore different levels of risk aversion we solve the problem for a range of parameter values. For the quadratic utility the value of s ranged from 1 to 20. For the negative exponential utility function the value of a ranged from 20 to 0.001. For the power utility the value of c ranged from 50 to 0.

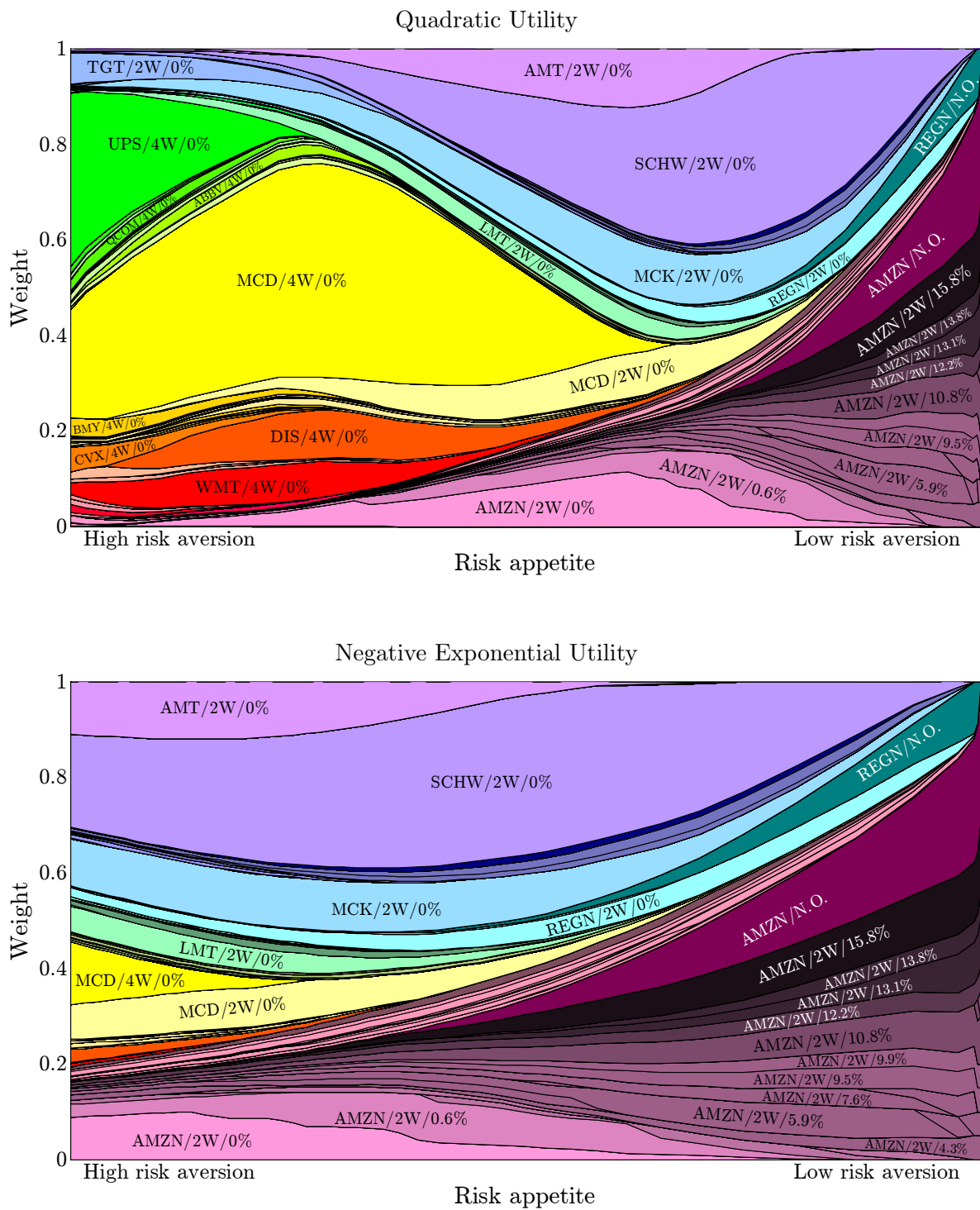


Figure 4.2

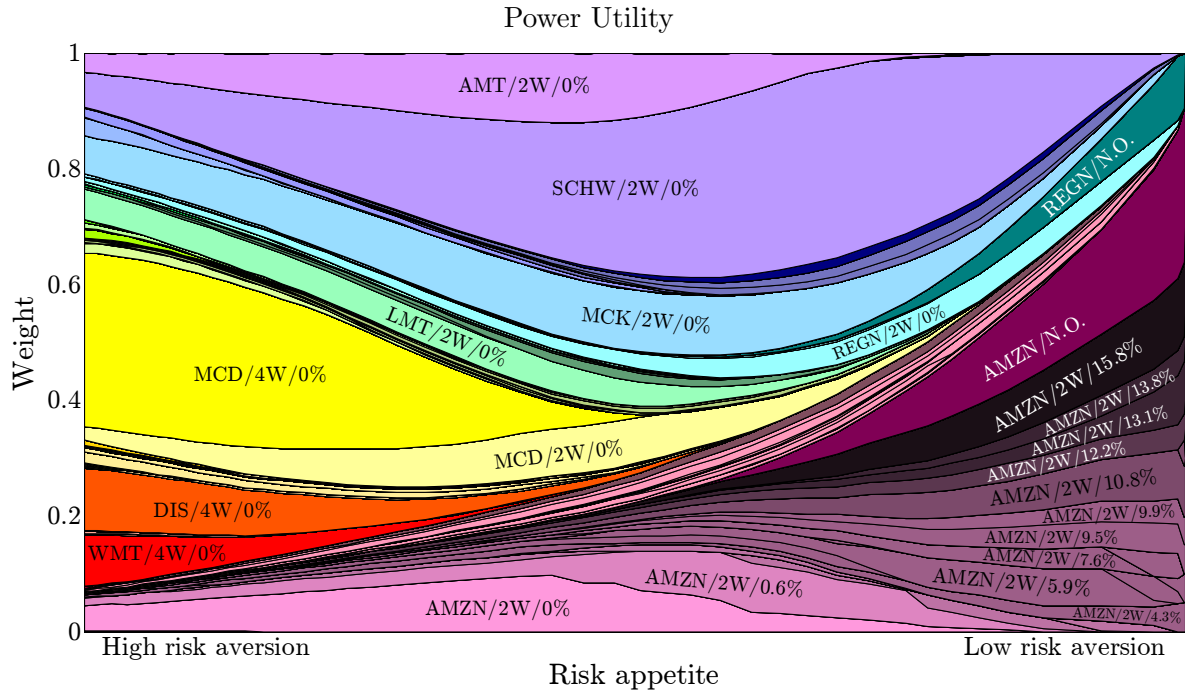


Figure 4.2: Blends of near-optimal first stage portfolios in November 2016. Areas simultaneously indicate underlying equity positions and call overwriting weights. Major positions are labelled in the format: Ticker/Maturity/Moneyness. Maturity is either two or four weeks, and moneyness is quoted as a percentage equal to the strike price divided by the underlying spot price minus one. 'N.O.' indicates equity weight held but not overwritten by the sale of call options.

4.3 Results

Figure 4.2 displays solutions averaged across 20 replications for November 2016 using $N_1 = N_2 = 40$. As risk aversion decreases all three utility functions converge to linear functions. Thus it can be seen in figure 4.2 that at low risk aversion all utility functions produce the same portfolio, the maximum return portfolio as we had predicted in section 4.1. At high risk aversion there is a large amount of overwriting, almost exclusively with ATM options. As risk aversion decreases the amount of overwriting decreases and the moneyness of options sold increases, this trend was also observed in chapter 3. Additionally we observe that at low risk aversion it is preferable to sell two-week-to-maturity options, while at high risk aversion a mix of two and four-week-to-maturity-options are generally sold. This is consistent with investor intuition that shorter dated options have the largest gap between implied and realized volatility and may offer disproportionately large premiums for a covered call. We find that under the assumed asset dynamics, i.e. skewness, kurtosis, and higher order moments driven by GARCH

volatility, variance of the return matching the implied ATM term structure, and expected return matching the historical return, that two-week-to-maturity options most often have lower call risk premiums (CRP, defined in Figelman 2008) than four-week-to-maturity options. A two-week-to-maturity option on some asset generally has a lower expected liability than a four-week-to-maturity option with a comparable price, and a two-week-to-maturity option on some asset generally has a higher price than a four-week-to-maturity option with a comparable expected liability. This suggests that a risk-averse investor maximizing the expectation of a linear utility function should prefer to sell two-week-to-maturity options in general. Optimal covered call portfolios can still contain short four-week-to-maturity options for many reasons: two-week-to-maturity options may not be available for some assets, or only for a limited range of strikes, or if options have sizeable transaction costs then the sale of two-week-to-maturity options twice as often as four-week options may negate the benefit of higher premiums.

The use of a rebalancing point between the first and second stages allows for more informed decision making at time zero, particularly when turnover is constrained. Compared to the portfolios in figure 4.2 optimized with a maximum equity turnover of 12.5% of wealth between stages, optimizing without turnover constraints produces portfolios which differ enormously except at very low risk aversion. At moderate to high risk aversion, first-stage equity holdings when optimizing without turnover constraints differ by 25 to 50% turnover from those of the portfolios in figure 4.2. This suggests that knowledge of options available at the end of the first stage and of asset dynamics during the second stage are useful in making decisions at the beginning of the first stage. It is not clear how to compare portfolios optimized over two stages against those optimized using only one stage since they fundamentally involve different assets. Out-of-sample testing is also difficult since it is not clear how to assess whether a portfolio's out-of-sample performance reflects its nominal in-sample expected utility. The exception is a linear utility, i.e. a maximum return portfolio, which we tested out-of-sample in chapter 3 for portfolios optimized over a single stage.

Considering the very small number of scenarios, $N_1 = N_2 = 40$, being used, optimal solutions are remarkably consistent across replications. When optimizing with low risk aversion in the first stage virtually all wealth is invested into Amazon in each of the 20 replications. At high risk aversion the optimal first-stage equity positions are stable across replications. Op-

tion positions are also stable, with each equity position typically coupled with one particular option. The exception is the Amazon position at low risk aversion. In a particular replication, the long position in Amazon, if overwritten, is fully overwritten with a two-week-to-maturity option with one particular strike, but this strike differs across replications. This suggests that as N_1 and N_2 approach infinity the optimal risk-neutral portfolio would involve a short position in a single option on Amazon. There is consensus across the replications that it should be a fairly far out-of-the-money option, the moneyness of the option sold ranges from 4.3% OTM to 15.8% OTM, which are unlikely to be exercised in a two week period. We can also imagine a non-overwritten equity position as being overwritten by an infinitely far out-of-the-money option, i.e. so far out-of-the-money that the premium and probability of exercise are 0. We could achieve a more precise solution by increasing N_1 and N_2 , a topic which we discuss later in this section.

Stability in the results is largely due to our adjustment of the sample scenarios to enforce particular values for the first and second order moments of asset returns. Adjusting the second order moments of samples is arguably justified since we are forcing them to match volatilities implied by option data, and we would like to make investment decisions which are consistent with implied option data. In contrast the estimation of first order moments is a subjective process. It has long been documented that portfolio optimization using point estimates for the expected returns and volatilities leads to concentrated asset positions, and observing the concentrated positions in Amazon in figure 4.2 we see that this is also true for covered calls. Thus adjusting the samples to reflect a point estimate of the expected returns is only justified if there is confidence in that estimate, otherwise we cannot trust the resulting concentrated positions. In figure 4.3 we see solutions averaged across 20 replications for November 2016 using $N_1 = N_2 = 40$, this time allowing sample first order moments to vary. Optimal portfolios at low risk aversion then contain a wide number of assets, reflecting uncertainty about which long equity and short call pair provides the highest expected return. Such a 'resampled' portfolio was most famously proposed by Michaud and Michaud (2008).

We find that optimizing using the negative exponential utility and the power utility produces nearly identical results. The negative exponential and power utilities have ARA coefficients of a and c/W respectively and reflect different risk attitudes. However since we are only optimizing

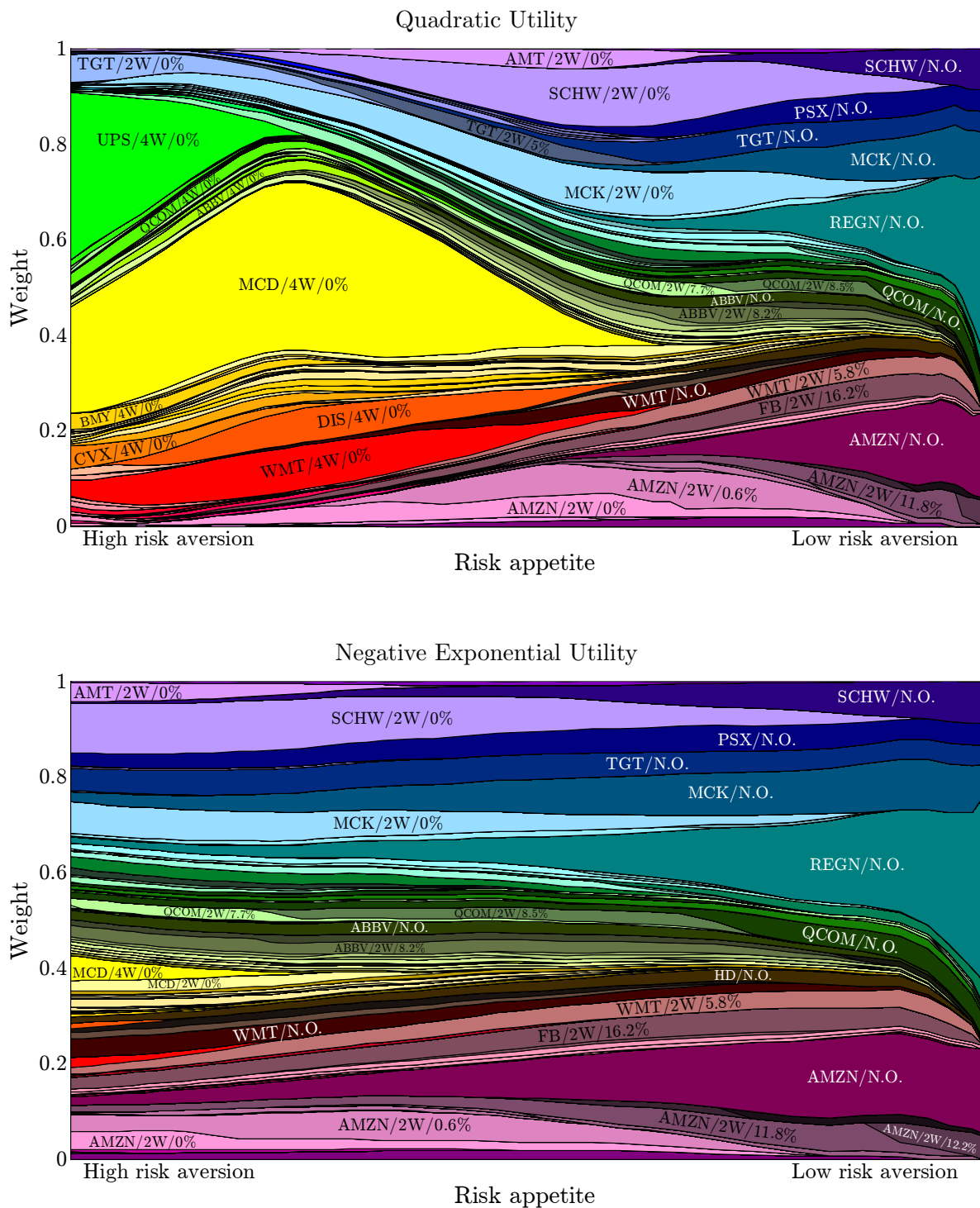


Figure 4.3

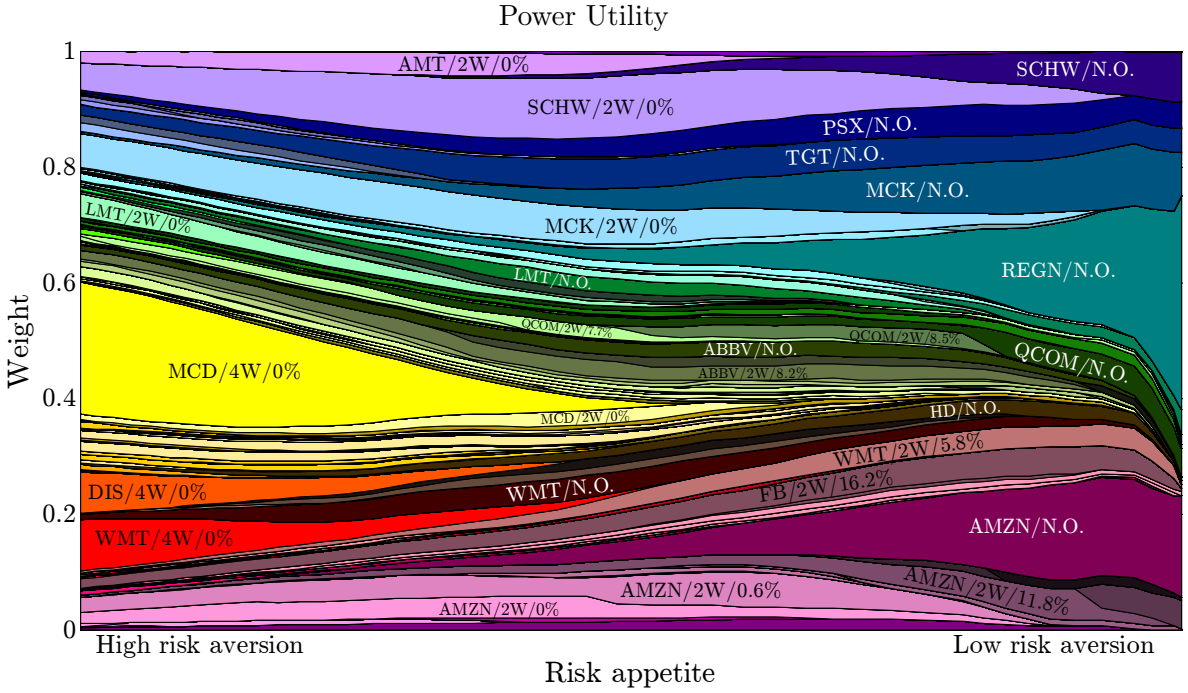


Figure 4.3: Near-optimal first stage portfolios in November 2016 when allowing first order sample moments to vary. Areas simultaneously indicate underlying equity positions and call overwriting weights. Major positions are labelled in the format: Ticker/Maturity/Moneyness. Maturity is either two or four weeks, and moneyness is quoted as a percentage equal to the strike price divided by the underlying spot price minus one. 'N.O.' indicates equity weight held but not overwritten by the sale of call options.

over a four week horizon the final wealth is often close to the assumed initial wealth, one. Thus the two utilities have near identical ARA coefficients when using $a = c$. In appendix I we prove that it is equivalent to optimize two utility functions with the same ARA coefficients. This is not an artefact of our assumption that the initial wealth is one, note that for the power utility $\arg \max U_P(W) = \arg \max U_P(W_0 W)$. The solutions differ at high risk aversion in figures 4.2 and 4.3 because we were only able to optimize the negative exponential utility up to $a = 20$ due to the problematic scaling of the term e^{-aW} . In contrast the key term in the power utility is W^{1-c} , which we optimized using $c = 50$ without difficulty. If we had longer maturity dates and the range of wealth outcomes were wider, then we would expect optimal solutions to differ between the two utilities.

We find that optimizing with the quadratic utility is generally an order of magnitude faster than when using the power or negative exponential utilities. Average solution times are shown in

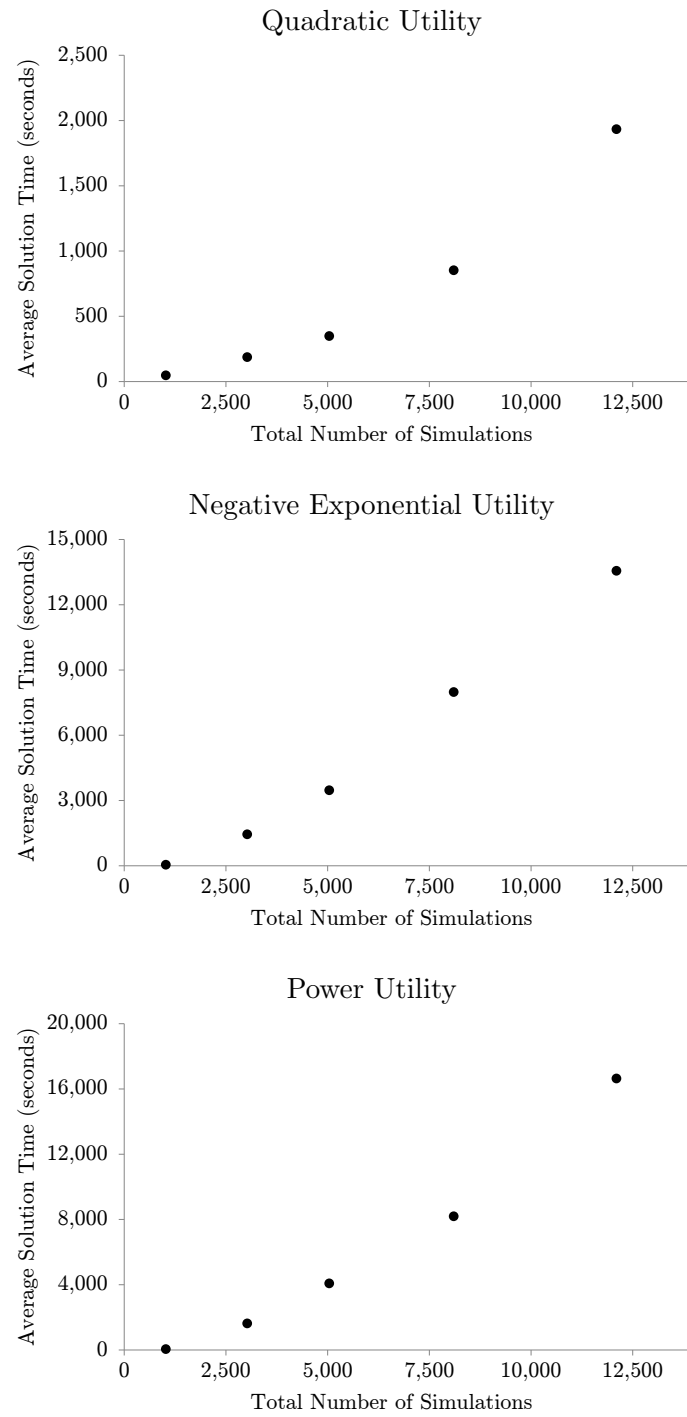


Figure 4.4: Average solution times versus number of scenarios in November 2016. Times shown are the total of solving using a particular utility function with five different parameter values, averaged over ten random number seed trials.

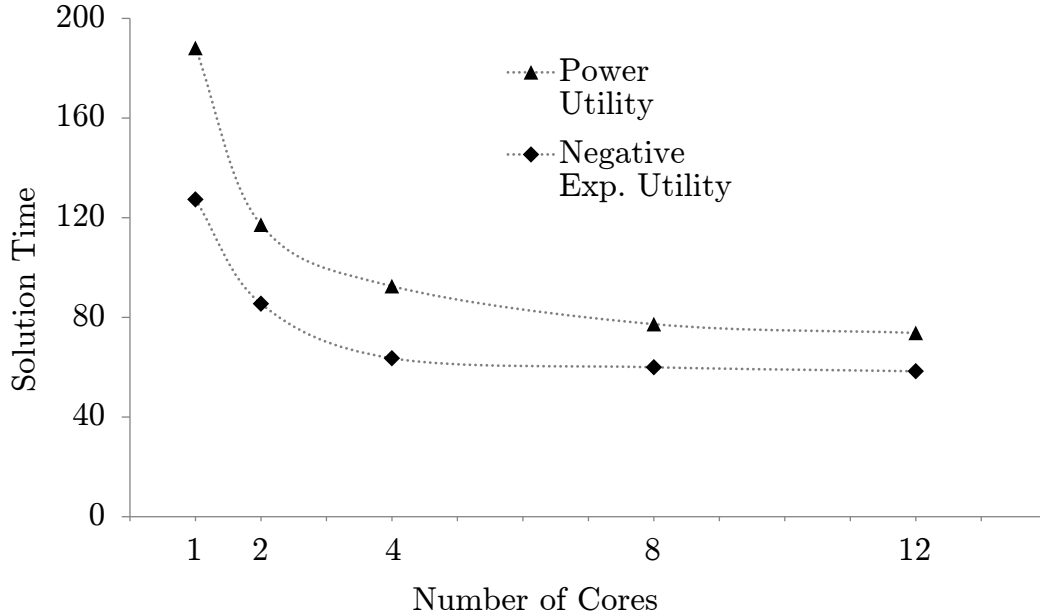


Figure 4.5: Typical solution time scaling versus number of cores (workers) when using the negative exponential and power utilities.

figure 4.4. Solution times vary across months roughly in proportion to differences in the number of available options, though across months times are well within an order of magnitude. Solution times do not differ substantially when varying the random number seed across replications. Although we used $N_1 = N_2 = 40$ for convenience to produce the large number of results needed to produce smooth figures, more accurate solutions can be achieved by increasing N_1 and N_2 . When using $N_1 = N_2 = 110$ the optimal first-stage equity positions in some replication differ on average from the blended portfolio by 8% when using the quadratic utility, and 16% when using the negative exponential or power utilities (compared to 18% and 25% respectively when using $N_1 = N_2 = 40$). Further increasing the number of scenarios would improve solution accuracy, but this causes solution times that are prohibitively slow for practical usage.

In figure 4.4 we see that solution times rise rapidly as the number of scenarios used increases. However it isn't possible to combat this problem with additional computing power. It is well known that the algorithms used to solve continuous problems, e.g. the simplex method or interior point methods, are highly serialized and difficult to distribute in parallel (see Rothberg 2013 for detail about parallelization of both simplex and barrier methods). In figure 4.5 we see that there is very little benefit to using more than four workers when solving using the

power utility or the negative exponential utility. We can expect similar scaling when using the quadratic utility which was solved with the quadratic simplex method in CPLEX. To address this problem we implement a progressive hedging decomposition.

4.4 Implementing the Progressive Hedging Algorithm

Instead of directly maximizing the expected utility using the formulation in section 4.1, we can use the progressive hedging decomposition first introduced in Rockafellar and Wets (1991). As part of the algorithm, each scenario im is solved as a separate subproblem and is allowed to have a full set of decision variables: $X^{im} = (w, q, q^0, w^i, q^i, z^i)^{im}$.

An important part of the progressive hedging algorithm are scenario bundles. A scenario bundle is a set of scenarios which are indistinguishable up until a particular time, say t^* . In order for a set of decisions X^{im} to be implementable, decisions made before t^* must be identical across all scenarios in each bundle at time t^* . At time zero all scenarios in our problem are indistinguishable; there is only one bundle and it contains all $N_1 N_2$ scenarios. The decision variables w , q , and q^0 are set at time zero, thus to be implementable they must be identical across all scenarios. All scenarios im where i is fixed are indistinguishable up until the end of the first stage. Thus there are N_1 scenario bundles at the end of the first stage, each containing N_2 scenarios. The decision variables w^i , q^i , and z^i are set at the end of the first stage. Thus to be implementable these variables must be identical across all X^{im} where i is fixed and m varies from 1 to N_2 . Since no decisions are made at the end of the second stage, scenario bundles at that time are irrelevant.

When solving for X^{im} it is assumed that scenario im is realized, at the end of the first stage asset prices are S_{1j}^i and call prices are C_{jl}^i , and at the end of the second stage asset prices are S_{2j}^{im} . The objective is to maximize the terminal utility for this scenario. This leads to optimal X^{im} which are not consistent across scenario bundles. The progressive hedging algorithm iteratively introduces a penalty into the objective function to address this inconsistency. The penalty forces optimal subproblem solutions to converge to an implementable solution. Rockafellar and Wets (1991) proves that this solution is optimal for the original non-anticipative stochastic program.

For our problem, the progressive hedging decomposition produces a large amount of overhead since each scenario is allowed to have a full set of decision variables. Table 4.1 displays subproblem sizes for different decomposition levels using $N_1 = N_2 = 80$, a total of 6,400 scenarios. When performing a full progressive hedging decomposition there are 6,400 subproblems, each corresponding to one individual scenario. Each subproblem is small, containing 2,030 variables and 272 constraints, but in aggregate there are over 12 million variables although the original problem contained less than 75,000. Additionally, a large number of iterations is required in order for all 6,400 duplicates of w , q , and q^0 and all 80 duplicates of each of the 80 sets of w^i and q^i to converge to an implementable solution. The full decomposition would only be useful if an exorbitant amount of computing power were available since all 6,400 subproblems can be solved in parallel.

Crainic et al. (2014) and Gade et al. (2016) both noted that it is not necessary to perform a full decomposition where each subproblem is an individual scenario. Instead, they suggested that a partial decomposition where each subproblem contains multiple scenarios could be advantageous. Crainic et al. (2014) found that since a partial decomposition has fewer subproblems than a full decomposition, fewer iterations were required to converge to an implementable solution. In our case we can greatly decrease the overhead produced by the progressive hedging decomposition by forming a partial decomposition where each subproblem contains scenarios im where i is fixed. These are scenarios which share the first stage scenario i , and thus share the second stage decision variables w^i , q^i , and z^i . If we take all N_2 scenarios im where i is fixed and m ranges from 1 to N_2 and place them within a single subproblem then duplication of the second stage decision variables is entirely avoided.

Table 4.1 shows the size of the subproblems using the partial decomposition described above. The number of variables and constraints per subproblem is scarcely larger than in the full decomposition, vastly lower than in the original problem. The total number of variables and constraints is on the same order of magnitude as the original problem, far lower than in the full decomposition. Since there are only 80 duplicates of w , q , and q^i , and no duplicates of the second stage variables, far fewer iterations are required to converge to an implementable solution versus using the full decomposition. We find that solving using the partial decomposition is several order of magnitude faster than using the full decomposition.

Decomposition type	No decomposition	Partial decomposition	Full decomposition
Number of subproblems	1	80	6,400
Number of variables per subproblem	74,789	2,109	2,030
Number of constraints per subproblem	22,708	351	272
Total number of variables	74,789	168,720	12,992,000
Total number of constraints	22,708	28,080	1,740,800
Iterations required for convergence	1	Few	Many
Parallelism	Difficult beyond 4 workers	Trivial up to 80 workers	Trivial up to 6,400 workers

Table 4.1: Problem sizes for different levels of progressive hedging decomposition using $N_1 = N_2 = 80$ in November 2016. The partial decomposition groups all scenarios im where i is fixed into subproblem i .

Using the partial decomposition described above, each subproblem i has a full set of first stage decision variables: $X^i = (w, q, q^0)^i$. Subproblem i also has the second stage decision variables w^i , q^i , and z^i . Since all scenarios belonging to a common scenario bundle at the end of the first stage are embedded in a single subproblem, there is no duplication of the second stage decision variables. Thus averaging and penalties are only required for the first stage decision variables w , q , and q^0 . The steps of the progressive hedging algorithm for our partial decomposition are as follows:

1. In iteration ν , for each subproblem i , obtain $X_{\nu+1}^i$ by solving the subproblem:

$$\underset{w, p, w^i, p^i, z^i, W^{im}}{\text{minimize}} \quad \sum_{m=1}^{N_2} \frac{-1}{N_2} U(W^{im}) + V_\nu^i \cdot X^i + 0.5r \|X^i - \hat{X}_\nu\|^2$$

$$\text{Subject to:} \quad w_j \geq 0 \quad \text{for } j = 1, \dots, n$$

$$\sum_{j=1}^n w_j = 1$$

$$q_{jl} \geq 0 \quad \forall j, l$$

$$q_{jl}^0 \geq 0 \quad \forall j, l$$

$$\begin{aligned}
& \sum_{l=1}^{n_j} q_{jl} + \sum_{l=1}^{n_j^0} q_{jl}^0 \leq w_j \quad \text{for } j = 1, \dots, n \\
& \sum_{j=1}^n \sum_{l=1}^{n_j^0} \frac{q_{jl}^0}{S_{0j}} (C_{jl}^0 e^{r_f T_1} - \max(S_{1j}^i - k_{jl}^0, 0)) \\
& + \sum_{j=1}^n \frac{w_j}{S_{0j}} (S_{1j}^i + D_{1j}) = \sum_{j=1}^n w_j^i \\
& w_j^i \geq 0 \quad \text{for } j = 1, \dots, n \\
& q_{jl}^i \geq 0 \quad \forall j, l \\
& \sum_{l=1}^{n_j} q_{jl} \frac{S_{1j}^i}{S_{0j}} + \sum_{l=1}^{n_j^i} q_{jl}^i \leq w_j^i \quad \text{for } j = 1, \dots, n \\
& \sum_{j=1}^n \sum_{l=1}^{n_j} \frac{q_{jl}}{S_{0j}} (C_{jl} e^{r_f (T_1 + T_2)} - \max(S_{2j}^{im} - k_{jl}, 0)) \\
& + \sum_{j=1}^n \sum_{l=1}^{n_j^i} \frac{q_{jl}^i}{S_{1j}^i} (C_{jl}^i e^{r_f T_2} - \max(S_{2j}^{im} - k_{jl}^i, 0)) \\
& + \sum_{j=1}^n \frac{w_j^i}{S_{1j}^i} (S_{2j}^{im} + D_{2j}) - \sum_{j=1}^n c_z z_j^i = W^{im} \quad \text{for } m = 1, \dots, N_2 \\
& w_j^i - w_j \frac{S_{1j}^i}{S_0} - z_j^i \leq 0 \quad \text{for } j = 1, \dots, n \\
& w_j \frac{S_{1j}^i}{S_0} - w_j^i - z_j^i \leq 0 \quad \text{for } j = 1, \dots, n \\
& \sum_{j=1}^n z_j^i \leq 2z_{max}
\end{aligned}$$

For the first iteration, we ignore the penalties in the objective function and only minimize the negative of the expected utility.

2. Compute $\hat{X}_{\nu+1}$ by averaging w , q , and q^0 over all subproblems (the sole time zero scenario bundle).
3. For each subproblem i , compute $V_{\nu+1}^i = V_\nu^i + r(X_{\nu+1}^i - \hat{X}_{\nu+1})$. We initialize $V_1^i = 0$ for all i in the first iteration.
4. Return to the first step with $\nu + 1$ replacing ν if the termination criteria aren't met.

There are still two important details missing in the algorithm: the value of r in the penalty

function and the termination criteria. Watson and Woodruff (2011) suggest setting r per element of the decision vector in proportion to the impact of that element on the objective value. In our problem the asset and option positions at time zero affect the final utility on a similar order of magnitude, thus we would like penalties to have a consistent magnitude across these decisions. In appendix J we show that a variable's penalty is proportional to r multiplied by the variable squared, and there is thus an equivalent choice between setting per variable values for r or rescaling decision variables. This observation motivated us to define the decision variables q , q^0 , and q^i to be the proportions of initial wealth overwritten by selling respective options, which gives them a similar order of magnitude as the other decision variables, w and w^i . Note that in chapter 3 we defined decision variables p to be the number of units of call options to sell, i.e. proportional to wealth overwritten divided by the asset price, typically far smaller than the option decision variables q . Using the old variables p the progressive hedging algorithm would have very poor convergence using a single value for r . Instead we use decisions variables which are within the same order of magnitude (w , q , q^0), and since their effects on the objective function are comparable, a single value of r is appropriate for the progressive hedging algorithm. It is then a simple matter of adjusting r upwards or downwards to balance convergence of the decision variables X^{im} and the multipliers V^{im} .

It is not necessary to run the algorithm until perfect convergence is achieved, i.e. $\hat{X}_{\nu+1} = \hat{X}_\nu$ and $V_{\nu+1}^i = V_\nu^i$ (which is equivalent to $X_{\nu+1}^i = \hat{X}_{\nu+1}$) for all i . We find that the terminal conditions $\|\hat{X}_{\nu+1} - \hat{X}_\nu\| < 0.001$ and $\frac{1}{N_1} \sum_{i=1}^{N_1} \|X_{\nu+1}^i - \hat{X}_{\nu+1}\| < 0.001$ consistently produce results which are nearly identical to those using the formulation in section 4.1. It is more convenient to impose terminal conditions based on X^i rather than V^i since we do not have an intuitive understanding of the magnitude of V^i . We would like to set the value of r so that both terminal conditions are met in roughly the same number of iterations. Depending on the value of the parameter s , when using the quadratic utility we find that values of r from 0.003 to 0.1 provide good convergence. When using the power utility we find that a value of $r = 0.2$ consistently produces good convergence for any risk appetite. Results were not collected for the negative exponential utility since the power utility produces nearly identical results and has better scaling.

Figure 4.6 shows solution times versus the number of workers using the partial decomposition

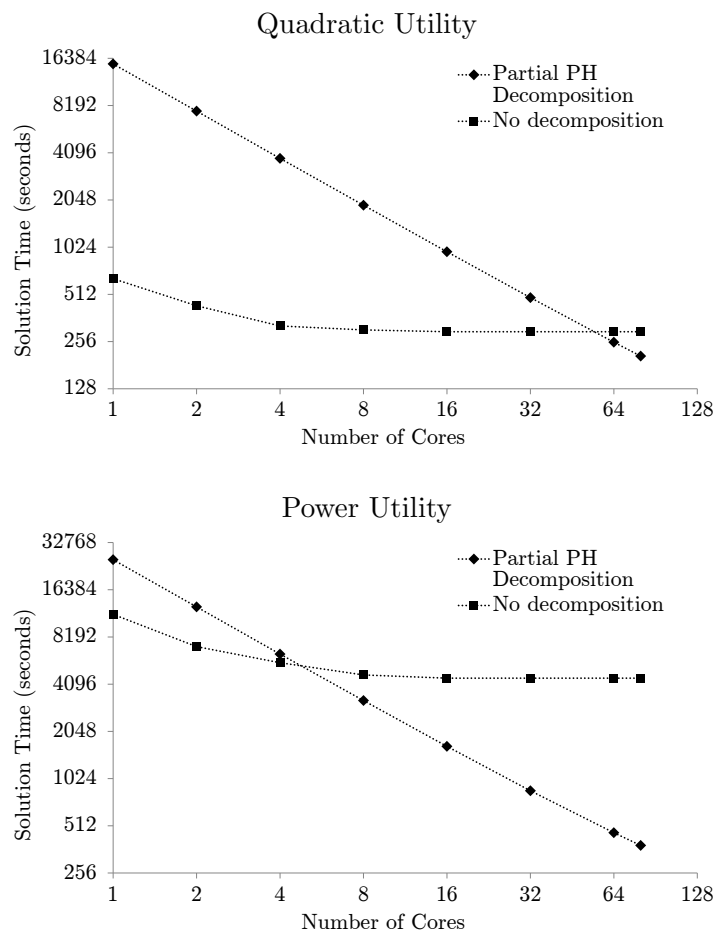


Figure 4.6: Estimated solution times versus number of cores (workers) using partial progressive hedging decomposition and without using decomposition. Optimization was performed using data from November 2016 using $N_1 = N_2 = 80$ with five different parameter values for each utility function.

described in section 4.4 and using the formulation from section 4.1. Although the partial decomposition has small subproblems so that each iteration is fast, there is still significant overhead since a large number of iterations are required, typically around 200. As the number of workers increases the progressive hedging decomposition demonstrates an advantage due to its trivial parallelism. Even with modest computing resources optimizing the power utility is much faster using progressive hedging. Progressive hedging was much less effective for the quadratic utility. Optimizing the quadratic utility without decomposition is fairly fast since once we have an optimal solution for the first parameter value for s subsequent problems are rapidly optimized by using a warm start (i.e. using the basis from the previous solution as a starting point, already likely close to optimal). This advantage of the quadratic utility is lost when using progressive hedging. In contrast interior point (barrier) methods used to optimize the power utility do not benefit from a supplied starting point.

With the advent of cloud computing the progressive hedging algorithm can be very useful. At the time of writing this article the on-demand cost to use a 72 core computing cluster optimized for computationally intensive tasks from Amazon Web Services is 3.06 USD per hour (see Amazon Web Services 2019). In one hour such a cluster could optimize the 67 asset two-stage covered call portfolio using $N_1 = N_2 = 80$ over 40 times using the power utility and around 80 times using the quadratic utility. In comparison the full problem without decomposition doesn't scale well with computing power as seen in figure 4.5.

4.5 Conclusion

We introduced a two-stage stochastic program for covered call portfolios. Instead of conventional risk-return optimization we optimized the expected utility across a number of scenarios, this allows for the use of any utility function by simply swapping the objective function. The model has only linear constraints, and a concave objective assuming a risk-averse utility function. While the previous models required that all options have a common maturity date, the two-stage model can optimize covered call portfolios with options of multiple expiries. Existing literature has not examined covered calls formed with options of different expiries sold simultaneously. When optimizing over a short investment horizon so that the total return is often close

to one, the negative exponential and power utilities have nearly identical ARA coefficients when using identical parameter values. We proved that this implies that they are equivalent from an optimization perspective, and thus produce near identical solutions. Though we first generated scenario returns randomly, to improve solution quality we then performed moment matching so that the sample expected returns and variances of scenario returns would match nominal values while preserving higher order moments. This adjustment was highly effective in decreasing the number of scenarios per stage required to produce consistent results. However due to the additional stage solution times become large when testing with two stages and 67 assets. Unlike conventional risk measures which are defined with reference to all scenario returns, we can compute the contribution of an individual scenario to the expected utility objective. This allowed us to apply a progressive hedging partial decomposition to decrease solution times. We found progressive hedging particularly effective when optimizing the power utility which we solved with an interior point solver, it was less effective when optimizing the quadratic utility which we solved with a quadratic simplex solver.

Chapter 5

Conclusion

By applying operations research we can cast the construction of covered call strategies of generalized forms as tractable scenario-based stochastic optimization problems with linear constraints and convex objective functions. In chapter 2 we presented a risk-return optimization formulation to select quantities and strike prices of options to sell with a common maturity date and a fixed position in a single underlying asset. The problem is highly tractable even with a large number of options under consideration. In chapter 3 we presented a risk-return optimization formulation which, for a fixed maturity date, selects equity weights and quantities and strike prices of options to sell to form optimal covered call portfolios. This problem is slower to solve than in chapter 2, but is still tractable for large numbers of underlying assets and options. In chapter 4 we presented an expected utility optimization formulation to construct portfolios of covered calls with multiple assets, and by selling different quantities of options with various strike prices and maturity dates. After applying moment matching and a progressive hedging decomposition this model is also tractable for large numbers of underlying assets and options which expire on two different maturity dates. We proved that progressive hedging with per-variable penalty values is equivalent to using a single penalty value and rescaling decision variables. The progressive hedging decomposition was particularly effective when optimizing the power utility which we solved using an interior point solver, and was less effective when optimizing the quadratic utility which we solved using a quadratic simplex solver.

Optimal covered calls are sensitive to assumptions about the first-order and second-order moments of the underlying asset price movements. As part of the optimization formulations it

is necessary to produce scenarios for the underlying asset prices on the option maturity dates. We found that optimal results are sensitive to the sample first-order and second-order moments present in the scenario set. Results were far less sensitive to changes in moments of the third order and above. In chapter 4 we found that controlling the first two sample moments by using moment matching greatly improved the stability of the results versus the number of scenarios used. We proved that the multidimensional moment matching we employed adjusts the first two sample moments to their desired values while preserving the correlations, skewness, and kurtosis present in the original samples.

Conventional covered call strategies which sell options based on a fixed level of moneyness or probability of exercise fail to consider the impact of the options' market prices. To form an optimized covered call strategy it is critical to consider the market prices of the available options. The payoff of a short call position is the option's market price less the liability at maturity. When an option's market price exceeds its expected liability at maturity the option has a negative call risk premium, and shorting the option produces an increase to the expected return of a covered call strategy. Out-of-sample tests in chapter 3 suggest that call options with negative CRPs do exist. In the single asset case of chapter 2, we proved that optimizing the expected return of a covered call strategy amounts to selling the option with the lowest CRP if it is negative, or simply holding the long equity position without call overwriting if all options have positive CRPs. In the case of a portfolio of covered calls in chapter 3, we proved that it amounts to selecting the asset-option pair which maximizes the expected return for the asset less the minimum of the option CRP and zero, i.e. the long asset-short option pair with the highest expected return. Thus a risk-neutral investor chiefly needs to concern themselves with assessing the expected returns and liabilities of the assets and options under consideration respectively.

Conventional covered call portfolios formed by overlaying short option positions on an existing portfolio, often an equally weighted portfolio, are not optimal in general. We found that optimal covered call portfolios display greater complexity in their structure compared to what has previously been examined in the literature and what has been implemented in practice. In many cases it was optimal to overwrite a single asset position with call options of different strikes simultaneously, or to only partially overwrite. In chapter 2 we observed that it is optimal

for a risk-minimizing investor to fully overwrite their asset position using an ATM option. In chapter 3 we observed that it is optimal for a risk-minimizing investor to hold a well diversified portfolio of assets, all fully overwritten by selling the respective ATM options. In chapter 4 we observed that it is optimal for an extremely risk-averse investor to hold a well diversified portfolio of assets fully overwritten with ATM options with four weeks to maturity (as opposed to with two weeks in maturity). These observations are intuitive since short ATM options provide the largest premiums and incur the largest liabilities, and thus produce covered call strategies with highly regularized returns versus the underlying long asset position alone. In chapter 2 we observed a structured policy for all tested risk measures where further OTM options are sold as risk aversion decreases. In chapter 3 we observed a structured policy for all tested risk measures where as risk aversion decreases: the average moneyness of options sold increases, the amount of wealth overwritten decreases, and underlying equity positions become concentrated into a small number of assets. In chapter 4 we observed a structured policy for all tested utility functions where as risk aversion decreases, in addition to the trends observed in chapter 3, overwriting shifts from four-week-to-maturity options which have the largest premiums to two-week-to-maturity-options which have the lowest CRPs.

In chapters 2 and 3 where we performed risk-return optimization we found that for all risk aversion levels results of optimizing different down-side risk measures (i.e. VaR, CVaR, and semivariance) do not differ meaningfully. Results differed substantially when minimizing variance though they still followed the solution policy described above. Given these findings, if a down-side risk measure is desired it is preferable to minimize CVaR since the resulting optimization problem is linear. In chapter 4 we performed expected utility maximization and observe that when optimizing over a short investment horizon so that the total return is close to one, the negative exponential and power utilities have nearly identical ARA coefficients when using identical parameter values. We proved that this implies that they are equivalent from an optimization perspective, and thus produce near identical solutions. Given this finding, it is preferable to optimize the power utility rather than the exponential utility due to the problematic scaling of the exponential term at high risk aversion. Results differed meaningfully when optimizing the quadratic utility, though they still followed the structured policy described above.

Throughout this work a number of innovations have been made which may be useful in other operations research settings. The moment-matching procedure in appendix G may be useful in improving solution stability in other scenario-based asset management problems. The proof of equivalence of optimizing expected utility functions with identical ARA coefficients in appendix I may be useful in any other optimization setting where expected utilities are being maximized. The partial progressive hedging decomposition of 4.4 serves as a concrete example of a case where a partial decomposition is preferable to a full decomposition, and the proof of equivalence of using per-variable penalties and variable rescaling in appendix J may provide an alternative perspective and guidance for the application of progressive hedging in other settings.

There are many possible topics for future study. Future work could focus on testing covered call optimization using different markets settings and asset classes. Future work could also include more extensive out-of-sample studies than we have performed, and could compare optimized covered calls against additional competing covered call heuristics. Another topic which could be analyzed in greater depth is the effect of the assumed underlying asset dynamics when generating scenarios. An interesting study could also be to adjust the frameworks to construct optimal put-write strategies and compare these against optimized covered calls.

Bibliography

- Alexander, S., T.F. Coleman, and Y. Li. Minimizing CVaR and VaR for a portfolio of derivatives. *Journal of Banking and Finance*, Vol. 30, No. 2 (2006), 583–605.
- Amazon Web Services. "EC2 Instance Pricing". <https://aws.amazon.com/ec2/pricing/on-demand/>. Accessed 11 Apr 2019.
- Bank of Montreal. 2018. BMO US High Dividend Covered Call ETF Fact Sheet. <https://www.bmo.com/gam/ca/advisor/products/etfs?fundUrl=/fundProfile/ZWH>. Accessed 2 Jan 2019.
- Bank of Montreal. 2019. Covered Call Option Strategy. https://bmogamhub.com/system/files/covered_call_option_strategy_eng.pdf. Accessed 5 Jun 2019.
- Bassett, G.W., R. Koenker, and G. Kordas. "Pessimistic portfolio allocation and Choquet expected utility." *Journal of Financial Econometrics*, Vol. 2, No. 4 (2004), 477–492.
- BlackRock. 2018. Enhanced Capital and Income Fund Fact Sheet. <https://www.blackrock.com/investing/literature/fact-sheet/cii-enhanced-capital-and-income-fund-factsheet-us09256a1097-us-en-individual.pdf>. Accessed 2 Jan 2019.
- Board, J., C. Sutcliffe, and E. Patrinos. "The performance of covered calls." *The European Journal of Finance*, Vol. 6, No. 1 (2000), 1–17.
- Bollerslev, T. "Generalized autoregressive conditional heteroskedasticity." *Journal of Econometrics*, Vol. 31, No. 3 (1986), 307–327.
- Callan Associates. "An Historical Evaluation of the CBOE S&P 500 BuyWrite Index Strategy." October 2006, www.cboe.com/micro/bxm/Callan_CBOE.pdf. Accessed 2 Jan 2019.
- Che, S.Y.S., and J.K.W. Fung. "The Performance of Alternative Futures Buy-Write Strategies." *Journal of Futures Markets*, Vol. 31, No. 12 (2011), pp. 1202–1227.

- Chicago Board Options Exchange. "Description of the CBOE S&P 500 BuyWrite Index." November 2010, www.cboe.com/micro/bxm/BXMDescription-Methodology.pdf. Accessed 23 Apr 2019.
- CI Financial. 2019. "First Asset Exchange Traded Funds Prospectus." https://www.firstasset.com/documents/0_prospectus_20190422.pdf. Accessed 5 Jun 2019.
- Cox, J.C., S.A. Ross, and M. Rubinstein. "Option Pricing: A Simplified Approach." *Journal of Financial Economics*, Vol. 7, No. 3 (1979), pp. 229–263.
- Crainic, T.G., M. Hewitt, and W. Rei. "Scenario grouping in a progressive hedging-based meta-heuristic for stochastic network design." *Computers & Operations Research*, Vol. 43 (2014), 90–99.
- Credit Suisse. 2019. X-Links Gold Shares Covered Call ETN. <https://notes.credit-suisse.com>Show/Details/GLDI>. Accessed 3 Jun 2019.
- Diaz, M., and R.H. Kwon. "Optimization of covered call strategies." *Optimization Letters*, Vol. 11, No. 7 (2017), 1303–1317.
- Diaz, M., and R.H. Kwon. "Portfolio optimization with covered calls." *Journal of Asset Management*, Vol. 20, No. 1 (2019), pp. 38–53.
- Eraker, B., M. Johannes, and N. Polson. "The Impact of Jumps in Volatility and Returns." *The Journal of Finance*, Vol. 58, No. 3 (2003), pp. 1269–1300.
- Estrada, J. "Mean-semivariance behaviour: An alternative behavioural model." *Journal of Emerging Market Finance*, Vol. 3, No. 3 (2004), 231–248.
- Feldman, B.E., and D. Roy. "Passive Options-Based Investment Strategies: The Case of the CBOE S&P 500 BuyWrite Index." *The Journal of Investing*, Vol. 14, No. 2 (2005), pp. 66–83.
- Figelman, I. "Expected Return and Risk of Covered Call Strategies." *The Journal of Portfolio Management*, Vol. 34, No. 4 (2008), 81–97.
- Figelman, I. "Effect of non-normality dynamics on the expected return of options." *The Journal of Portfolio Management*, Vol. 35, No. 2 (2009), 110–117.
- Gade, D., G. Hackebeil, S.M. Ryan, J.P. Watson, R.J.B. Wets, and D.L. Woodruff. "Obtaining lower bounds from the progressive hedging algorithm for stochastic mixed-integer programs." *Mathematical Programming*, Vol. 157, No. 1 (2016), 47–67.

- Gao, R., and A.J. Kleywegt. 2016. Distributionally robust stochastic optimization with Wasserstein distance. *arXiv preprint arXiv:1604.02199*.
- Gatheral, J. *The Volatility Surface: A Practitioner's Guide*. John Wiley & Sons, 2006.
- Gerber, H.U., and G. Pafumi. "Utility functions: from risk theory to finance." *North American Actuarial Journal*, Vol. 2, No. 3 (1998), 74–81.
- Global X. 2019. Nasdaq 100 Covered Call ETF. <https://www.globalxfunds.com/funds/qyld/>. Accessed 3 Jun 2019.
- Hanoch, G., and H. Levy. "Efficient Portfolio Selection with Quadratic and Cubic Utility." *The Journal of Business*, Vol. 43, No. 2 (1970), 181–189.
- He, D.X., J.C. Hsu, and N. Rue. "Option-Writing Strategies in a Low-Volatility Framework." *Journal of Investing*, Vol. 24, No. 3 (2015), 116–128.
- Hill, J.M., V. Balasubramanian, K. Gregory, and I. Tierens. "Finding Alpha via Covered Index Writing." *Financial Analysts Journal*, Vol. 62, No. 5 (2006), pp. 29–46.
- Horizons. 2019. Horizons Exchange Traded Funds Prospectus. https://www.horizonsetfs.com/horizons/media/pdfs/prospectus/CoveredCall_Prospectus.pdf. Accessed 5 Jun 2019.
- Høyland, Kjetil, M. Kaut, and S.W. Wallace. "A heuristic for moment-matching scenario generation." *Computational optimization and applications*, Vol. 24, No. 2-3 (2003), pp. 169–185.
- Invesco. 2019. Invesco S&P 500 BuyWrite ETF. <https://www.invesco.com/portal/site/us/investors/etfs/product-detail?productId=PB#>. Accessed 3 Jun 2019.
- Kapadia, N., and E. Szado. "The Risk and Return Characteristics of the Buy-Write Strategy on the Russell 2000 Index." *Journal of Alternative Investments*, Vol. 9, No. 4 (2007), 39–56.
- Maidel, S., and K. Sahlin. "Capturing the volatility premium through call overwriting." *Russell Research*, December 2010, www.cboe.com/micro/Buywrite/Russell-2010-12-VolatilityPremiumthroughCallOverwriting.pdf. Accessed 2 Jan 2019.
- Manulife. 2018. Manulife Covered Call U.S. Equity Fund Fact Sheet. <https://funds.manulife.ca/api/mutual/pdf/240e-en-us>. Accessed 2 Jan 2019.
- Markowitz, H. "Portfolio selection." *Journal of Finance*, Vol. 7, No. 1 (1952), 77–91.
- McIntyre, M.L., and D. Jackson. "Great in practice, not in theory: An empirical examination

- of covered call writing.” *Journal of Derivatives & Hedge Funds*, Vol. 13, No. 1 (2007), 66–79.
- Michaud, R.O., and R.O. Michaud. 2008. *Efficient Asset Management: A Practical Guide to Stock Portfolio Optimization and Asset Allocation*. Oxford University Press.
- Mulvey, J.M., and W.T. Ziemba. 1998. *Worldwide asset and liability modeling*. Cambridge University Press.
- Pratt, J.W. ”Risk Aversion in the Small and in the Large.” *Econometrica*, Vol. 32, No. 1/2 (1964), 122–136.
- Rockafellar, R.T., and R.J.B. Wets. ”Scenarios and policy aggregation in optimization under uncertainty.” *Mathematics of operations research*, Vol. 16, No. 1 (1991), 119–147.
- Rockafellar, R.T., and S. Uryasev. Optimization of conditional-value-at-risk. *Journal of Risk*, Vol. 2 (2000), 21–42.
- Römisch, Werner. ”Scenario generation.” *Wiley Encyclopedia of Operations Research and Management Science* (2010).
- Rothberg, E. ”Parallelism in Linear and Mixed Integer Programming.” *Parallel and Distributed Algorithms for Inference and Optimization*, October 2013, <https://simons.berkeley.edu/talks/ed-rothberg-2013-10-24>.
- Saliby, E. ”Descriptive sampling: a better approach to Monte Carlo simulation.” *Journal of the Operational Research Society*, Vol. 41, No. 12 (1990), 1133–1142.
- Shapiro, A., D. Dentcheva, and A.P. Ruszczyński. *Lectures on Stochastic Programming: Modeling and Theory*. Society for Industrial and Applied Mathematics, 2009.
- Watson, J.P., and D.L. Woodruff. ”Progressive hedging innovations for a class of stochastic mixed-integer resource allocation problems.” *Computational Management Science*, Vol. 8, No. 4 (2011), 355–370.
- Whaley, R.E. ”Return and risk of CBOE buy write monthly index.” *The Journal of Derivatives*, Vol. 10, No. 2 (2002), 35–42.
- Yang G.Z. 2011. Buy-Write or Put-Write: An Active Index Writing Portfolio to Strike it Right. Working paper. Available at www.ssrn.com/abstract=1827363. Accessed 2 Jan 2019.
- Zenios, S.A., and W.T. Ziemba. 2007. *Handbook of Asset and Liability Management: Applications and case studies*. Vol. 2. Elsevier.

Zymler, S., B. Rustem, and D. Kuhn. Robust Portfolio Optimization with Derivative Insurance Guarantees. *European Journal of Operational Research*, Vol. 210, No. 2 (2011), 410–424.

Appendix A

Monotonicity of a Single Asset Covered Call

Here we prove that the return r in section 2.1 is a monotonically increasing function of the asset price at maturity S_T . This permits the convenient formulations for VaR and CVaR seen in section 2.1.

Theorem 2. *The return of a covered call on a single asset is a monotonically increasing function of the asset price on the option expiry date.*

Proof. Consider the return of the strategy at maturity as a function of the asset price at maturity:

$$r(S_T) = \frac{1}{S_0} \left(S_T + \frac{\eta}{n} D - S_0 + \sum_{j=1}^{N_c} p_j (C_j e^{r_f T} - \max(S_T - k_j, 0)) \right)$$

Now consider the impact of any increase $\delta > 0$ in the asset price at maturity:

$$\begin{aligned} r(S_T + \delta) - r(S_T) &= \frac{1}{S_0} \left(S_T + \delta + \frac{\eta}{n} D - S_0 + \sum_{j=1}^{N_c} p_j (C_j e^{r_f T} - \max(S_T + \delta - k_j, 0)) \right) \\ &\quad - \frac{1}{S_0} \left(S_T + \frac{\eta}{n} D - S_0 + \sum_{j=1}^{N_c} p_j (C_j e^{r_f T} - \max(S_T - k_j, 0)) \right) \end{aligned}$$

$$= \frac{1}{S_0} \left(\delta + \sum_{j=1}^{N_c} p_j (\max(S_T - k_j, 0) - \max(S_T + \delta - k_j, 0)) \right)$$

The lowest possible value of $(\max(S_T - k_j, 0) - \max(S_T + \delta - k_j, 0))$ is $-\delta$ when $S_T \geq k_j$:

$$r(S_T + \delta) - r(S_T) \geq \frac{1}{S_0} \left(\delta + \sum_{j=1}^{N_c} p_j (-\delta) \right)$$

Since we have the constraint $0 \leq \sum p_j \leq 1$, the lowest possible value of $\sum p_j (-\delta)$ is $-\delta$.

$$r(S_T + \delta) - r(S_T) \geq \frac{1}{S_0} (\delta - \delta)$$

$$r(S_T + \delta) \geq r(S_T)$$

Since the above holds for any $\delta > 0$ and any value of S_T , the return is a monotonically increasing function of the asset price at maturity. \square

Appendix B

Linearity of Covered Call Constraints

Here we show that in section 2.1 the VaR and CVaR optimization problems are linear programs and our variance and semivariance optimization problems are quadratic programs. The decision variables are p , r , $\mathbb{E}(r)$, and z ; all other symbols represent known constants. Our formulations have the following objectives and constraints:

Variance optimization:

$$\underset{p,r,\mathbb{E}(r)}{\text{minimize}} \quad \lambda \left(\frac{1}{N-1} \sum_{i=1}^N (r_i - \mathbb{E}(r))^2 \right) - (1-\lambda)\mathbb{E}(r) \quad (\text{B.1})$$

Semivariance optimization:

$$\underset{p,r,\mathbb{E}(r),z}{\text{minimize}} \quad \lambda \left(\frac{1}{N} \sum_{i=1}^N z_i^2 \right) - (1-\lambda)\mathbb{E}(r) \quad (\text{B.2})$$

VaR optimization:

$$\underset{p,r,\mathbb{E}(r)}{\text{minimize}} \quad \lambda (-r_{(1-\alpha)N}) - (1-\lambda)\mathbb{E}(r) \quad (\text{B.3})$$

CVaR optimization:

$$\underset{p, r, \mathbb{E}(r)}{\text{minimize}} \quad \lambda \left(\frac{-1}{(1-\alpha)N} \sum_{i=1}^{(1-\alpha)N} r_i \right) - (1-\lambda)\mathbb{E}(r) \quad (\text{B.4})$$

Common constraints:

$$\sum_{j=1}^{N_c} p_j \leq 1 \quad (\text{B.5})$$

$$0 \leq p_j \leq 1, \quad j = 1, \dots, N_c \quad (\text{B.6})$$

$$r_i = \frac{S_T^i + \frac{\eta}{n}D - S_0 + \sum_{j=1}^{N_c} p_j (C_j e^{r_f T} - \max(S_T^i - k_j, 0))}{S_0} \quad i = 1, \dots, N \quad (\text{B.7})$$

$$\mathbb{E}(r) = \frac{1}{N} \sum_{i=1}^N r_i \quad (\text{B.8})$$

Additional constraints for semivariance:

$$-z_i \leq r_i - e^{r_f T} \quad i = 1, \dots, N \quad (\text{B.9})$$

$$z_i \geq 0 \quad i = 1, \dots, N \quad (\text{B.10})$$

Objectives (B.1) and (B.2) can be put into the standard quadratic optimization form: $x^T Q x + c^T x$. For both objectives the vector c contains only zeros with the exception of the coefficient of $\mathbb{E}(r)$ which is $(1-\lambda)$. Expanding the summation in (B.1):

$$\begin{aligned} & \lambda \left(\frac{1}{N-1} \sum_{i=1}^N (r_i^2 - 2r_i \mathbb{E}(r) + \mathbb{E}(r)^2) \right) - (1-\lambda)\mathbb{E}(r) \\ &= \left(\frac{\lambda}{N-1} \sum_{i=1}^N (r_i^2 - 2r_i \mathbb{E}(r) + \mathbb{E}(r)^2) \right) - (1-\lambda)\mathbb{E}(r) \\ &= \left(\frac{\lambda N}{N-1} \mathbb{E}(r)^2 + \sum_{i=1}^N \frac{\lambda}{N-1} (r_i^2 - 2r_i \mathbb{E}(r)) \right) - (1-\lambda)\mathbb{E}(r) \end{aligned}$$

For objective (B.1), the matrix Q contains $\lambda N / (N-1)$ in the diagonal corresponding to $\mathbb{E}(r)^2$, $\lambda / (N-1)$ in the diagonals corresponding to r_i^2 , $-\lambda / (N-1)$ in the columns and rows corresponding to the cross terms $r_i \mathbb{E}(r)$, and zero elsewhere. The matrix Q for objective (B.2)

contains λ/N in the diagonals corresponding to z_i^2 and zero elsewhere.

Objectives (B.3) and (B.4) are in standard linear optimization form: $c^T x$. We assume that α and N are selected so that $(1 - \alpha)N$ is an integer, otherwise this value may not be used as an index for r_i . Noting this, (B.3) and (B.4) are evidently linear.

Constraints (B.5) through (B.10) can all be put into one of the standard linear forms: $a^T x \leq b$, $a^T x \geq b$, or $a^T x = b$. Constraints (B.5) and (B.6) are in linear form. Constraint set (B.7) can be rearranged into linear form:

$$S_0 r_i + \sum_{j=1}^{N_c} p_j (\max(S_T^i - k_j, 0) - C_j e^{r_f T}) = S_T^i + \frac{\eta}{n} D - S_0 \quad i = 1, \dots, N$$

Note that S_T^i is a simulated value which is input to the optimization as a constant, thus the max function is also a constant. Constraint (B.8) is in linear form if we group the expressions on the left-hand side and equate them to zero. Constraint (B.9) is in linear form if we move r_i to the left-hand side and note that the exponential term is a constant. Constraint (B.10) is in linear form.

Since all constraints are linear, the problems of optimizing VaR or CVaR are linear programs, and the problems of optimizing variance or semivariance are quadratic programs. In appendix C we show that the quadratic terms are convex, so that minimizing them is tractable.

Appendix C

Convexity of Variance and Semivariance

Although the variance and semivariance objectives in section 2.1 are quadratic, minimizing a quadratic function is only tractable if it is convex. Here we show that the sample variance and sample semivariance are convex functions.

Consider the sample variance which is a function of the variables r_i and $\mathbb{E}(r)$:

$$\sigma_r^2 = \frac{1}{N-1} \sum_{i=1}^N (r_i - \mathbb{E}(r))^2$$

Consider the Hessian of the function $(r_i - \mathbb{E}(r))^2$ for a fixed value of i :

$$H = \begin{bmatrix} 2 & -2 \\ -2 & 2 \end{bmatrix}$$

This Hessian has eigenvalues of 4 and 0, and is thus positive semi-definite. Therefore the function $(r_i - \mathbb{E}(r))^2$ is convex for each i . Since the sample variance is a sum of convex functions multiplied by a positive scalar, it is also a convex function.

Similarly, consider the sample semivariance which is a function of z_i :

$$\text{semivariance} = \frac{1}{N} \sum_{i=1}^N z_i^2$$

For each i the function z_i^2 is convex. Since the sample semivariance is a sum of convex functions multiplied by a positive scalar it is also a convex function.

Since the sample variance and semivariance are convex, the objective of minimizing them in a quadratic program is tractable.

Appendix D

Description of Michaud Resampling

Here we describe the Michaud resampling procedure as used in section 3.4. The procedure comprises the following steps:

1. Using geometric Brownian motion and the point estimates in table 3.1, $S = 252$ daily returns are simulated.
2. The sample expected return and covariance matrix of the simulations produced in step 1 are computed.
3. The sample statistics from step 2 are used to produce $N = 2,000$ simulations of the asset prices at maturity.
4. For the chosen risk measure, the formulation from section 3.1 and the simulations from step 3 are used to produce an efficient frontier of 50 points. The corresponding portfolio positions are stored.
5. Steps 1 to 4 are performed a total of $L = 50$ times.
6. The stored portfolio positions are blended by averaging over the L resampling iterations.

Though we have used geometric Brownian motion, in practice an investor can substitute a stochastic process which they believe describes the underlying assets.

The quantity S should be carefully selected to reflect the investor's degree of confidence in their point estimates. A higher value reflects a higher degree of confidence and will lead to

estimates in step 2 which are closer to the point estimates used in step 1. A lower value reflects a lower degree of confidence and will lead to estimates in step 2 which have a wider spread. An investor should look at the spread of estimates outputted from step 2 and confirm that they match their degree of confidence regarding the point estimate used in step 1. We use $S = 252$ which reflects a relatively low degree of confidence. This produces a broad range of resampled expected returns and covariances and consequently produces blended portfolios which contain positions in a wide range of assets and options.

When formulating in step 4 we use the dividend rates from table 3.1 since they are known in advance and certain. Efficient frontiers are obtained by first solving for the minimum risk portfolio and the maximum expected return portfolio. We then optimize for 48 expected return targets equally spaced between the expected return of the minimum risk portfolio and the maximum expected return.

The number of resampling iterations, L , should be sufficiently large to produce consistent results. However, each of the L iterations must solve for an efficient frontier, thus too large a number can be prohibitively slow despite the fact that the iterations can be computed in parallel. We choose $L = 50$ which we find produces consistent results.

From each of the L frontiers we select the portfolio with the lowest expected return target, i.e. the minimum risk portfolio. The first blended portfolio is created by averaging these L portfolio positions. From each of the L frontiers we then select the portfolio with the next lowest expected return, averaging these positions produces the second blended portfolio. And so on until the last blended portfolio is the average of the L maximum expected return positions.

While we have applied a simple blending procedure, Michaud and Michaud (2008) use utility functions to select portfolios to average. A number of other blending procedures also exist in the literature. Further guidelines for Michaud resampling can be found in Michaud and Michaud (2008).

Appendix E

Description of GARCH Volatility

Here we describe the use of GARCH volatilities to produce results found in figure 3.3 in section 3.4. Details about GARCH models can be found in Bollerslev (1986). We fit a GARCH(1,1) model on the volatility of monthly log-returns of the S&P 500, EAFE, and EM indices using data from 1988 to 2016. In step 3 of the procedure described in appendix D the resampled mean and correlation matrix from step 2, and the fitted GARCH models are used to produce simulations of the asset returns at maturity. Each simulated scenario is used to drive the GARCH volatilities in the subsequent scenario. The simulated returns are then rescaled so that their variance matches the resampled variance from step 2. This ensures that the first and second moments do not differ whether using geometric Brownian motion with static volatilities or with the GARCH volatility models; the resulting simulation distributions differ only in higher order moments. The remainder of the procedure from appendix D is unchanged.

Appendix F

Two-Stage Covered Call Optimization Formulation

This appendix contains the formulation and a full list of the symbols from section 4.1.

$$\begin{aligned}
& \underset{w, p, z, W}{\text{maximize}} \quad \frac{1}{N_1 N_2} \sum_{i=1}^{N_1} \sum_{m=1}^{N_2} U(W_0 W^{im}) \\
& w_j \geq 0 \quad \text{for } j = 1, \dots, n \\
& \sum_{j=1}^n w_j = 1 \\
& q_{jl} \geq 0 \quad \forall j, l \\
& q_{jl}^0 \geq 0 \quad \forall j, l \\
& \sum_{l=1}^{n_j} q_{jl} + \sum_{l=1}^{n_j^0} q_{jl}^0 \leq w_j \quad \text{for } j = 1, \dots, n \\
& \sum_{j=1}^n \sum_{l=1}^{n_j^0} \frac{q_{jl}^0}{S_{0j}} (C_{jl}^0 e^{r_f T_1} - \max(S_{1j}^i - k_{jl}^0, 0)) \\
& + \sum_{j=1}^n \frac{w_j}{S_{0j}} (S_{1j}^i + D_{1j}) = \sum_{j=1}^n w_j^i \quad \text{for } i = 1, \dots, N_1 \\
& w_j^i \geq 0 \quad \text{for } i = 1, \dots, N_1 \text{ and } j = 1, \dots, n \\
& q_{jl}^i \geq 0 \quad \text{for } i = 1, \dots, N_1 \text{ and } \forall j, l
\end{aligned}$$

$$\begin{aligned}
& \sum_{l=1}^{n_j} q_{jl} \frac{S_{1j}^i}{S_{0j}} + \sum_{l=1}^{n_j^i} q_{jl}^i \leq w_j^i \quad \text{for } i = 1, \dots, N_1 \text{ and } j = 1, \dots, n \\
& \sum_{j=1}^n \sum_{l=1}^{n_j} \frac{q_{jl}}{S_{0j}} (C_{jl} e^{r_f(T_1+T_2)} - \max(S_{2j}^{im} - k_{jl}, 0)) \\
& + \sum_{j=1}^n \sum_{l=1}^{n_j^i} \frac{q_{jl}^i}{S_{1j}^i} (C_{jl}^i e^{r_f T_2} - \max(S_{2j}^{im} - k_{jl}^i, 0)) \\
& + \sum_{j=1}^n \frac{w_j^i}{S_{1j}^i} (S_{2j}^{im} + D_{2j}) - \sum_{j=1}^n c_z z_j^i = W^{im} \quad \text{for } i = 1, \dots, N_1 \text{ and } m = 1, \dots, N_2 \\
& w_j^i - w_j \frac{S_{1j}^i}{S_0} - z_j^i \leq 0 \quad \text{for } i = 1, \dots, N_1 \text{ and } j = 1, \dots, n \\
& w_j \frac{S_{1j}^i}{S_0} - w_j^i - z_j^i \leq 0 \quad \text{for } i = 1, \dots, N_1 \text{ and } j = 1, \dots, n \\
& \sum_{j=1}^n z_j^i \leq 2z_{max} \quad \text{for } i = 1, \dots, N_1
\end{aligned}$$

- U is the investor's utility function for wealth.

Constants:

- N_1 and N_2 are the number of scenarios or simulations in the first and second stages respectively.
- W_0 is the initial wealth of the investor.
- n is the number of assets available.
- S_{0j} is the initial price of asset j .
- At time zero there are n_j different options available to sell on asset j which mature T_1+T_2 days after time zero. They have strike prices k_{jl} and market prices C_{jl} .
- At time zero there are n_j^0 different options available to sell on asset j which mature T_1 days after time zero. They have strike prices k_{jl}^0 and market prices C_{jl}^0 .
- r_f is the risk-free rate of return.
- T_1 is the number of days from time zero to the end of the first stage.

- D_{1j} is the value of dividends paid per unit of asset j during the first period grown at the risk-free rate from the distribution date to the end of the first stage.
- D_{2j} is the value of dividends paid per unit of asset j during the second period grown at the risk-free rate from the distribution date to the end of the second stage.
- T_2 is the number of days from the end of the first stage to the end of the second stage.
- c_z is the transaction cost of one unit of wealth.
- z_{max} is the maximum proportion of wealth which can be reinvested into a different asset at the end of the first stage.

Simulated constants:

- S_{1j}^i is the price of asset j at the end of the first stage in scenario i .
- At the beginning of the second stage in scenario i there are n_j^i different options available to sell on asset j which mature T_2 after being sold. They have strike prices k_{jl}^i and market prices C_{jl}^i .
- S_{2j}^{im} is the price of asset j at the end of the second stage in scenario im .

Optimization variables:

- w_j is the proportion of each unit of initial wealth invested in asset j at the beginning of the first stage.
- q_{jl} is the proportion of each unit of initial wealth overwritten at time zero by selling a call option on asset j struck at k_{jl} and maturing $T_1 + T_2$ days after time zero.
- q_{jl}^0 is the proportion of each unit of initial wealth overwritten at time zero by selling a call option on asset j struck at k_{jl}^0 and maturing T_1 days after time zero.
- w_j^i is the proportion of each unit of initial wealth invested in asset j at the beginning of the second stage in scenario i .

- q_{jl}^i is the proportion of each unit of initial wealth overwritten at the beginning of the second stage in scenario i by selling a call option on asset j struck at k_{jl}^i and maturing T_2 days after the beginning of the second stage.
- z_j^i is the turnover in asset j per unit of wealth between the end of the first stage and the beginning of the second stage in scenario i .
- W^{im} is the total return plus one at the end of the second stage in scenario im .

Appendix G

Two-Stage Scenario Generation

Here we describe the production of scenario prices S_{1j}^i and S_{2j}^{im} in section 4.2. We produce returns using geometric Brownian motion with GARCH volatilities, then we adjust the resulting log-returns so that the sample volatilities match the volatilities implied by the market prices of ATM options, and so that the sample average simple returns matches the historical simple return.

We first assume that daily log-returns are jointly distributed according to a multivariate normal distribution with a constant vector of drifts, a constant correlation matrix, and a vector of variances each following a GARCH(1,1) process. For a single asset j :

$$r(j, t, i) = (\mu_j - \frac{1}{2} \sigma(j, t, i)^2) + \sigma(j, t, i) Z(j, t, i)$$

Where:

- $r(j, t, i)$ is the log-return of asset j on day t in scenario i .
- μ_j is the historical drift of the daily log-return of asset j , gross of dividends
- $\sigma(j, t, i)^2$ is the variance of the daily log-return of asset j on day t in scenario i , modeled as a GARCH(1,1) process.
- $Z(j, t, i)$ are standard normal random variables which are jointly distributed across assets: $\text{corr}(Z(j, t, i), Z(k, t, i)) = \text{corr}(r(j, t, i), r(k, t, i)) = \rho_{j,k}$.

The drifts and correlations are estimated using historical data from November 2006 to November 2016 and are assumed to be constant. GARCH(1,1) processes are fitted on the daily

log-return residuals over the same time period. From fitting the GARCH processes we have variance estimates for all assets at time $t = 1$, denoted by $\sigma(j)$. We use these volatilities as the starting point of the GARCH processes in all scenarios, i.e. $\sigma(j, t = 1, i) = \sigma(j)$ for all scenarios i and all assets j . For each scenario i we can simulate $Z(j, t = 1, i)$ for all assets j from a multivariate normal distribution with means equal to zero, variances equal to one, and covariance matrix $\rho = [\rho_{j,k}]$. Then, for all assets j in each scenario i , the log-return $r(j, t = 1, i)$ can be computed and the GARCH variances can be updated through the equation $\sigma(j, t + 1, i)^2 = \alpha_j^0 + \alpha_j \sigma(j, t, i)^2 Z(j, t, i)^2 + \beta_j \sigma(j, t, i)^2$, where α_j^0 , α_j , and β_j are the fitted GARCH(1,1) parameters for asset j . We can then proceed to $t = 2$. In this fashion log-returns are simulated one day at a time for $t = 1$ to T_1 .

For an asset j and a scenario i , the log-return during the first stage is given by:

$$r_{1j}^i = \sum_{t=1}^{T_1} r(j, t, i)$$

Consider the sample expectation and variance of r_{1j}^i across the simulated scenarios:

$$\begin{aligned} \text{var}(r_{1j}) &\equiv \hat{\sigma}_j^2 T_1 \\ \mathbb{E}(r_{1j}) &\equiv M_j \equiv (\hat{\mu}_j - \frac{1}{2} \hat{\sigma}_j^2) T_1 \end{aligned}$$

Suppose that we would like to transform the values of r_{1j}^i so that the sample daily variance is equal to the daily variance implied by the market price of the ATM two-week-to-maturity call option on asset j , $\tilde{\sigma}_j^2$, and so that the sample average simple return matches that implied by the historical rate μ_j . Furthermore we would like to preserve higher order moments and correlations present in the samples. We can do this by applying the transformation:

$$\begin{aligned} \tilde{r}_{1j}^i &= \tau(r_{1j}^i - M_j) + \tilde{M}_j \\ \tau &= \frac{\tilde{\sigma}_j}{\hat{\sigma}_j} , \quad \tilde{M}_j = (\mu_j - \frac{1}{2} \tilde{\sigma}_j^2) T_1 \end{aligned}$$

Then:

$$\begin{aligned}\mathbb{E}(\tilde{r}_{1j}) &= \tilde{M}_j \\ \text{var}(\tilde{r}_{1j}) &= \text{var}(\tau(r_{1j} - M_j) + \tilde{M}_j) \\ &= \tau^2 \text{var}(r_{1j}) \\ &= \tilde{\sigma}_j^2 T_1\end{aligned}$$

Thus the transformed variable exhibits the desired sample variance. Now let us assume that r_{1j} is approximately normally distributed:

$$r_{1j} \approx (\hat{\mu}_j - \frac{1}{2}\hat{\sigma}_j^2)T_1 + \hat{\sigma}_j \sqrt{T_1}Z$$

Where Z is a standard normal random variable. Then:

$$\begin{aligned}\tilde{r}_{1j} &\approx \tau(\hat{\sigma}_j \sqrt{T_1}Z) + \tilde{M}_j \\ &= (\mu_j - \frac{1}{2}\tilde{\sigma}_j^2)T_1 + \tilde{\sigma}_j \sqrt{T_1}Z\end{aligned}$$

Thus the sample expected simple return approximately matches the simple return given by the historical drift:

$$\mathbb{E}(\exp(\tilde{r}_{1j})) \approx \exp(\mu_j T_1)$$

We could of course embed a small correction into \tilde{M}_j to achieve perfect equality, but in practice we find that the difference is negligible. As an alternative to adjusting the sample expected simple return we could have set $\tilde{M}_j = (\hat{\mu}_j - \frac{1}{2}\tilde{\sigma}_j^2)T_1$. Then the sample expected simple return would be unchanged from that of the untransformed samples.

Consider the standardized moment of degree v of \tilde{r}_{1j} :

$$\begin{aligned}\bar{\mu}_v(\tilde{r}_{1j}) &= \frac{\mathbb{E}((\tilde{r}_{1j} - \tilde{M}_j)^v)}{\text{var}(\tilde{r}_{1j})^{\frac{v}{2}}} \\ &= \frac{\mathbb{E}((\tau(r_{1j} - M_j))^v)}{(\tau^2 \text{var}(r_{1j}))^{\frac{v}{2}}}\end{aligned}$$

$$\begin{aligned}
&= \frac{\tau^v \mathbb{E}((r_{1j} - M_j)^v)}{\tau^v \text{var}(r_{1j})^{\frac{v}{2}}} \\
&= \frac{\mathbb{E}((r_{1j} - M_j)^v)}{\text{var}(r_{1j})^{\frac{v}{2}}} \\
&= \bar{\mu}_v(r_{1j})
\end{aligned}$$

Thus the transformation preserves the skewness, kurtosis, and higher moments that were present in the original samples. Consider the correlation between the transformed returns of two different assets:

$$\begin{aligned}
\text{corr}(\tilde{r}_{1j}, \tilde{r}_{1k}) &= \frac{\text{cov}(\tilde{r}_{1j}, \tilde{r}_{1k})}{\text{var}(\tilde{r}_{1j})^{\frac{1}{2}} \text{var}(\tilde{r}_{1k})^{\frac{1}{2}}} \\
&= \frac{\text{cov}(\tau r_{1j}, \tau r_{1k})}{\tau \text{var}(r_{1j})^{\frac{1}{2}} \tau \text{var}(r_{1k})^{\frac{1}{2}}} \\
&= \frac{\text{cov}(r_{1j}, r_{1k})}{\text{var}(r_{1j})^{\frac{1}{2}} \text{var}(r_{1k})^{\frac{1}{2}}} \\
&= \text{corr}(r_{1j}, r_{1k})
\end{aligned}$$

Thus the transformation preserves the correlations between assets that were present in the original samples.

We compute the price of asset j in scenario i at the end of the first stage: $S_{1j}^i = S_{0j} \exp(\tilde{r}_{1j}^i) - D_{1j}$, where if an ex-dividend date falls between $t = 1$ to T_1 then D_{1j} is the value of that dividend, or zero otherwise.

Production of scenarios for the second stage is nearly identical. In the second stage the GARCH volatilities are initialized to their final realized value from the first stage simulations, i.e. $\sigma(j, t = T_1 + 1, im) = \sigma(j, t = T_1 + 1, i)$ for all assets j and scenarios im . For the second stage the target variance $\tilde{\sigma}_j$ is set to be the inferred ATM implied volatility from $t = T_1$ to $t = T_1 + T_2$ based on the daily volatilities implied by the ATM four-week-to-maturity and two-week-to-maturity options at time zero. This ensures that the volatility of log-returns from $t = 0$ to $t = T_1 + T_2$ matches the implied volatility of ATM four-week-to-maturity options. The remainder of the procedure is unchanged, we set: $S_{2j}^{im} = S_{1j}^i \exp(\tilde{r}_{2j}^{im}) - D_{2j}$.

Appendix H

Option Market Price Estimation

Here we describe the procedure used in section 4.2 to estimate the market prices of call options at the beginning of the second stage in each scenario i , i.e. C_{jl}^i . Supposing that we have produced scenario prices S_{1j}^i for all assets at the end of the first stage, we then require some method for estimating the market prices of call options such that they are consistent with the scenario asset prices. The maturity date is in T_2 days, i.e. at the end of the second stage. The risk-free rate is assumed to be known, and the assets' spot prices are given by the scenario prices. From an option pricing perspective the only other parameters needed are the strike prices and volatilities.

We pick strike prices for each asset's options by first assuming that the number of OTM options available for some asset is equal to the number of T_1 -days-to-maturity OTM options which were available at the beginning of the first stage, i.e. $n_j^i = n_j^0$ for all assets j in each scenario i . Strike prices for a particular asset are generally given by multiples of some number centered around the spot price, e.g. multiples of 1, 5, 10, etc. We observe this strike price multiplier for each asset using the n_j^0 options available at time zero. We set the strike price of the ATM option on asset j at the beginning of the second stage in scenario i by rounding the spot price S_{1j}^i down to the closest strike price multiple. Subsequent OTM strikes are set by increasing the ATM strike by the observed multiplier until $n_j^i = n_j^0$.

We require an estimate of the implied volatility curve where the expiry is in T_2 days. A substantial amount of literature exists in modelling implied volatility surfaces, much of which is collected in Gatheral (2006). In our case we may view the entire volatility surface for each

asset at time zero. Since there are only T_1 days to the end of the first stage it is reasonable to assume that changes in the volatility surface over this time period ought to be small. We assume that for an asset j the implied volatility curve for T_2 -days-to-maturity options at the beginning of the second stage, as a function of moneyness, is unchanged from that of time zero. This assumption is known as the 'sticky delta' rule. We estimate market prices by first computing implied volatilities of T_2 -days-to-maturity options at time zero using a Cox-Ross-Rubinstein (CRR) binomial tree (see Cox et al. 1979 for details), then estimate options' market prices at the beginning of the second stage using a CRR tree with the implied volatilities and the relevant strike prices. It is possible to apply sophisticated models if needed; since the scenario prices are exogenous inputs to the optimization model, prices generated using any model can easily be substituted.

Appendix I

Utilities With Identical Arrow-Pratt Coefficients

Here we prove that it is equivalent to optimize the expectation of two increasing utility functions which have the same Arrow-Pratt ARA coefficient.

Theorem 3. If two smooth, monotonically increasing functions $f : \mathbb{R} \mapsto \mathbb{R}$ and $g : \mathbb{R} \mapsto \mathbb{R}$ satisfy the condition $f''(x)/f'(x) = g''(x)/g'(x)$ then $\exists a, b \in \mathbb{R}$ such that $f(x) = a + b g(x)$.

Proof. Proof by recognizing that $f''(x)/f'(x) = \frac{d}{dx} \log(f'(x))$. Then:

$$\begin{aligned}\frac{f''(x)}{f'(x)} &= \frac{g''(x)}{g'(x)} \\ \frac{d}{dx} \log(f'(x)) &= \frac{d}{dx} \log(g'(x)) \\ \log(f'(x)) &= \log(g'(x)) + c \\ f'(x) &= e^c g'(x) \\ f(x) &= a + b g(x)\end{aligned}$$

Where $c \in \mathbb{R}$ is a constant and defining $b = e^c$. □

Proof. Alternatively consider a Taylor expansion of $f(x)$ and $\tilde{g}(x) = a + b g(x)$ around an

arbitrary point x_0 . To ensure $f(x_0) = \tilde{g}(x_0)$ and $f'(x_0) = \tilde{g}'(x_0)$:

$$a = f(x_0) - b g(x_0), \quad b = \frac{f'(x_0)}{g'(x_0)}$$

From the theorem statement:

$$\frac{f''(x)}{f'(x)} = \frac{b g''(x)}{b g'(x)} = \frac{\tilde{g}''(x)}{\tilde{g}'(x)}$$

Evaluating at x_0 :

$$\frac{f''(x_0)}{f'(x_0)} = \frac{\tilde{g}''(x_0)}{\tilde{g}'(x_0)} = \frac{\tilde{g}''(x_0)}{f'(x_0)}$$

Thus $f''(x_0) = \tilde{g}''(x_0)$.

Rearranging the theorem statement we have: $f''(x) \tilde{g}'(x) = \tilde{g}''(x) f'(x)$. Consider taking the n th order derivative of both sides (where n is a positive integer):

$$\frac{d^n}{dx^n} (f''(x) \tilde{g}'(x)) = \frac{d^n}{dx^n} (\tilde{g}''(x) f'(x))$$

This yields the following functional expressions:

$$\begin{aligned} LHS &= f^{(2+n)}(x) \tilde{g}'(x) + \sum_{k=1}^n m_k f^{(k+1)}(x) \tilde{g}^{(2+n-k)}(x) \\ &= RHS = \tilde{g}^{(2+n)}(x) f'(x) + \sum_{k=1}^n m_k \tilde{g}^{(k+1)}(x) f^{(2+n-k)}(x) \end{aligned}$$

Where $m_k \in \mathbb{Z}$ for $k = 1 \dots n$ are constant integers which can be determined by carrying out the differentiation, their exact values are unimportant. Suppose that $f^{(i)}(x_0) = \tilde{g}^{(i)}(x_0)$ is true for $i = 1 \dots n+1$. Then:

$$\begin{aligned} LHS|_{x=x_0} &= f^{(2+n)}(x_0) f'(x_0) + \sum_{k=1}^n m_k f^{(k+1)}(x_0) f^{(2+n-k)}(x_0) \\ &= RHS|_{x=x_0} = \tilde{g}^{(2+n)}(x_0) f'(x_0) + \sum_{k=1}^n m_k \tilde{g}^{(k+1)}(x_0) f^{(2+n-k)}(x_0) \end{aligned}$$

Thus $f^{(i)}(x_0) = \tilde{g}^{(i)}(x_0)$ true for $i = 1 \dots n + 1$ implies $f^{(2+n)}(x_0) = \tilde{g}^{(2+n)}(x_0)$. We already showed under the required choice of b that $f'(x_0) = \tilde{g}'(x_0)$ and $f''(x_0) = \tilde{g}''(x_0)$. By induction $f^{(i)}(x_0) = \tilde{g}^{(i)}(x_0)$ is true for all positive integers i . We also selected a such that $f(x_0) = \tilde{g}(x_0)$. Therefore $f(x)$ and $\tilde{g}(x) = a + b g(x)$ have the same infinite order Taylor expansion at any arbitrary point x_0 , and are thus effectively identical functions. \square

Applying theorem 3, two monotonically increasing utility functions with the same ARA coefficients differ by only a linear transformation. Maximizing $\mathbb{E}(U(x))$ is equivalent to maximizing $\mathbb{E}(a + b U(x))$ given that $b > 0$ since both functions are increasing and $\mathbb{E}(a + b U(x)) = a + b\mathbb{E}(U(x))$.

Appendix J

Progressive Hedging Penalties With Variable Rescaling

Here we demonstrate that setting per element values of r in the progressive hedging algorithm is equivalent to using a single value of r for all variables and rescaling the decision variables.

Theorem 4. When using the progressive hedging algorithm with a penalty parameter r rescaling a decision variable x_k by multiplying it by a constant n_k is equivalent to using the variable specific penalty value $r_k = r n_k^2$.

Proof. Consider the penalty associated with a single decision element x_k in iteration ν of the progressive hedging algorithm for some particular subproblem:

$$\begin{aligned} & V_{\nu,k} x_k + 0.5r(x_k - \hat{x}_{\nu,k})^2 \\ &= (\sum_2^\nu r(x_{\nu,k} - \hat{x}_{\nu,k}))x_k + 0.5r(x_k - \hat{x}_{\nu,k})^2 \end{aligned}$$

Consider replacing x_k with a rescaled variable $y_k = n_k x_k$. The optimization problem is unchanged assuming we make the substitution $x_k = y_k/n_k$ in the subproblem's constraints and original objective function. Consider the penalty that progressive hedging would impose on y_k in iteration ν :

$$(\sum_2^\nu r(y_{\nu,k} - \hat{y}_{\nu,k}))y_k + 0.5r(y_k - \hat{y}_{\nu,k})^2$$

Transforming back to the original variable (assuming for now that $y_{\nu,k} = n_k x_{\nu,k}$, which also implies $\hat{y}_{\nu,k} = n_k \hat{x}_{\nu,k}$):

$$\begin{aligned} &= \left(\sum_2^{\nu} r(n_k x_{\nu,k} - n_k \hat{x}_{\nu,k}) \right) n_k x_k + 0.5r(n_k x_k - n_k \hat{x}_{\nu,k})^2 \\ &= \left(\sum_2^{\nu} r n_k^2(x_{\nu,k} - \hat{x}_{\nu,k}) \right) x_k + 0.5r n_k^2(x_k - \hat{x}_{\nu,k})^2 \\ &= \left(\sum_2^{\nu} r_k(x_{\nu,k} - \hat{x}_{\nu,k}) \right) x_k + 0.5r_k(x_k - \hat{x}_{\nu,k})^2 \end{aligned}$$

Where we defined $r_k = r n_k^2$. This is identical to the original penalty for x_k except with r replaced by r_k . It remains to show $y_{\nu,k} = n_k x_{\nu,k}$. The first iteration is solved without penalties, thus for each subproblem $y_{2,k} = n_k x_{2,k}$ is true, and $\hat{y}_{2,k} = n_k \hat{x}_{2,k}$ is true. Suppose that we use the penalty parameter $r_k = r n_k^2$ for element x_k in the original subproblems and the penalty r in the rescaled subproblems. Then the penalties are identical in the second iteration since $y_{2,k} = n_k x_{2,k}$, and the problems have the same solution, $y_{3,k} = n_k x_{3,k}$. By induction this is true for all subsequent iterations. Therefore, the progressive hedging algorithm with x_k rescaled by n_k is equivalent to performing progressive hedging using the value $r_k = r n_k^2$ for element x_k . \square

Since the progressive hedging penalty is separable across variables, the proof holds when multiple variables are rescaled.